The Genetic Regulation of CO_2 Neuron Formation in *Drosophila melanogaster*

Marion Hartl

Dissertation zur Erlangung des Doktorgrades
der Fakultät für Chemie und Pharmazie
der Ludwig–Maximilians–Universität München

The Genetic Regulation of CO_2 Neuron Formation in *Drosophila melanogaster*

Marion Hartl

Marion Hartl
aus Bad Reichenhall

2012

Erklärung

Diese Dissertation wurde im Sinne von §7 der Promotionsordnung vom 20.November 2011 von Herrn Prof.Dr. Klaus Förstemann der Fakultät für Chemie und Pharmazie betreut.

Eidesstaatliche Versicherung

Diese Dissertation wurde eigenständig und ohne unerlaubte Hilfe erarbeitet.

München, den 25.04.2012

_____

Marion Hartl

Dissertation eingereicht am 27.04.2012

Erstgutachter: Prof.Dr. Klaus Förstemann

Zweitgutachter: Prof.Dr. Dietmar Martin

Tag der mündlichen Prüfung: 15.06.2012

Contents

List of Figures

Summary

CO_2 is a ubiquitous gas that is perceived by many insects via their olfactory system. Comparing *Drosophila melanogaster* and blood feeding mosquitoes illustrates how CO_2 elicits species specific behavior. While flies strongly avoid CO_2, mosquitoes are attracted by the gas and use it for host detection. In parallel, the anatomical localization of the responsive neurons and their synaptic connectivity differs in the two species. *Drosophila* CO_2 neurons sit on the antennae and target to the V-glomerulus in the antennal lobe, while mosquito CO_2 neurons sit on the maxillary palp and target to the food odor responsive medial glomerulus. A previously discovered mutant of *miR-279* shed some light on the molecular evolution of CO_2 neuron formation in flies and mosquitoes (Cayirlioglu et al., 2008). A mutation of *miR-279* causes the formation of ectopic CO_2 neurons on the maxillary palp, which mistarget to a medial glomerulus in the antennal lobe. On the molecular level, *miR-279* was shown to repress the neurogenic transcription factor Nerfin-1 (Cayirlioglu et al., 2008). In the presented work, I followed-up the study by focusing on the molecular network surrounding the studied microRNA. I wanted to identify an upstream regulator of *miR-279* and the factors that control downstream of *miR-279* the suppression of CO_2 neurons on the maxillary palp.

A hypomorphic allele of the transcription factor Prospero, *pros*^{IG2227}, was found to exhibit a similar expression of ectopic CO_2 neurons on mutant palps. I compared the phenotypes of the *miR-279* and Prospero mutants on the anatomical, electrophysiological and developmental level. On the anatomical level, both mutations led to the development of ectopic CO_2 neurons on adult maxillary palps without influencing the development of antennal CO_2 neurons. The ectopic maxillary palp neurons wired in the labial nerve and innervated the V-glomerulus together with the antennal CO_2 neurons but grew further to innervate a medial glomerulus. In addition to the newly identified hypomorphic allele of Prospero, two more Prospero alleles were analyzed. A complete loss-of function allele, *pros*^{17} (Doe et al., 1991), and another hypomorphic allele, *pros*^{voila78}(Grosjean et al., 2001). In parallel to *pros*^{IG2227}, the two other mutant alleles showed the same expression of ectopic CO_2 neurons which mistargeted to the medial glomerulus in the antennal lobe. Moreover, the full loss-of-function allele of Prospero showed in addition to the mistargeting phenotype an overall loss of neurons. This observation was in line with previous studies on the sensory neurons on the thorax of the fly (Manning and Doe, 1999).

Apart from the CO_2 neuron receptor, also two more receptor classes, Or42a and Or59c, were

affected by mutations in *miR-279* and Prospero. Or42a and Or59c expressing neurons are in the wildtype located on the maxillary palp and target a medial glomerulus. In the *miR-279* and Prospero mutant background, the axons targeted first the V-glomerulus before reaching the medial glomerulus.

Single sensillum recordings (SSR) on the hybrid sensilla revealed that the ectopic neurons were functionally responding to CO_2 and to the key ligands of either Or42a or Or59c, iso-amylacetate or 3-octanol.

Analyzing the development of the maxillary palp, I found in collaboration with Dr. Laura Loschek that in the wildtype, both, Prospero and *miR-279* were co-expressed throughout pupal development, although the onset of *miR-279* was slightly delayed as compared to Prospero. In both mutants, the ectopic neurons formed within the basiconic sensilla on the maxillary palp by augmenting the neuron number from two to three. The full loss of Prospero, showed again additional phenotypes. Apart from the three neuron sensilla, *pros*^{17} mutants showed either misdifferentiation of the olfactory neurons or a conversion of the neuronal to the non-neuronal fate.

Based on the phenotypical similarity and the overlap in expression, I tested the genetic interaction of Prospero and *miR-279*. By re-expressing *miR-279*, the Prospero mutant phenotype was almost completely rescued indicating that Prospero acts upstream of *miR-279* during MP CO_2 neuron suppression. In contrast, re-expression of Prospero in the *miR-279* mutant background, only slightly reduced the mistargeting phenotype. This slight rescue suggested that Prospero might also act independently on the suppression of MP CO_2 neurons although less efficient.

To test whether Prospero is controlling the microRNA in a direct way, I screened for predicted Prospero binding sites in the putative *miR-279* enhancer. The putative *miR-279* enhancer fragment contained the genomic region 2kb upstream of the microRNA gene and was previously shown to rescue the *miR-279* phenotype (Cayirlioglu et al., 2008). Within the enhancer, 18 putative Prospero binding sites were identified wherein 5 turned out to be highly conserved among 6 *Drosophila* species. To test for direct binding of Prospero to one of these sites, I performed an Electromobility Shift Assay (EMSA). In this *in vitro* assay, Prospero bound strongly to oligos containing one of the predicted sites (P4), which lay outside the 1.2 kb long primary transcript of *miR-279*.

As Prospero was shown to act as repressor as well as activator (Choksi et al., 2006), I tested the effect of Prospero binding to the *miR-279* enhancer in a S2 cell reporter assay. In S2 cells the enhancer reporter was highly expressed. By mutating all four predicted Prospero binding sites or reducing the levels of Prospero using RNAi, the expression of the enhancer reporter was highly reduced. Increasing the levels of Prospero through overexpression, did not lead to a change neither of the wildtype nor the mutated reporter indicating a saturation of the reporter expression.

To verify *in vivo* binding of Prospero to the promotor, I performed a Chromatin Immunoprecipitation (ChIP) asssay. The α-FLAG-Prospero immunoprecipitated fraction of chromatin was tested via PCR for the presence of *miR-279* enhancer fragments surrounding the predicted binding sites.

Corroborating with the *in vitro* assay, a fragment containing the conserved P4 site was amplified. *In vivo*, an enhancer reporter of *miR-279* was repressed in the Prospero mutant background. This effect was observed in the developing maxillary palp as well as in adult palps. In summary, *in vitro* and *in vivo* data showed that Prospero is acting upstream of *miR-279*. Upon direct binding of Prospero to the *miR-279* enhancer, the microRNA is activated and acts together with the transcription factor on the suppression of CO_2 neuron formation on the maxillary palp.

To find downstream targets of both regulators that influence the observed phenotype, I focused on a combination of experimentally verified targets of Prospero (Choksi et al., 2006) and predicted targets of *miR-279* using online tools like e.g. Target Scan. The overlap of the two lists contained 20 common targets. Functional classification of these using Gene Ontology (GO) term analysis revealed that the identified common targets cluster into three categories: neuronal development, cell fate determination and neurogenesis. Reducing the levels of these candidate genes in the mutant background revealed, that RNAi of Nerfin-1 was able to rescue the *miR-279* mutant phenotype to 100% and the *pros*^{IG2227} phenotype to 80%. A second predicted target, Escargot, was shown to be expressed in early stages of MP development. In S2 cells, *miR-279* downregulated 3'UTR luciferase reporter of Nerfin-1 and Escargot. *In vivo*, the expression of Escargot was significantly increased in the background of both mutants.

As these results suggested that Escargot and Nerfin-1 are repressed by *miR-279* and Prospero, I tested whether reduction of the target level in the mutant background would affect the number of ectopic CO_2 neurons. As a result, decreasing the level of either Nerfin-1, Escargot or a combination of both, reduced the number of ectopic CO_2 neurons in both mutants to comparable levels. Increasing the level of either Escargot or Nerfin-1 in the wildtype did not induce the formation of CO_2 neurons on the MP. However, a combination of the two targets, led to the formation of ectopic CO_2 neurons on the MP which performed mistargeting to a medial glomerulus.

Taken together, the presented work describes a regulatory network consisting of a transcription factor and a microRNA which cooperate to suppress the development of a mosquito-like CO_2 receptor neuron on the maxillary palp of *Drosophila melanogaster*. Here, the neurogenic transcription factor Prospero is repressing the expression of Escargot and Nerfin-1 in a coherent feed-forward loop employing *miR-279*. Furthermore, the two target molecules are shown to be necessary and sufficient to suppress CO_2 neuron development on the maxillary palp.

Chapter 1

Introduction

1.1 The Adult Olfactory System of *Drosophila melanogaster*

Navigating through their natural environments, animals are immersed in odors. Based on species specific receptor repertoires, odors can be interpreted and thus allow to locate food sources, to identify mates, promoting reproduction and to avoid predators and thus guaranteeing survival. Olfactory cues differ from visual and auditory signals in many ways. First, they cannot be characterized by simple parameters like wavelength or frequency. The complexity of interpreting odorous cues is reflected in the large set of different receptors that have been evolved to tackle this challenge. Second, the discrimination of odors relies on combinatorial coding at every single step of olfactory processing. The functional organization of olfactory systems resemble each other across the phyla suggesting that different species share common strategies of how to detect odors.

Flies perceive odors via two olfactory appendages attached to their head: the antennae and the maxillary palps. Both appendages carry olfactory sensilla containing one to up to four olfactory sensory neurons (OSNs) that express different combinations of olfactory receptors. On the antenna roughly 1200 olfactory neurons are found (Stocker, 2001) which project via the antennal nerve bundle together with fibers form auditory, hygro-sensitive and thermo-sensitive sensory neurons to the antennal lobe. The olfactory sensilla are exclusively found on the third segment of the antennae. The shaft of the sensilla encapsulates the dendrites of the olfactory sensory neurons (OSN) (Zacharuk, 1980) and support cells ensure that the neurons are electrically separated from neighboring cells. Three different types of sensilla are found on the antenna: small and large basiconics, trichoids and coeloconics (Shanbhag et al., 2000). The distribution of the three types is very stereotyped and the amount of trichoid and large basiconic

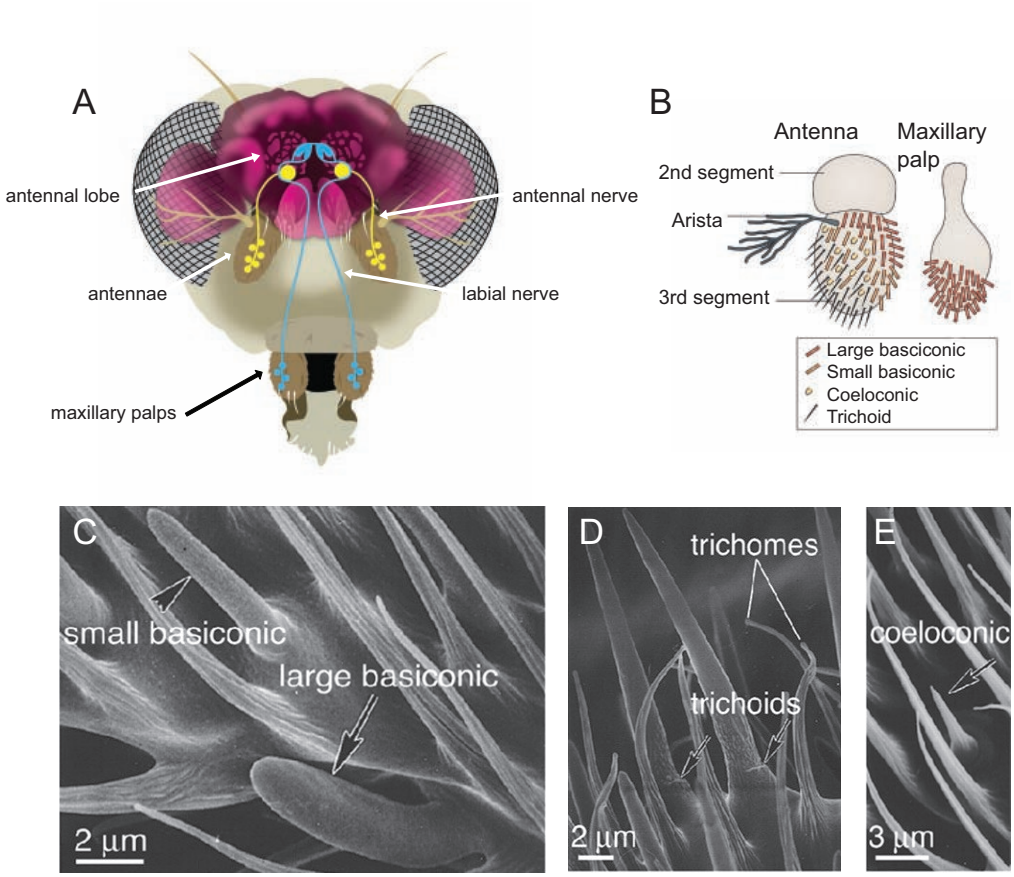

Figure 1.1: The olfactory system of *Drosophila melanogaster* A. Schematic drawing of a fly head indicating the position of antennae, maxillary palps, antennal nerve, labial nerve and the antennal lobe (copyright Julia Froehlich). **B**. Schematic of relative positions of different sensilla types on antenna and maxillary palp (Kaupp, 2010). **C**-**E**. Electronmicrographs of small and large basiconic (C), trichoid (D) and coeloconic (E) sensilla.

sensilla is sexually dimorphic (Stocker, 2001) indicating a putative role in pheromone detection. Anatomically, the maxillary palp has a simpler structure with only 120 olfactory neurons. The OSNs on the maxillary palp are exclusively housed in one sensilla type, the basiconic with only two neurons per sensillum. The axons of these OSNs fasciculate with gustatory neurons and travel via the labial nerve through the suboesophagal ganglion (SOG) to the antennal lobe.

1.1.1 Odorant Receptors

The odor response pattern of the sensilla subtypes differs. Basiconic sensilla respond largely to food odors (Goldman et al., 2005; Hallem and Carlson, 2006). Trichoid sensilla were found to respond to the pheromone cis-vaccenyl acetate (cVA)(Ha and Smith, 2006) and coeloconic

sensilla are tuned to acids, ammonia, and humidity (Yao et al., 2005). The response specificity of the different sensilla types is based on the expression of distinct chemoreceptors. To detect odors, the fly uses two different subsets of receptors, the olfactory receptors (ORs) and the recently characterized ionotropic receptors (IRs) (Benton et al., 2006). In *Drosophila* 60 genes

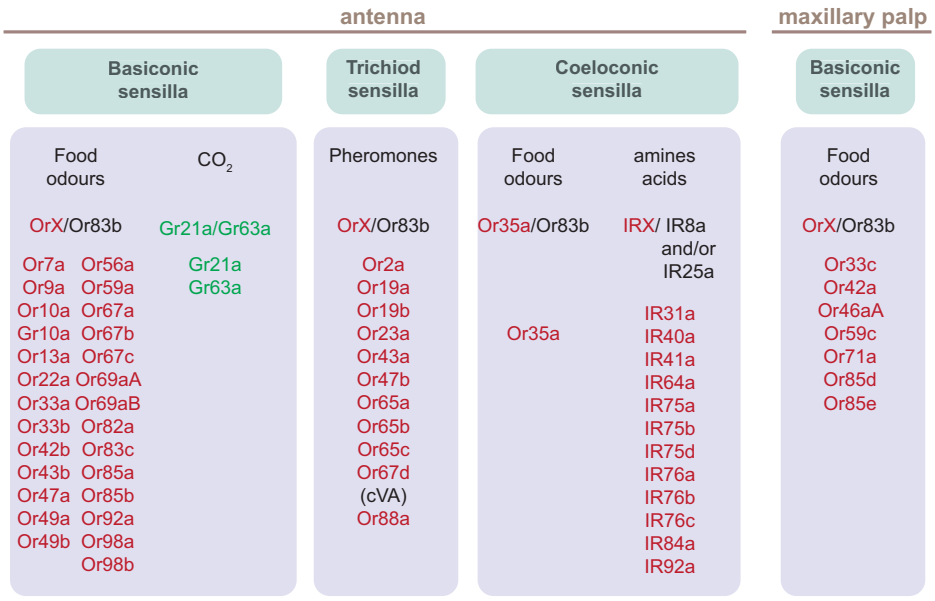

Figure 1.2: Response properties of sensilla subtypes. Overview of response properties of different sensilla types and their respective olfactory receptors (adapted from Vosshall and Stocker (2007)).

code for 62 olfactory receptors as two are subject to alternative splicing (Robertson et al., 2003). In mammals, reptiles, birds, amphibians, fish and nematodes chemosensory cues are detected via receptors of the transmembrane domain G protein-coupled receptor (GPCR) superfamily (Buck and Axel, 1991; Troemel et al., 1995; Bargmann, 2006). The invertebrate receptors were found in a bioinformatic screen searching for seven transmembrane proteins in the *Drosophila* genome. Unlike vertebrate receptors, insect chemoreceptors are not related to GPCRs (Vosshall et al., 1999; Benton et al., 2006; Wistrand et al., 2006). Mechanistically, the chemoreceptors function as odor-gated ion channels (Sato et al., 2008; Wicher et al., 2008). In comparison, vertebrate ORs resemble metabotropic receptors such as the glutamate receptor. All insect ORs are expressed as a heterodimer along with the co-receptor ORCO (previously know as Or83b) (Benton et al., 2006). The co-receptor together with an odor specific OR is expressed in the ciliated dendrites of OSNs. ORCO was shown to be necessary and sufficient for receptor targeting to the ciliated dendrites and for establishing a functional receptor dimer (Benton et al., 2006). The broad function of ORCO is reflected in the expression in almost all olfactory sensilla

types except for coeloconic sensilla. Apart from ORCO, all OR genes are expressed in a defined subpopulation of neurons.

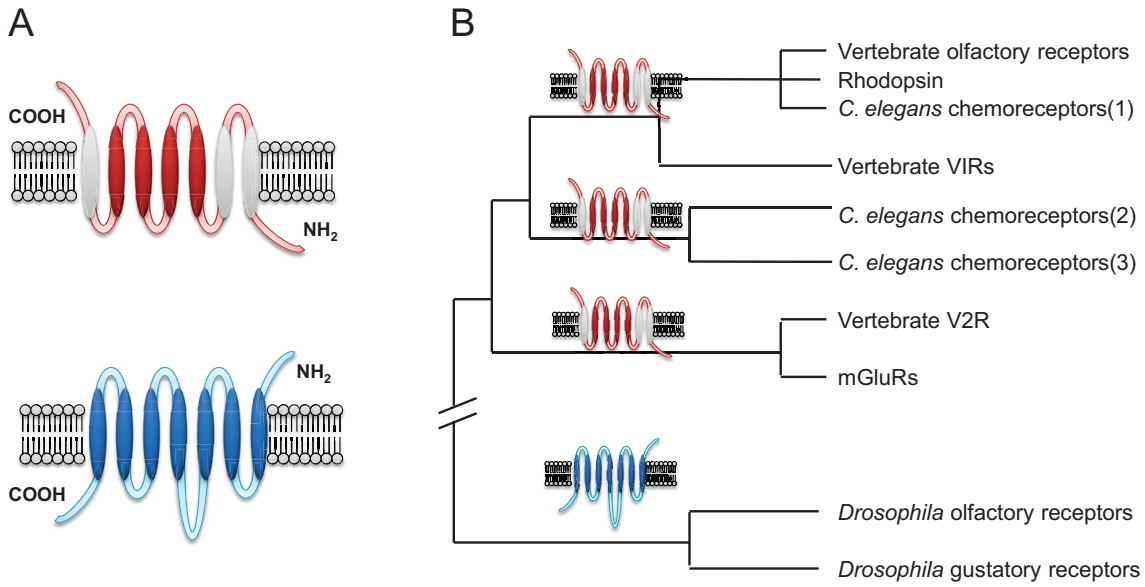

Figure 1.3: Comparison of vertebrate and invertebrate chemoreceptors A. Membrane topology of vertebrate GPCRs (red) and insect seven transmembrane domain olfactory receptors (blue). **B**. Phylogenetic tree showing the distribution of the two different chemoreceptor types in the animal kingdom (adapted from Bargmann (2006)).

Based on a bioinformatic screen searching for insect genes that are enriched in OSNs, members of the ionotropic glutmate receptor (iGluR) gene family were found to accumulate in coeloconic sensilla (Benton et al., 2009). These members of variant iGluRs were further characterized as a new class of chemosensory receptors. Structurally, they differ from the well known kainate, AMPA and NMDA classes of iGluRs as they show divergent ligand-binding domains and the lack of a glutamate binding residue. IRs function as heteromers consisting of one receptor with either one or two broadly expressed co-receptors (IR8a and IR25a) (Abuin et al., 2011). IRs respresent an evolutionary old way of chemodetection as they are conserved in bacteria, plants and animals (Benton et al., 2009). An interesting example for the function

of IRs is the involvement of IR84a in courtship behavior (Grosjean et al., 2011).

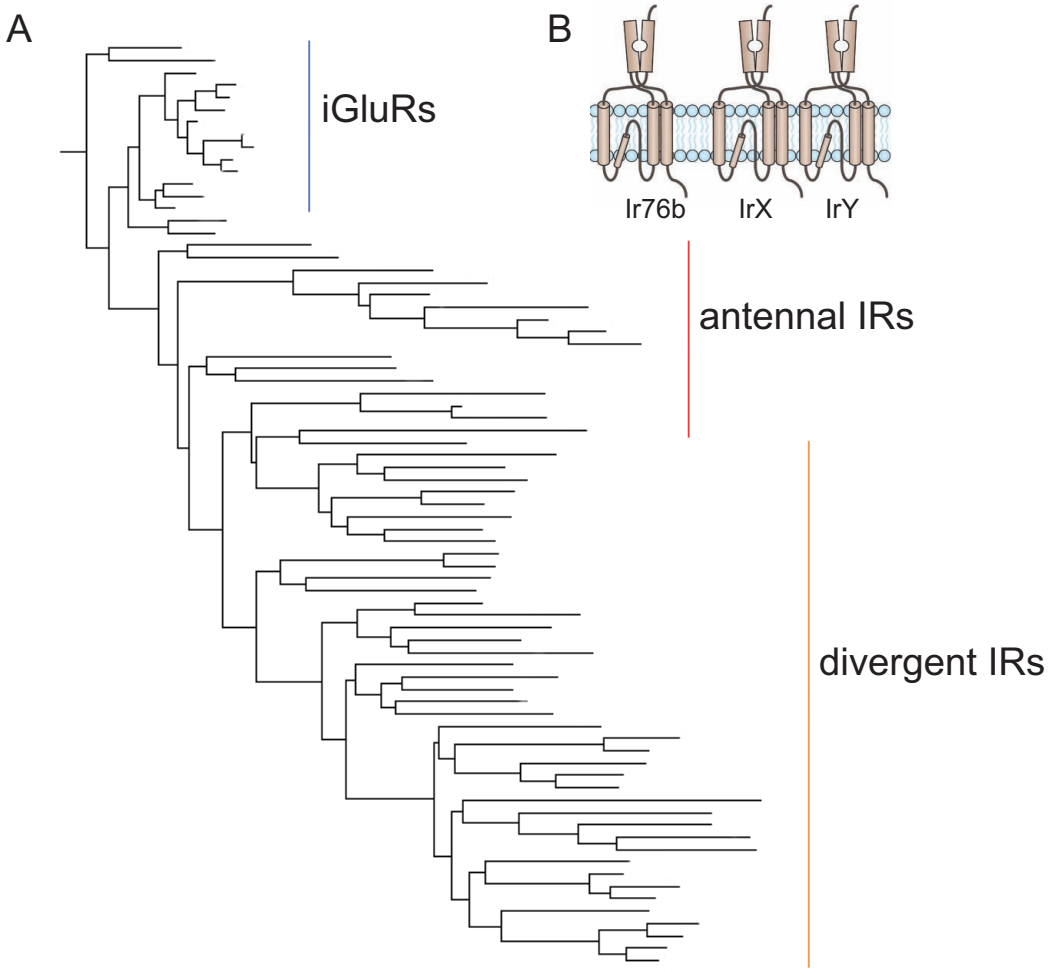

Figure 1.4: Evolution of ionotropic receptors (IRs) A. Phylogenetic tree indicating the evolutionary distance of iGluRs e.g. NMDA1, antennal ionotropic receptors (IRs) and divergent IRs (Benton et al., 2006). **B**. Schematic structure of an IR complex (Kaupp, 2010).

1.1.2 The Pathway of Olfactory Information

From the antenna and maxillary palp, neurons that express either a specific set of ORs or IRs send their axons to the primary relay center of olfactory information in the central nervous system (CNS), the antennal lobe (AL). The AL comprises around 46 structures called glomeruli. In each glomerulus the axons of OSNs coming from the peripheral appendages form synapses

with the dendrites of projection neurons that relay the olfactory information to higher brain centers. All OSNs which express the same OR, target to a distinct glomerulus in a stereotyped pattern. Based on that observation, the enhancer regions of the receptor genes can be used to generate reporters to label a specific glomerulus. Thereby, a topographic representation of the olfactory information was defined and every glomerulus was assigned to a specific OR (Couto et al., 2005; Fishilevich and Vosshall, 2005). The few glomeruli that were unassigned could be later defined as the target areas of IRs (Benton et al., 2009). From the initial description of the

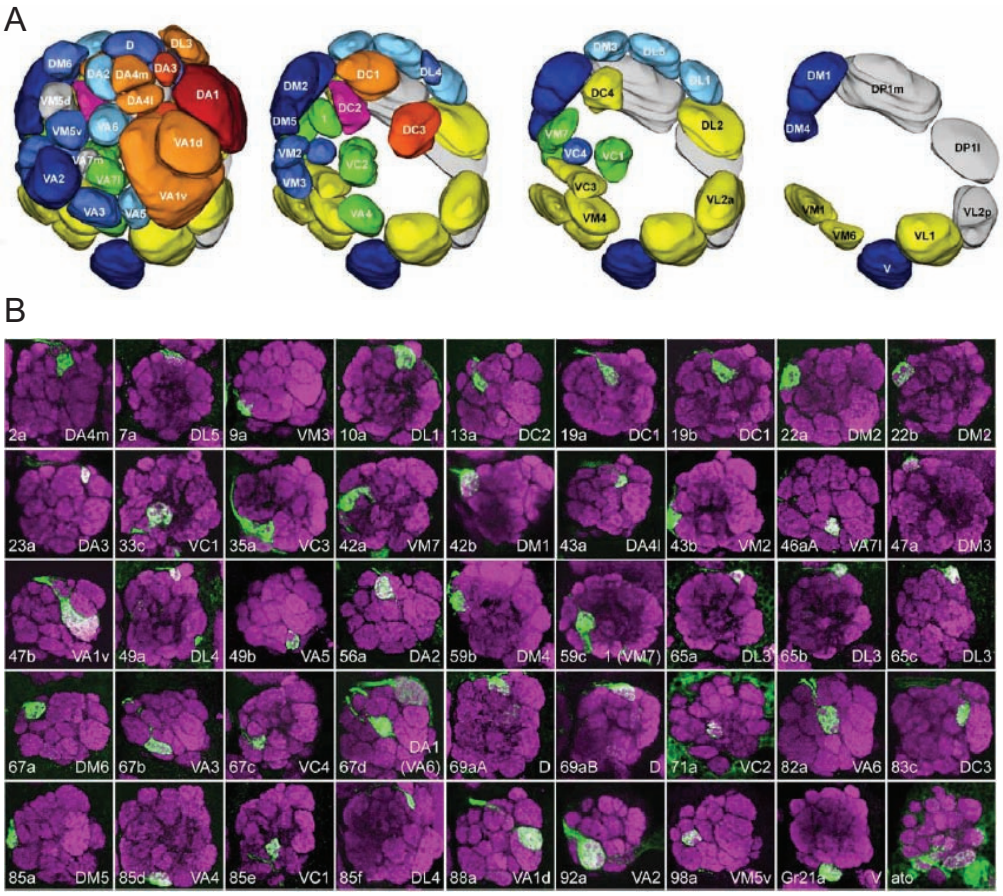

Figure 1.5: The olfactory map in *Drosophila melanogaster* A. 3D reconstrcution of a male antennal lobe. The position of 49 glomeruli starting from the anterior to the posterior glomeruli, are shown. **B**. The location of glomeruli targeted by or reporter constructs. The constructs are direct fusions of ORX-Gal4 and UAS mcD8GFP (green). To stain the neuropil the α- nc82 antibody (magenta) was used Couto et al. (2005).

olfactory map some organization principles could be deducted. First, sensilla of the same type target to a similar area in the antennal lobe, for instance antennal basiconic sensilla occupy the medial edge. Second, two large lateral glomeruli were found to be sexually dimorphic. As

a third design principle, 45 olfactory receptors converge in 36 glomeruli (Couto et al., 2005; Fishilevich and Vosshall, 2005), while the remaining nine are innervated by IRs (Benton et al., 2009). Finally, it was hypothesized that neurons tuned to similar odors also target similar areas in the AL (Couto et al., 2005; Fishilevich and Vosshall, 2005; Hallem and Carlson, 2006).

The targeting logic of IRs is largely similar to the ORs (Fig.1.6). Most IRs target one glomerulus except for IR64a innervating two glomeruli. Similarly, IR40a has a more complex columnar targeting pattern (Silbering et al., 2011). Moreover, the majority of the IRs project to the contralateral antennal lobe, although a subset of IRs (IR40a and IR75d) exclusively target ipsilateral postsynaptic targets (Silbering et al., 2011). The glomeruli that are innervated by IRs and ORs are separated from each other in the antennal lobe. However, second order neurons integrate the information of both subsystems and interdigitate them in higher brain centers. In line with this anatomical pairing of IR and OR pathways, behavioral responses of flies rely on a combination of both chemoreceptor pathways (Silbering et al., 2011).

The synaptic arrangement within the antennal lobe is complex. Two classes of neurons send their dendrites to the antennal lobe: The lateral interneurons (LNs) and the projection neurons (PNs). Lateral interneurons horizontally connect the glomeruli with each other, while PNs transmit the olfactory information vertically to the higher brain centers. Given this arrangement, the question arose whether the lateral connections together with PNs modify odor information already at the level of the antennal lobe or whether the antennal lobe only functions as relay station. Using functional imaging, no evidence for a modifying role of the antennal lobe was found. Instead, the odor-evoked activity of incoming OSNs and PN dendrites seemed to be identical (Ng et al., 2002; Wang et al., 2003). In contrast, whole cell patch clamp experiments revealed that PNs are more broadly tuned than OSNs and have a temporally more complex firing pattern (Wilson et al., 2004). This finding supports the idea of a "cross-talk" in the antennal lobe based on LNs (Sachse and Galizia, 2002; Ng et al., 2002). Most of the LNs are GABAergic. Supported by electronmicroscopy data, inhibitory LNs directly connect to PNs and therefore establish a network of lateral inhibition (Mori et al., 1999; Sachse and Galizia, 2002; Christensen et al., 1993). This GABA-mediated effect provides a mechanism to modulate olfactory gain on the level of the antennal lobe (Olsen and Wilson, 2008). These modifications might differ from glomerulus to glomerulus depending on the precision versus dynamic range that is needed to detect a given odor. Moreover, cholinergic LNs were identified which form mixed chemical-electrical synapses with inhibitory LNs and solely electrical synapses with PNs. It seems that every excitatory LN is connected to every PN thereby forming a broad recurrent inter-connective network (Yaksi and Wilson, 2010; Huang et al., 2010). Thus excitatory LNs can

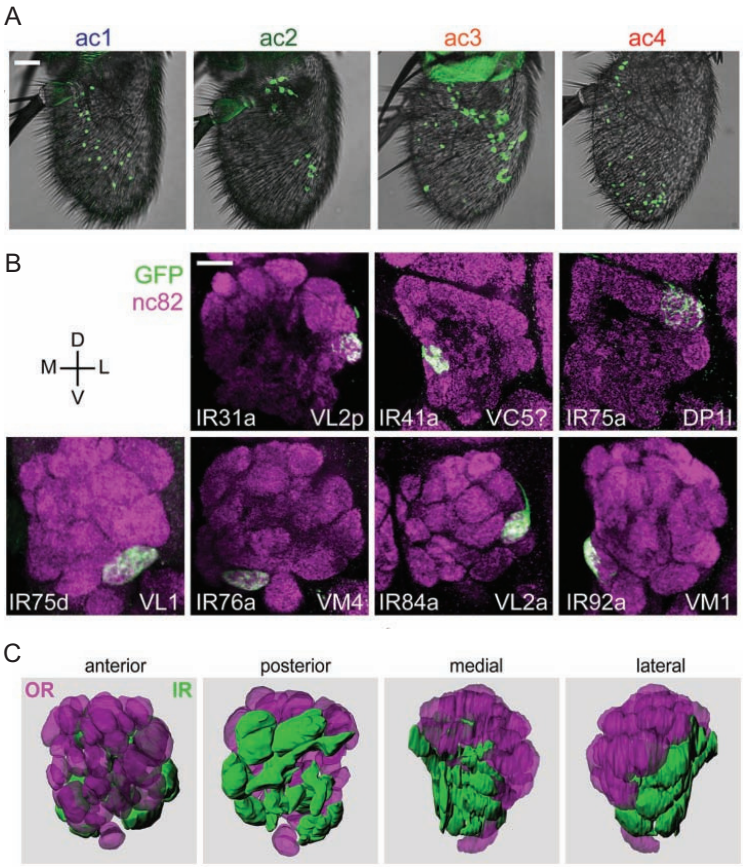

Figure 1.6: Localisation and targeting of ionotropic receptors (IRs) A. The position of coeloconic sensilla subtypes is indicated using reporter lines for ac1 (IR92a), ac2 (IR41a, ac3 (or35a) and ac4 (IR84a) driving the expression of UAS-nls-GFP. Scale bar indicates 20 μm. **B**. IRX-Gal4 reporter lines express UASmcD8GFP (green) to label the targeted area in the antennal lobe. The neuropil is stained with nc82 (magenta). Scale bar 20 μm. **C**. 3D reconstruction of a female antennal lobe. The areas targeted by IRs (green) and ORs (purple) are indicated. (Silbering et al., 2011)

elicit a broad excitation of divers PNs upon stimulation with an odor. Moreover, the network can lead to a synchronization of PN activity, which might improve the detection of weak odors (Wilson, 2011). On the other hand, excitatory LNs are thought to activate inhibitory LNs that in turn inhibit PNs. Thereby, a balance between overall excitation and inhibition might be achieved (Yaksi and Wilson, 2010).

Following the pathway of olfactory information, the PNs target two higher brain centers: the mushroom body (MB) and the lateral horn (LH). Higher brain centers also exhibit a topographic map of odor representation, but are yet differently organized compared with the antennal lobe. Axons from distinct PNs follow four different tracts to reach the mushroom body and the

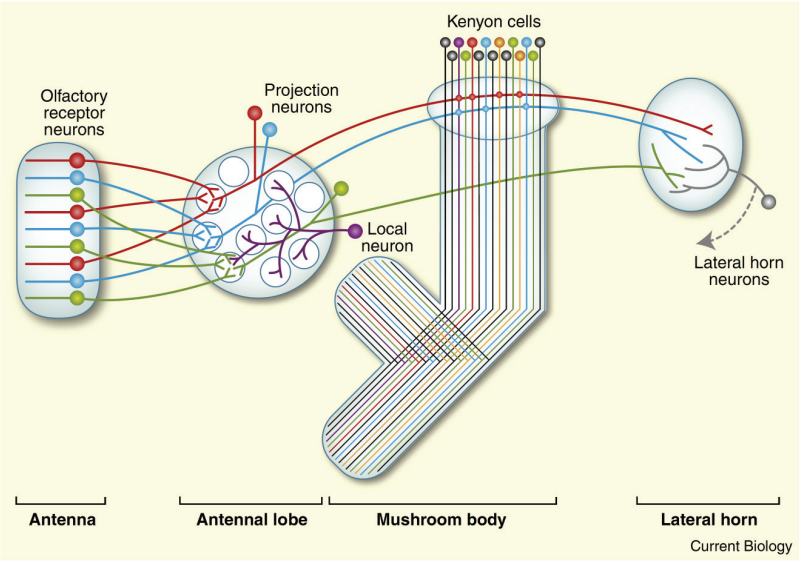

Figure 1.7: The pathway of olfactory information. A schematic drawing showing the steps of olfactory information processing in the fly. OSNs from the periphery target the antennal lobe and synapse to the dendrites of projection neurons (PNs), which further transmit the information to higher brain centers (Mushroom Body and Lateral Horn) (Masse et al., 2009)

lateral horn: the inner antennocerebral tract (iACT), the outer antennocerebral tract (oACT), the middle antennocerebral tract (mACT) and the inner-middle antennocerebral tract (imACT) (Tanaka et al., 2008). Among these tracts the iACT is the most prominent.

Following mostly the iACT, PNs from specific glomeruli target distinct zones in the MB and the LH. In the MB, the major input region is the calyx. Here, the PNs synapse with roughly 2500 intrinsic MB neurons called Kenyon cells (Strausfeld et al., 2003). Based on their axonal projections, Kenyon cells divide into at least three different subsystems (α/β; α'/β'; γ) (Crittenden et al., 1998; Lee et al., 1999). Within the calyx, the Kenyon cells are aligned in concentric zones targeted by distinct PNs originating from specific glomeruli. The output pattern of the Kenyon cells reflects the combined activity of several PNs and might therefore be used for coincidence detection. Hence, the MB can integrate a wide range of odor information. Previous studies have shown that the MB has a strong impact on olfactory learning (de Belle and Heisenberg, 1994; Heisenberg et al., 1985; Zars, 2000; Heisenberg, 2003; Keene and Waddell, 2007). Moreover, the anatomical subdivisions correlate with different functions. The α β and the α' β' system correlate with intermediate and long term memory, whereas the γ lobe is involved in short term memory (Akalal et al., 2006; Krashes et al., 2007; McGuire et al., 2001; Pascual and Préat, 2001; Zars, 2000). In the LH, PN axons target the dorso-ventral and the

antero-posterior axes. These distinct zones are again linked to different brain areas. Unlike the MB, the LH is presumably involved in innate and experience-independent odor recognition (de Belle and Heisenberg, 1994; Heimbeck et al., 2001; Tanaka et al., 2004). Given the recent effort in defining the neuronal circuits in the fly brain, some described aspects of the higher brain centers will have to be revised.

1.2 Development of the Olfactory System

1.2.1 Sensilla Develop Through a Series of Assymmetric Cell Divisions

Sensory neurons are housed in sensilla that are comprised of different cell types (neurons, hair, socket and sheath cells) (Rodrigues and Hummel, 2008). As these different cell types are derived from a single sensory organ precursor (SOP), sensilla became a well established model system to study cell fate determination. Apart from the celluar diversity, different sensilla types exhibit a great morphological diversity for instance in the number of innervating neurons or form and presence of external structures. Due to the diverse morphology, the ontogeny of different sensilla types has been a matter of debate. Intense studies on the bristle sensilla sitting on the thorax of the fly in comparison with other sensory sensilla revealed, that throughout development the basic series of asymmetric cell divisions and transcription factors employed are highly similar. Based on these observations, a canonical model of sensillum development was proposed (Lai and Orgogozo, 2004). According to the canonical model of sensilla formation, four cell divisions occur to give rise to the different cell types. In the first division, the SOP divides into a pIIa (outer cell lineage) and pIIB (neuronal lineage) cells. The pIIb divides before the pIIa cell into the pIIIb cell and one glia cell. While the pIIa cell finally divides to generate 2 external cells, the neuronal pIIIb cell divides one more time to give rise to a sheath cell and a neuron. Throughout the cell division a specific set of transcription factors are switched to distinguish the fate of sibling cells. The canonical model may provide the basis of the development of most different sensilla types. So far, the development of many different sensilla types is not understood, and currently a subject of investigation.

Olfactory sensilla are innervated by up to 4 neurons. The SOP divides first to give rise to the precursors cell of outer (pIIa) and inner (pIIb) cell lineages. In the following step pIIa appears to divide in pOa and pOb that are positive for the transcription factor cut and further differentiate into shaft and socket cells, which continue to express the transcription factor cut. The inner or neuronal lineage precursor pIIb divides further in pNa and pNb. Both are positive

for Senseless, Elav and Prospero but differ in the expression of Seven-up in pNa and Pon in pNb. The pNb cell divides one more time and differentiate into two neurons that are positive for Elav. The pNa cell also undergoes one more division and gives rise to one repo positive cell and one additional precursor, the pNa' cell. The pNa' cell expresses high Notch levels. After an additional division, the pNa' cell divides into two neurons that express Elav. This model remains to be proven but would illustrate the formation of one sensillum with totally four neurons and four outer cells (Fig.1.8). Olfactory sensilla with less neurons probably follow this model of cell divisions but undergo apoptosis to remove the dispensable cells (Rodrigues and Hummel, 2008).

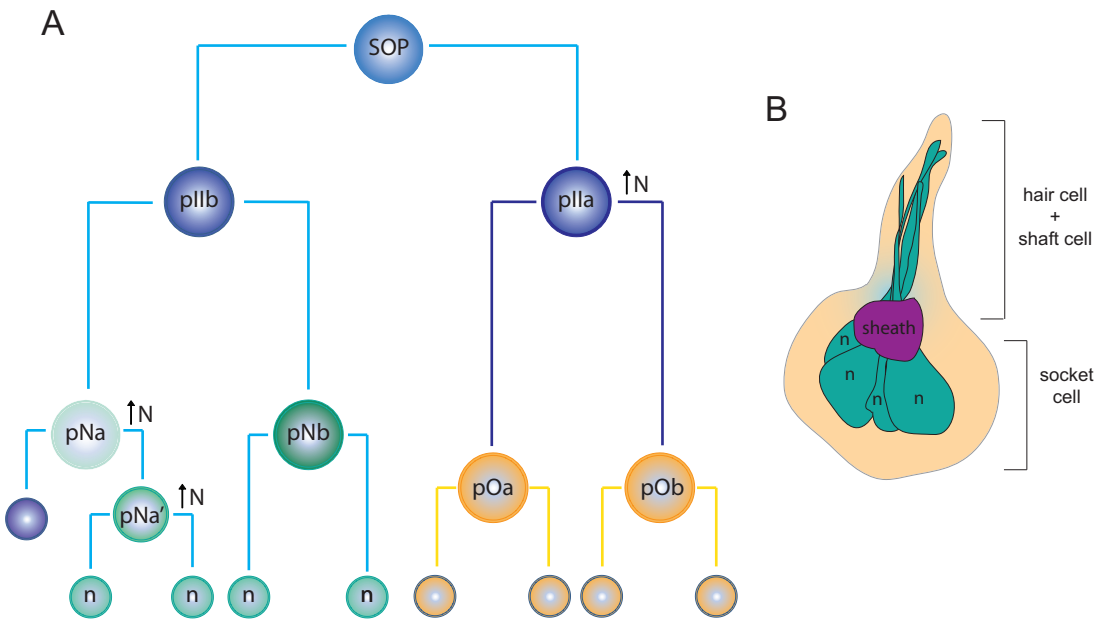

Figure 1.8: Lineage formation in the olfactory system. A. Scheme of the series of asymmetric cell divisions that give rise to an olfactory sensillum innervated by four neurons. SOP, sensory organ precursor; N, Notch levels; B. Scheme of a sensilla containing four neurons (n), one sheath cell and the surrounding cell types (socket, hair and shaft cell).

1.2.2 Development of Olfactory Sensilla Subtypes

In the olfactory system three different morphologies of sensilla are found: basiconica, trichoidea and coeloconica (Fig1.1). The choice between the different types is driven by the expression of pro-neuronal genes. Which type of sensilla is formed is dependent on the expression of two basic helix-loop-helix transcription factors, Amos and Atonal. As a consequence, loss-of function of *atonal* resulted in loss of coeloconic sensilla (Gupta and Rodrigues, 1997b). While mis-expression of *atonal* converts the basiconic and trichoidea sensilla into coeloconic (Jhaveri et al., 2000) Therefore, *atonal* is defining the fate of coeloconic sensilla. The expression of *atonal* is driven by patterning genes like *Hedgehog* and *Wingless* (Jhaveri et al., 2000). The trichoid and basiconic sensilla types are depending on the expression of *amos* (Goulding et al., 2000). A complete loss of *amos* removes all basiconic sensilla from the antenna while trichoidea are only partly affected (Gupta et al., 1998). This led to the assumption that additional factors are upstream of *amos* to define the trichoidea cell fate. In contrast, basiconic sensilla on the maxillary palp are defined by *atonal* (Gupta and Rodrigues, 1997a).

1.2.3 Notch Signaling Defines Sensilla Differentiation and Diversifies the Neuronal Lineages

The best studied sensilla are the microaechaete bristles or external sensory (ES) organs on the thorax of the fly. Due to the similar ontogeny of these mechanosensory structures and other ES organs many parallel events in the lineages have been described (Jan and Jan, 1994). In the bristle lineage a cluster of undifferentiated epidermal cells acquires the potential to become neuronal by expressing the proneuronal genes Amos and Atonal and also the ES organ specific Achaete, Scute and Lethal of Scute genes also referred as AS-C class (García-Bellido, 1979; Campuzano and Modolell, 1992; Ghysen et al., 1993). Within a cluster only one cell retains the neuronal potential, the sensory organ precursor or SOP. The signaling pathway responsible is the Notch-signaling pathway. The Notch receptor receives inputs from Delta and Jagged/Serrate membrane bound ligand families. Upon binding proteolytic events take place and release the intracellular domain of Notch (NICD) to the cytoplasm. The NICD travels to the nucleus and activates the expression of Notch dependent genes. At all steps many co-factors and suppressors were found to modify Notch signaling. The subsequent asymmetric cell divisions are further dependent on Notch. After a cell division one of the sister cell sends Notch signals while the other becomes a Notch signal receiver. Excess Notch signaling, e.g. due to mis-expression of Notch pathway components or loss of numb, remodels all sister cells in signal receiving

cells, while loss of Notch signaling results in cells that only send Notch signals. An extreme result of these events are cells that form sensilla only with external structures or sensilla only with neurons. Notch signaling throughout sensilla development is unidirectional and leads to an asymmetric distribution of cell fate determinants. In a recent study, Notch was shown to influence cell cycle arrest in ES organ cells. Upon forcing post-mitotic cells to proliferate by overexpression of cyclinE, only cells that are independent of Notch underwent extra divisions. In this process, Notch cooperated with the neuronal fate determinant Prospero (see section 1.4)(Simon et al., 2009).

In the olfactory system Notch signaling was shown to influence lineage formation as well as odor receptor choice and targeting (Endo et al., 2007). Mutants of the activator of Notch signaling, mastermind (mam) and an inhibitor of Notch signaling, numb, gave some insights into the asymmetric role of Notch signaling in these two different aspects of olfactory system development. First, early in development Notch signaling influences lineage formation. When Notch activity is reduced throughout sensillum development by loss-of-function of mam, the pIIa lineage is converted to the pIIb and the pNa acquires a pNb fate. As a result, all progenies acquire a pNb fate and the external lineage is not formed. In contrast, mutations in numb exclusively affect the development of inner cell lineages, such that all cells in the pNb lineage are transformed into a pNa fate. Hence, Notch does not directly influence the identity of pNa progeny. But probably has an impact on the precursors of pNa and pNb. Second, Notch signaling influences odor receptor choice and targeting. The set of glomeruli can also be separated in glomeruli that are targeted by cells with high Notch levels (Notch-ON) and by cells with low Notch levels (Notch-OFF) (Fig.1.9). The asymmetry in Notch levels is achieved during cell divisions. Mutants of mam show a multiplication of neurons which follow the Notch-OFF pathway. While neurons exhibit a normal targeting, instead of one, two OSNs per sensillum are formed (Endo et al., 2007). A recent follow-up study in the olfactory system showed how Notch signaling can be further modified through expression of Hamlet. During cell division the daughter cell inherits the Notch activity of the parental cell. Expression of Hamlet is able to erase this inherited Notch state, and thereby Hamlet modifies the subsequent signaling. In this process, Hamlet acts as chromatin remodeling protein that specifically makes the Notch target promotor accessible for Supressor of Hairless (Su(H)) (Endo et al., 2011).

1.2.4 Prospero a Neurogenic Transcription Factor

Prospero was first identified in a screen for regulators of neuronal fate in the embryonic central (CNS) and peripheral nervous system (PNS). Mutants of Prospero developed abnormal cell

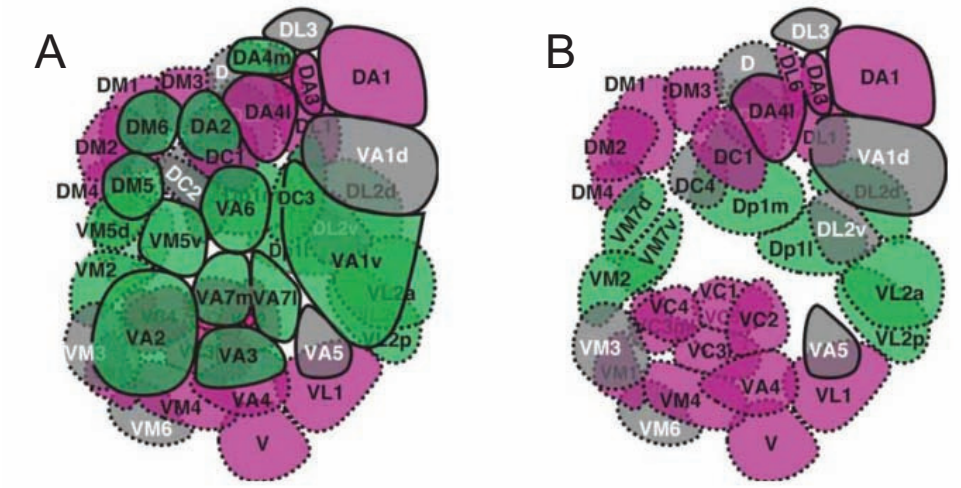

Figure 1.9: Notch signaling influences the targeting of the antennal lobe. Schematic drawing of the glomeruli in the antennal lobe indicating the glomeruli targted by OSNs with high Notch levels (Notch-ON; magenta) versus low Notch levels (Notch-OFF; green) (Endo et al., 2007).

lineages in both the embryonic CNS and PNS producing neurons with defects in axon pathfinding (Doe et al., 1991). Later, it was shown that Prospero is asymmetrically localized in the basal cortex of a differentiating neuroblast (Spana and Doe, 1995). To do so, Prospero requires the co-factor *Miranda* (Shen et al., 1997). In the adult eye sense organ and in the external sensory organ on the notum, Prospero is expressed in the early pIIb cell, which belongs to the neuronal lineage. Loss-of-function of Prospero, causes the formation of a "double bristle" indicating a conversion of the pIIb into the pIIa lineage. In this case, the hair and socket cells duplicate at the expense of neurons and glia cells. The conversion of the pIIb into the pIIA lineage was more frequently observed in the eye sense organ than in notum sensilla. Similar to the CNS, neurons mis-differentiate and have defects in axons and dendrites (Fig.1.10) (Manning and Doe, 1999). Gain-of-function experiments with Prospero resulted in sensilla with more neurons and glia cells than hair and socket cell. Here, the opposite conversion from pIIa to pIIb lineage occurred (Manning and Doe, 1999). In the fully differentiated sensilla, Prospero expression labels the sheath cell. Structurally, Prospero is an atypical homeobox transcription factor which binds to two distinct DNA binding motifs (Hassan et al., 1997; Cook et al., 2003). In order to understand the molecular function of Prospero, target genes had to be identified. Therefore, the genome-wide binding profile of Prospero in *Drosphila* embryos was studied using a methylation-based chromatin profiling technique called DamID (Choksi et al., 2006). In this assay, Prospero was fused to the *E.coli* adenine methyltransferase (Dam) and ubiquitously expressed *in vivo*. Upon DNA binding, the Dam enzyme leaves a methyl group

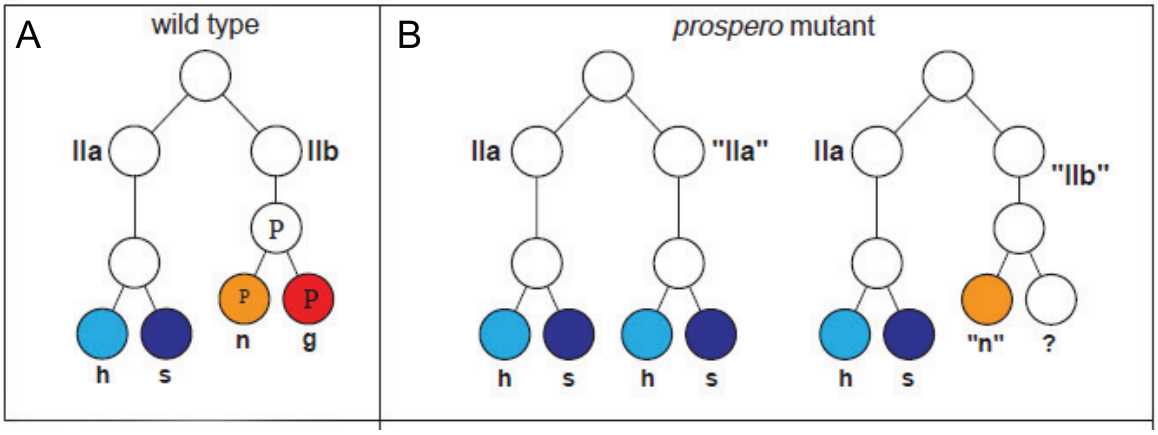

Figure 1.10: Prospero is required for proper sensillum differentiation A. Schematic on wildtype sensillum development. **B**. Loss-of-function of *Prospero* leads to conversion of the pIIB into pIIa lineage or to mis-differentiated pIIb lineage resulting in neurons lacking a wildtype axon and dendrite morphology (Manning and Doe, 1999).

on local adenines, which are embedded in a GATC sequence. Methylated whole genomic DNA extracts were further cut with a methylgroup sensitive restriction enzyme, DpnI. The resulting fragments were labeled and analyzed on a tilling array. Using this technique around 1.602 *in vivo* binding sites of Prospero were identified. An annotation of these genes using GO (gene ontology) term analysis revealed that most of the targets fall into three categories: Cell fate determination, nervous system development and regulation of transcription. Interestingly, 41% of all annotated neuroblast fate genes, 45% of genes involved in gliogenesis and 9% of all known cell cycle genes were close to *in vivo* Prospero binding sites (Choksi et al., 2006). Expression analysis of these genes comparing wildtype and mutant embryos, revealed that Prospero is activating genes that are important for differentiation e.g. *zfh* and *Lim-1* (Garces and Thor, 2006; Lilly et al., 1999) or *FasI* and *FasII* (Elkins et al., 1990; Lin et al., 1994). On the other hand, Prospero acts as a tumor suppressor, because neuroblasts in Prospero mutants overproliferate and fail to differentiate (Fig.1.11). Therefore, Prospero has a dual role in inhibiting proliferation presumably through repression of mitosis and actively inducing cell differentiation (Choksi et al., 2006).

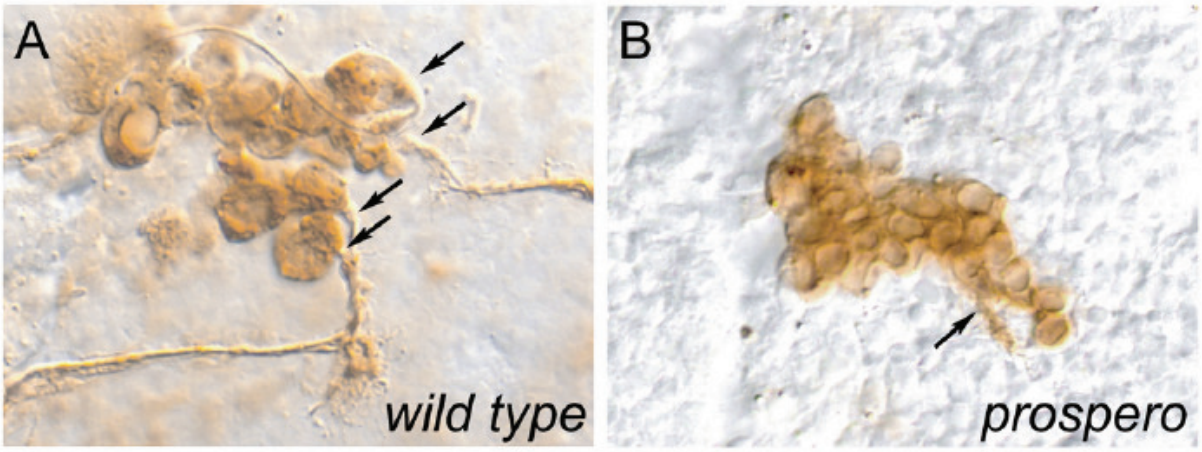

Figure 1.11: Neuroblast clones of wildtype (A). and of *prospero* mutant(B) in the embryonic CNS stained with the lipophilic dye DiI **A**. wildtype clone from a single neuroblast extend their axons (arrows)which is normal for neurons in the CNS. **B**.*Prospero* mutant clones produce more cells and rarely form outgrowths. Neurites in mutant clones are short and blunt (arrow) (Choksi et al., 2006)

1.3 CO_2 Neurons are Highly Specialized Olfactory Neurons in Insects

1.3.1 CO_2 as a behavioral trigger in *Drosophila* and *Mosquito*

CO_2 is an ubiquitous gas, which is perceived by many insect species. In some species it allows the animal to find an appropriate source for egg laying, some larvae find profitable food sources and bees control their O_2 versus CO_2 levels in the stock in order to establish optimal atmospheric conditions (Guerenstein and Hildebrand, 2008). In *Drosophila melanogaster*, larvae and adult, strongly avoid CO_2 (Suh et al., 2004). CO_2 elicits an immediate escape response as being the main component of the Drosophila stress odor (dSO), which is emitted by stressed flies. In experimental conditions, stress is triggered through vigorous shaking or electric shock. Hence, self-emitted CO_2 might act as a conspecific alarm signal which allows other flies to flee from dangerous situations (Suh et al., 2004). In contrast, in their natural environment, flies feed on rotten fruits that highly emit CO_2. During the ripening process, some studies found that the CO_2 emission decreases. Therefore, CO_2 could allow the fly to find a profitable food source (Guerenstein and Hildebrand, 2008). In contrast, these major food sources such as fruits and yeast on fermenting fruits were shown to strongly emit CO_2 (Faucher et al., 2006; Golding et al., 1999). Moreover, other studies found CO_2 in the headspace of both unripe and ripe fruits. In climacteric plants e.g. banana CO_2 emission increases with ripening. The

question arises why flies can overcome the aversive cue and still approach fruits and yeast, which is required in order to find appropriate food sources. It was hypothesized, that other compounds are emitted by fermenting fruits, which reduce the innate avoidance behavior of flies through directly binding and inhibiting the CO_2 receptors. Indeed two volatiles, 1-hexanol and 2,3-butandione were found to inhibit the electrophysiological and the behavioral response toward CO_2 (Turner and Ray, 2009). Both are emitted by fruits and yeast whereas 1-hexanol is directly synthesized through oxidation of unsaturated fatty acids and 2,3 butandione is a by-product of fermentation. The concentration of both compounds is drastically increased upon ripening. Interestingly, unlike flies, blood-feeding mosquitoes are highly attracted by CO_2 for host detection. Female mosquitoes change their flight direction toward a CO_2 plume (Dekker et al., 2005). Synergistically with components of human sweat, (L+)lactic acids and 1-octen-3-ol, CO_2 leads to high attraction of several mosquito species (Dekker et al., 2002). Mosquitoes in a wind tunnel that are tested on a filamentous plume that resembles the stimulus of a distant host, try eagerly to approach the source (Guerenstein and Hildebrand, 2008).

1.3.2 The Anatomical and Molecular Basis of CO_2 Detection in *Drosophila* and *Anopheles*

In the olfactory system, CO_2 is a unique cue as the perception relies completely on a pair of specialized receptors in OSNs which target only a single glomerulus in the antennal lobe. The pair of receptors was previously assigned to the class of gustatory receptors and therefore maintained their names: Gr21a and Gr63a (Jones et al., 2007; Kwon et al., 2007). In the adult fly, 25-30 neurons on the antenna housed in ab1c sensilla express the receptor pair (de Bruyne et al., 2001; Suh et al., 2004). These neurons innervate the ventral (V-) glomerulus in the antennal lobe (Fig.1.12). When tested in a binary choice assay, adult flies with an inactivated Gr21a expressing neuron fail to distinguish between the two sides (Suh et al., 2004). Generally, gas sensors in other animals e.g. the guanylate cyclases in *C.elegans* are present in the cytosol, the Gr21a/Gr63a receptor pair was the first membrane associated gas sensor described (Jones et al., 2007; Kwon et al., 2007). Whether other cytosolic compounds are necessary for CO_2 detection or the actual metabolite of CO_2 that is recognized by Gr21a/Gr63a receptor complex remains to be solved. Moreover, the higher brain centers involved in CO_2 processing remain to be identified.

Interestingly, the CO_2 receptor pair homologue in mosquito (*aga-Gr22* and *aga-Gr24*) shares a high similarity in sequence with the fly receptors. In contrast, the location of the *Anopheles*

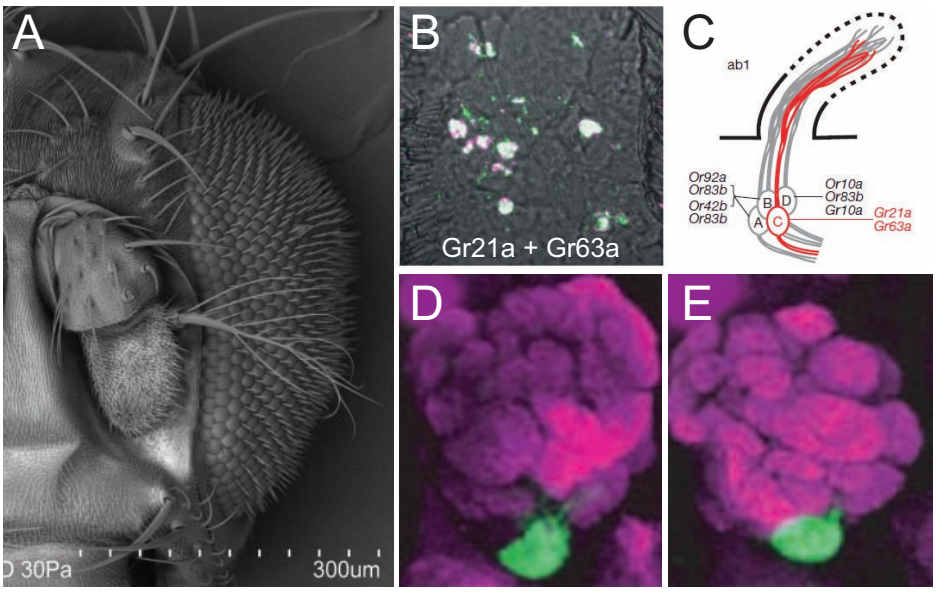

Figure 1.12: CO_2 detection in *Drosophila melanogaster*. **A**. Electronmicrograph of a *Drosophila* antenna (taken by Siju Purayil). **B**. *In situ* of Gr21a and Gr63a receptors showing co-expression on the fly antenna (Jones et al., 2007). **C**. Scheme of the ab1C sensillum housing Gr21a/Gr63a positive sensilla (Jones et al., 2007). **D** and **E**. Reporter lines for *Gr21a-Gal4* (D) and *Gr63a-Gal4* (E) driving the expression of *UAS-sytGFP* (green), label the V-glomerulus (Kwon et al., 2007).

gambiae neurons and the targeting pattern differs. Unlike fly CO_2 neurons, mosquito CO_2 neurons are exclusively located on the maxillary palp and target medial glomeruli in the mosquito antennal lobe (Fig.1.13). The medial glomeruli are associated with food sources and therefore reflect the ecologically important function of CO_2 in host detection and blood feeding (see section 1.5).

1.3.3 *miR-279* Is Involved in CO_2 Neuron Development

In general, only few factors were identified which lead to the formation of odor specific sensilla. In case of CO_2 neuron carrying sensilla, a microRNA was identified which acts on suppression of CO_2 neurons on the maxillary palp. microRNAs are small 21-23 nucleotide long non-coding RNAs and act as repressors of target mRNAs through complementary binding of the 3'untranslated region (3'UTR). They are transcribed as longer pri-miRNAs (500-3000 bases), which are cleaved into shorter pre-miRNAs (around 70 bases long) by the enzyme complex Drosha/Pasha and exported into the cytoplasm. The pre-miRNA is further trimmed to the double stranded 21-23 bases long miRNA, which is further processed into a single stranded active microRNA

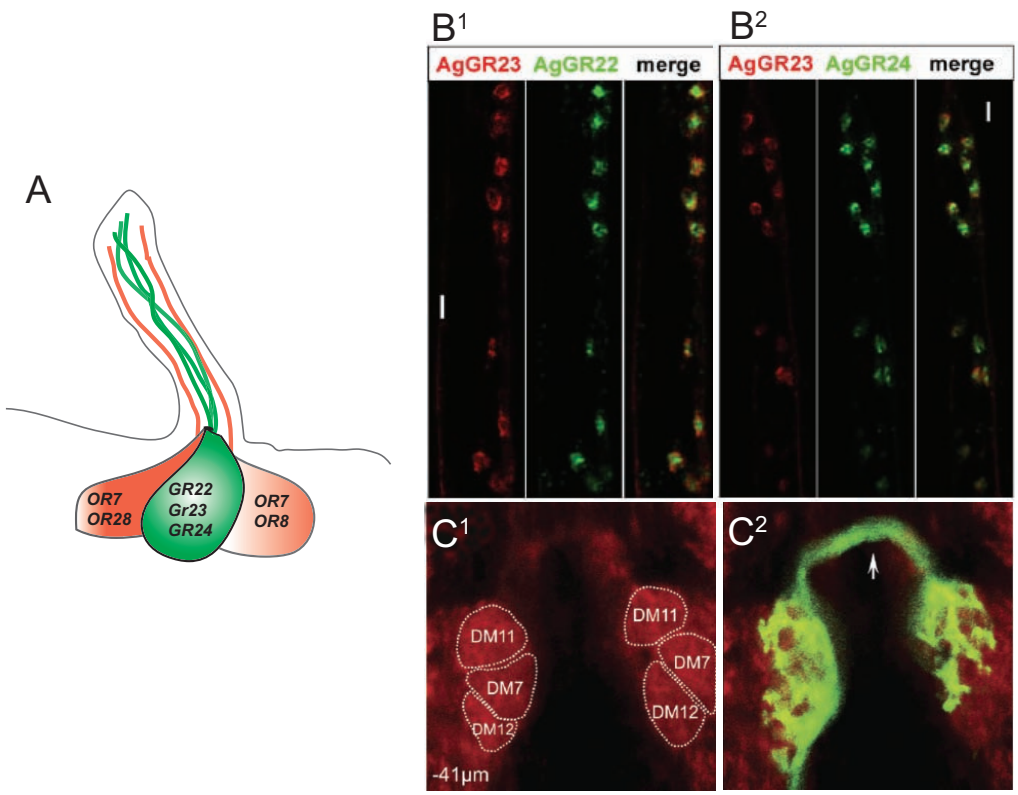

Figure 1.13: CO_2 detection in *Anopheles gambiae* A. Scheme of a capitate peg sensillum on the MP of *Anopheles gambiae*. The sensillum is innervated by three neurons, one expressing the receptors which mediate CO_2 detection, namely Gr22, Gr23 and Gr24 (Lu et al., 2007). **B^1 and B^2**. *In situ* for CO_2 receptors on the MP of *Anopheles gambiae* (Lu et al., 2007). **C**. Confocal image of the mosquito antennal lobe indicating the targeted glomeruli of capitate peg sensilla (Ghaninia et al., 2007).

(Bartel, 2004; He and Hannon, 2004; Meister and Tuschl, 2004). MicroRNAs detect their binding partners via their so-called seed region. The seed region stretches from nucleotide 2-7 and allows perfect pairing to the 3'UTR of the target mRNA (Bartel, 2009). The efficiency of these sites is characterized by two properties: the seed-pairing stability (SPS) and the target-site abundance (TA)(Garcia et al., 2011). Surprisingly, microRNAs with low proficiency and therefore few targets like the nematode *lys-6* and the mammalian *miR-23* share a low seed-pairing stability but a high target-site abundance. By reducing these two parameters the binding changes toward a random binding or "off-target" effect. As these two properties are only connected to the seed region, an influence of surrounding regions can be largely excluded (Garcia et al., 2011). MicroRNAs are integrated in a RNA-protein containing complex (RISC complex or miRNP)(Ambros, 2004; Bartel, 2004; Cullen, 2004; He and Hannon, 2004). Within

this complex, microRNAs attenuate the translation of the respective target mRNA. Three models exist which explain the mechanism after the mRNA is recognized by the microRNA. The common model is the inhibition of translation initiation: RNA binding proteins are thought to bind to the cap region of the mRNA and therefore compete with the translation initiation factors like eIF4E (Kiriakidou et al., 2007). In contrast to this model, two more possible explanations exist, which are both concentrating on post-initiation events. One model states a premature ribosome drop-off (Petersen et al., 2006) and in another study the degradation of the nascent protein chain was proposed (Nottrott et al., 2006). Understanding the mechanism of how mRNAs are degraded upon microRNA binding will help to refine experiments that aim to describe the effect of a suppression mediated by a microRNA within a certain cell type or tissue.

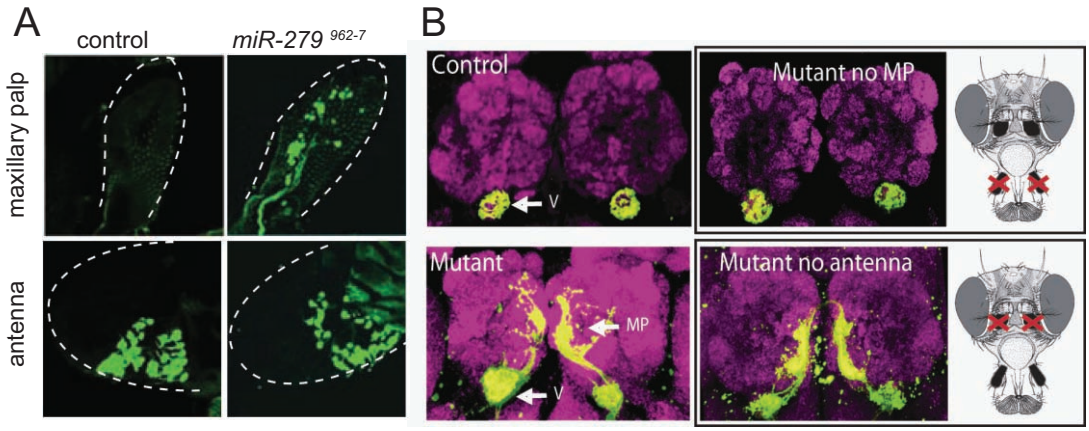

Figure 1.14: ***miR-279* controls CO_2 neuron development in *Drosophila melanogaster*** **A**. Antennae and maxillary palp expressing *Gr21a-Gal4* driving *UAS mcD8-GFP* (green) label CO_2 neurons on antennae in control flies. Flies carrying a mutation for *miR-279* $^{962-7}$ show ectopic CO_2 neurons on the maxillary palp. **B**. The CO_2 neuron reporter line labels the V-glomerulus in the antennal lobe of control flies, while *miR-279* $^{962-7}$ mutants show additional mistargeting to a medial glomerulus (Cayirlioglu et al., 2008).

MicroRNAs represent an evolutionary old strategy to regulate mRNA expression. In general, two different concepts try to understand the underlying mechanisms of evolutionary changes. First, changes in expression and function occur because of random, non-synonymous mutations within the coding regions of genes. Second, changes in protein output occur due to changes in the cis-regulatory regions of genes e.g. mutations in enhancer regions and in 3'UTRs. Hence, altering the possibility of microRNA binding could shift the expression patterns of their target mRNAs. The two models are not conflicting and examples for both mechanisms are found in the literature (Stern and Orgogozo, 2008). *Drosophila* and *Anopheles gambiae* diverged around 250

million years ago. Among many other species specific adaptations, flies and mosquitoes acquired a different behavior toward CO_2 which is accompanied by a relocation of the sensory neurons. A specific microRNA, *miR-279*, was found to play a role in the suppression of CO_2 neuron formation on the maxillary palp of *Drosophila*. Mutants of *miR-279* expressed ectopic CO_2 neurons on the maxillary palp that mistargeted to a medial glomerulus (Cayirlioglu et al., 2008) (Fig.1.14). The antennal CO_2 neurons were not affected in number and targeting. Interestingly, the location and the targeting pattern of the mutant CO_2 neurons highly resembled the CO_2 neurons found in mosquito (Fig.1.13). Based on this high similarity, it was hypothesized that *miR-279* acts as a molecular switch in the evolution of the chemosensory system of flies and mosquitoes (Cayirlioglu et al., 2008).

The transcription factor Nerfin-1 was identified as downstream target of *miR-279*. The ectopic CO_2 neurons on the MP were found to express elevated levels of Nerfin-1 (Fig.1.15). In S2 cells, the nerfin-1 3'UTR reporter was found to be directly targeted and repressed by *miR-279* (Cayirlioglu et al., 2008). The 1.6 kb long 3'UTR of Nerfin-1 contains 21 predicted binding sites for 18 different microRNAs (Kuzin et al., 2007), which puts Nerfin-1 under a tight post-transcriptional control. Out of the 21 sites, 6 sites are recognized by *miR-279* (Cayirlioglu et al., 2008).

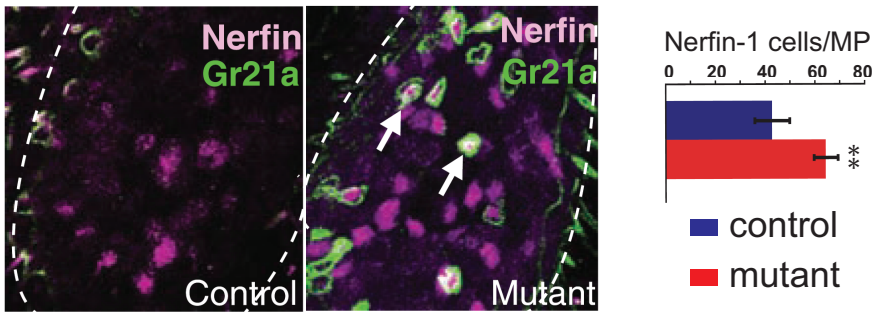

Figure 1.15: *mir-279* represses Nerfin-1. Control palps do not express CO_2 neurons on the MP but do have cells positive for Nerfin-1 (magenta). *mir-279* $^{962-7}$ mutant palps show ectopic CO_2 neurons (green) that overlap with α Nerfin-1 staining (magenta). Overall the number of Nerfin-1 positive cells is elevated on mutant MPs compared to control flies (see quantification).

Nerfin-1 together with Nerfin-2 was found in an *in situ* screen to affect nervous system development. Nerfin-1 mutant embryos exhibit altered axon guidance especially in commissural and connective axon fascicles in the embryonic CNS. In line with this phenotype, Nerfin-1 was shown to act upstream of axon guidance molecules like *robo*, *lar* and *futsch*. The expression of Nerfin-1 itself seems to be dependent on Prospero (Kuzin et al., 2005).

1.4 Aims of the Thesis

The following work continues the analysis of *miR-279* on the supression of CO_2 neuron development on the maxillary palp (MP) of *Drosophila melanogaster*. Based on the observation that a hypomorphic allele of Prospero, *pros*^{IG2227}, developed a highly similar phenotype as the microRNA, I studied whether Prospero is an upstream factor directly controlling the expression of *miR-279*. Generally, work on microRNAs focused on the identification of downstream targets. Although it is conceptually approved that transcription factors are controlling the activity of microRNAs (Hobert, 2008), only a few studies dealt with the identification of these factors (Bethke et al., 2009). I started with a detailed comparison of the mutant phenotype of *miR-279* and *pros*^{IG2227} in pupae and in adult flies. As a result, both mutants switch CO_2 sensing neurons into a mosquito-like fate by inducing the development of MP CO_2 neurons which perform mistargeting to a medial glomerulus. To establish the relationship of Prospero and *miR-279*, I undertook a series of *in vitro* and *in vivo* experiments which proved that Prospero is directly binding to the enhancer region of *miR-279*. Furthermore, I was interested to find factors that are involved in suppressing CO_2 neurons on the MP of *Drosophila melanogaster*. To this end, I tested predicted common targets of *miR-279* and Prospero. From the list of common targets, I focused on two neurogenic transcription factors, Escargot and Nerfin-1. Using S2 cell assays and *in vivo* analysis, I could show that both are repressed by *miR-279* and Prospero. Moreover, raising the level of Escargot and Nerfin-1 in the wildtype background led to the formation of ectopic CO_2 neurons on the maxillary palp. These results suggested that Escargot and Nerfin-1 are necessary and sufficient to suppress the formation of ectopic CO_2 neurons.

To summarize, the presented work describes the regulatory network suppressing CO_2 neuron development on the MP of *Drosophila*. The transcription factor Prospero employs in a coherent feed-forward loop *miR-279* to tightly control and repress the common targets Escargot and Nerfin-1. Elevated levels of both target genes were shown to be necessary and sufficient to induce formation of ectopic CO_2 neurons on the MP.

The results of the thesis are published in Hartl et al. (2011).

Chapter 2

Results

2.1 *miR-279* and Prospero Supress CO_2 Neurons on the Maxillary Palp

In a previous study a P-element insertion into the locus of *miR-279* resulted in the formation of ectopic CO_2 neurons on the maxillary palp, while wildtype CO_2 neurons were exclusively found on the antenna. Additionally to the gain of neurons, these extra cells mistargeted to a medial glomerulus in the antennal lobe (Cayirlioglu et al., 2008). The targeting of the ectopic neurons from the maxillary palp occurred via the labial nerve, whereas wildtype antennal CO_2 neurons targeted via the antennal nerve (see Fig.1.1). Hence, *miR-279* was shown to be essential for the suppression of CO_2 neuron formation on the *Drosophila* maxillary palp. Since the location and the targeting pattern of the ectopic CO_2 neurons resembled the arrangement of CO_2 neurons found in mosquito (Fig.1.13), the microRNA was hypothesized to act as a molecular switch in the evolution between flies and mosquitoes. In order to gain insight into the mechanisms regulating the microRNA, I analyzed a mutant allele of Prospero that showed a similar phenotype as the *miR-279* mutant. The new hypomorphic allele of Prospero, $pros^{IG2227}$, was found in a collection of lethal ethane methyl sulfonate (EMS) mutants. The point mutation resulted in a change of amino acid 850 from a Leucine into an Arginine in one of the Prox-1 domains (Fig.2.1). Similar to the *miR-279* mutant, the hypomorphic allele of Prospero was lethal in early stages of development. To analyze the phenotype in the olfactory system, I induced mutant clones using eyFLP combined with MARCM. Early in development, mutant clones in the eye and the olfactory organs were induced using eyFLP while the brain remained wildtype. The mutant cells expressing one of the receptors for CO_2, Gr21a, were labeled with

GFP. Using MARCM and cell lethal only the mutant cells expressing the respective Gal4 reporter were labeled. In our case, neurons expressing the CO_2 receptor reporter, Gr21a (*Gr21a-Gal4 UAS-mcD8 GFP*) were analyzed. In control flies, CO_2 neurons were restricted to the antenna and targeted the V-glomerulus via the antennal nerve. In the *pros*^{IG2227} mutant background, every maxillary palp analyzed developed ectopic CO_2 neurons (15±0.9). In comparison, on MPs of *miR-279* $^{962-7}$ mutants around 16±0.6 ectopic CO_2 neurons were expressed. Similar to *miR-279* $^{962-7}$ also Prospero mutant palps targeted a medial glomerulus in the antennal lobe via the labial nerve (Fig.2.2 A,B). In contrast, the number and targeting of CO_2 neurons on the antennae was not affected by any of the analyzed mutations. Exposing organisms to EMS can

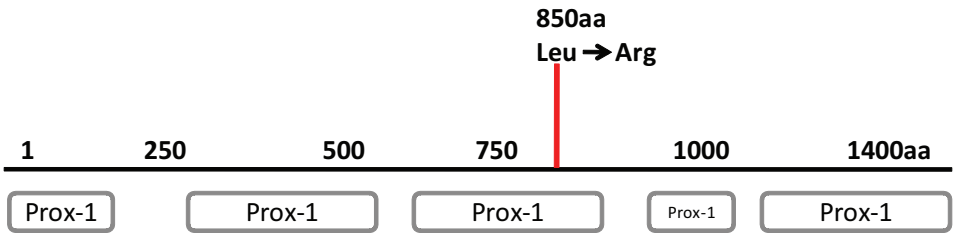

Figure 2.1: The point mutation in the hypomorphic Prospero allele, *pros*^{IG2227}. A sketch of the EMS induced point mutation into the Prospero locus indicating the length of the protein and the relative position of the five Prox-1 domains. The EMS point mutation causes a change of amino acid 850 from a Leucin into an Arginin.

lead to a variety of mutagenic effects such as deletions or point mutations which are due to the transition in methylation of guanidin residues. In addition, the DNA defects occur randomly throughout the genome. To test whether the EMS generated mutant was really specific for Prospero, I analyzed two more mutant alleles of Prospero for the presence of ectopic CO_2 neurons on the maxillary palp and the mistargeting to the medial glomerulus. One of the mutant alleles was a null mutant of Prospero, *pros*^{17} (Manning and Doe, 1999), while the other one was a hypomorphic allele *pros*^{voila78} (Grosjean et al., 2001). The *voila* allele resulted from a P-element insertion into the enhancer region of Prospero followed by an imprecise excision (Grosjean et al., 2001). During sensillum formation, *pros*^{17} caused a partial conversion of the neuronal to the non-neuronal lineage (Manning and Doe, 1999) (see Introduction). In line with these previous results, I saw that the overall CO_2 neuron number on the antenna in the *pros*^{17} mutant background was reduced to 51.5% (19.4 ± 4 to 10 ± 1.3 cells) (Fig.2.2 F). Nevertheless, the mutant brains exhibited the mistargeting phenotype in the antennal lobe due to ectopic CO_2 neuron formation in the maxillary palp. But as the number of neurons was overall reduced in the *pros*^{17} background, the axon bundles from both antennal and labial nerve

were thinner (Fig.2.2 D^3). Therefore, also the number of ectopic CO_2 neurons was reduced in *pros*^{17} mutant palps (Fig.2.2 F). *pros*^{voila78} mutant flies showed a similar phenotype as compared to *pros*^{IG2227}, both, in number and expression of ectopic neurons on the MP (Fig.2.2 F).

To test whether the mutations of *miR-279* and Prospero also affected the targeting of other olfactory receptors (OR) a set of different OR markers (*OrX-Gal4-UASmcD8GFP*) was tested. Among all olfactory receptors analyzed, only the targeting of two additional classes, Or42a and Or59c, was affected by the mutations (Fig.2.3, Fig.2.4 A-E).

Wildtype Or42a and Or59c neurons are expressed in sensilla on the maxillary palp and target the medial glomerulus via the labial nerve (Fig.1.1). In both, *miR-279* $^{962-7}$, *pros*^{IG2227}, *pros*^{17} and *pros*^{voila78} mutants, neurons expressing these receptor classes mistargeted the V-glomerulus (Fig.2.4 B,C,D,E). Using *in situs*, I observed a co-expression of Or42a or Or59c receptor with the ectopic Gr21a receptors (Fig.2.4 F). Hence, the mutant hybrid sensilla expressed additional neurons that co-express Gr21a with either Or42a or Or59c receptors. And although the wildtype Or42a and Or59c receptors were found on the MP and targeted according to their wildtype innervation pattern, the set that was co-expressed in the hybrid sensilla performed a mistargeting to the V-glomerulus.

The antennae and MPs in *pros*^{17} mutants exhibited additionally an overall neuron loss for all OR marker tested (Fig.2.3 B). Hence, complete loss of Prospero during sensilla development resulted in two phenotypes, a more general defect leading to an overall neuron loss and a more specific phenotype highly similar to the one observed for *pros*^{IG2227} and *miR-279* $^{962-7}$ mutants. The general effect was in line with previous reports on other sensilla types e.g., bristles on the thorax of the fly (Manning and Doe, 1999).

Figure 2.2 *(following page)*: *mir-279* and Prospero affect location and targeting of CO_2 neurons. Mutations in *pros*^{IG2227} (B1) and *miR-279* $^{962-7}$ (C1) cause the formation of ectopic CO_2 neurons on the maxillary palp. These ectopic CO_2 neurons mistarget to a medial glomerulus in the antennal lobe (B3,B3,C3,C4) while wildtype neurons innervate the V-glomerulus (A3,A4). Also, a loss-of-function mutant of Prospero *pros*^{17} develops ectopic CO_2 neurons that perform medial mistargeting (D1-D4), although the overall neuron number is reduced on both antennae and maxillary palps (F). This neuron loss effects also the thickness of the axon bundle as it appears thinner (D3). Another hypomorphic Prospero allele, *pros*^{voila78}, resulted in a comparable phenotype as *pros*^{IG2227}(E1-E4). **F**. Quantification of Gr21a positive cells on control and mutant MPs and antennae.

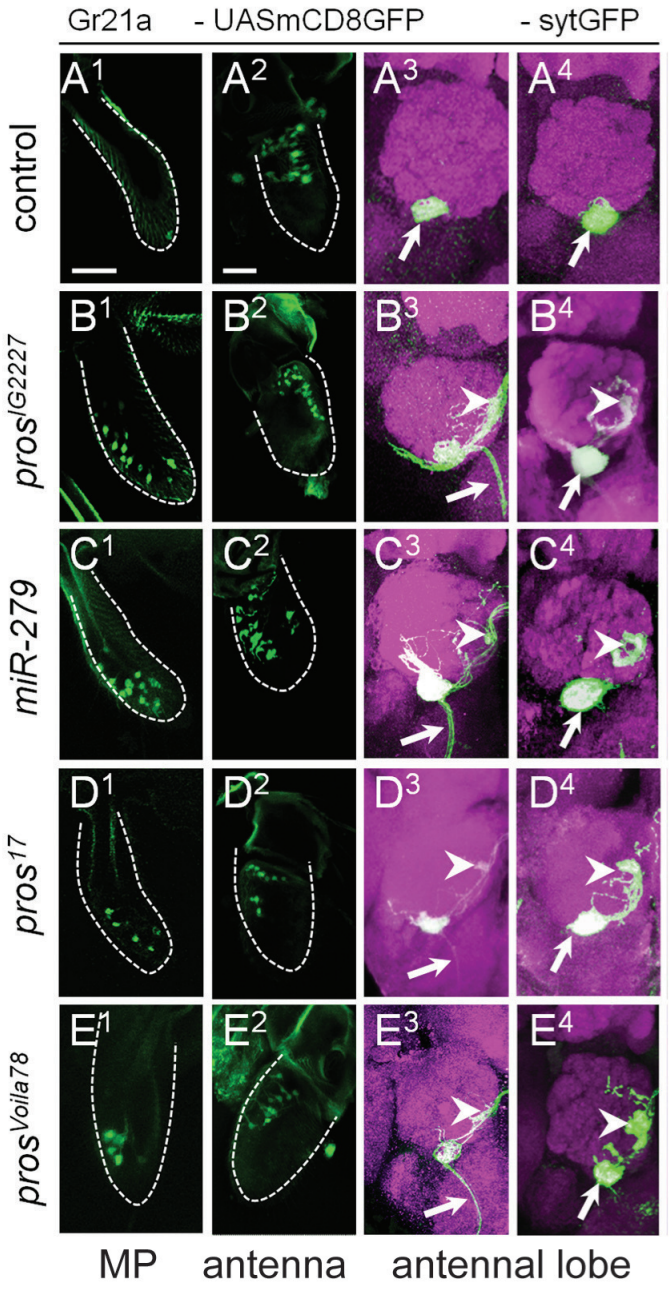
Gr21a
- UASmCD8GFP
- sytGFP
control
prosIG2227
miR-279
pros17
prosVoila78
A1
A2
A3
A4
B1
B2
B3
B4
C1
C2
C3
C4
D1
D2
D3
D4
E1
E2
E3
E4
MP
antenna
antennal lobe

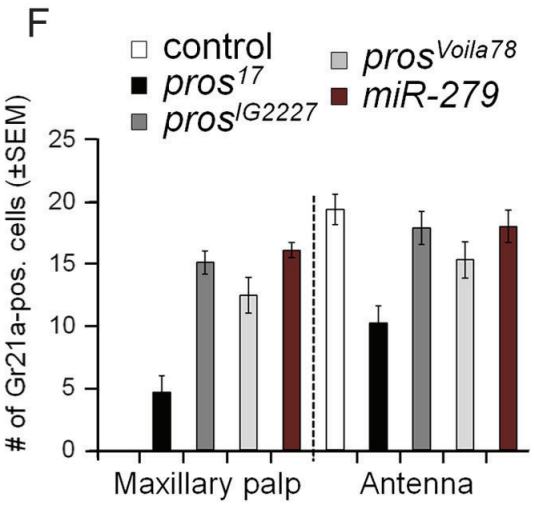
F
control
pros17
prosIG2227
prosVoila78
miR-279
# of Gr21a-pos. cells (±SEM)
25
20
15
10
5
0
Maxillary palp
Antenna

To address whether the ectopic neurons were also functionally responding to CO_2, single sensillum recordings (SSR) were performed by Dr.Siju Purayil, a postdoctoral fellow in the laboratory. To this end, recordings from mutant sensilla on the MP were performed while stimulating the neurons with CO_2 as ligand for Gr21a receptors (Jones et al., 2007; Kwon et al., 2007). Since the ectopic neurons co-expressed the receptors for Or42a and Or59c, the ligands, isoamyl-acetate and 3-octanol (de Bruyne et al., 1999) were tested to show whether these receptors were functionally in the hybrid sensilla. Unlike wildtype sensilla, hybrid sensilla of *miR-279* $^{962-7}$ and *pros*^{IG2227} mutants responded to CO_2 with a comparable spike number (Fig.2.5 A,B). Moreover, the same mutant sensilla which were sensitive to CO_2 additionally responded to the ligands of Or42a and Or59c (Fig.2.5 C). In line with the anatomical results of the mutant lines, the ectopic CO_2 neurons that either co-expressed Or42a or Or59c in basiconic sensilla on the MP also responded to ligands of the respective receptors.

Taken together, mutant palps of *miR-279* and Prospero failed to suppress the formation of CO_2 neurons and developed a similar amount of ectopic CO_2 neurons which mistargeted via the labial nerve to a medial glomerulus in the antennal lobe. Additionally, both mutations led to mistargeting of two more olfactory receptors, Or42a and Or59c. In the mutant background, the two receptor classes mistargeted the V-glomerulus, while wildtype Or42a and Or59c expressing neurons innervate a medial glomerulus. *In situs* for the receptors showed that the ectopic MP CO_2 neurons co-expressed either Or42a or Or59c. In single sensillum recordings, the ectopic CO_2 neurons of both mutants were responding to CO_2 as well as to the key ligands of Or42a and Or59c. Therefore, the mutant allele of *miR-279* and the hypomorphic Prospero allele, *pros*^{IG2227}, exhibited an anatomically and physiologically highly similar phenotype.

Figure 2.3 *(following page)*: Most OR marker are unaffected by *miR-279* $^{962-7}$ and *pros*^{IG2227} A. A set of antennal and maxillary palp OR marker in the mutant background of *miR-279* $^{962-7}$, *pros*^{IG2227} and *pros*^{17} show no phenotype. **B**. Quantification of Or83b positive neurons on MP in control, *pros*^{IG2227} and *pros*^{17} flies.

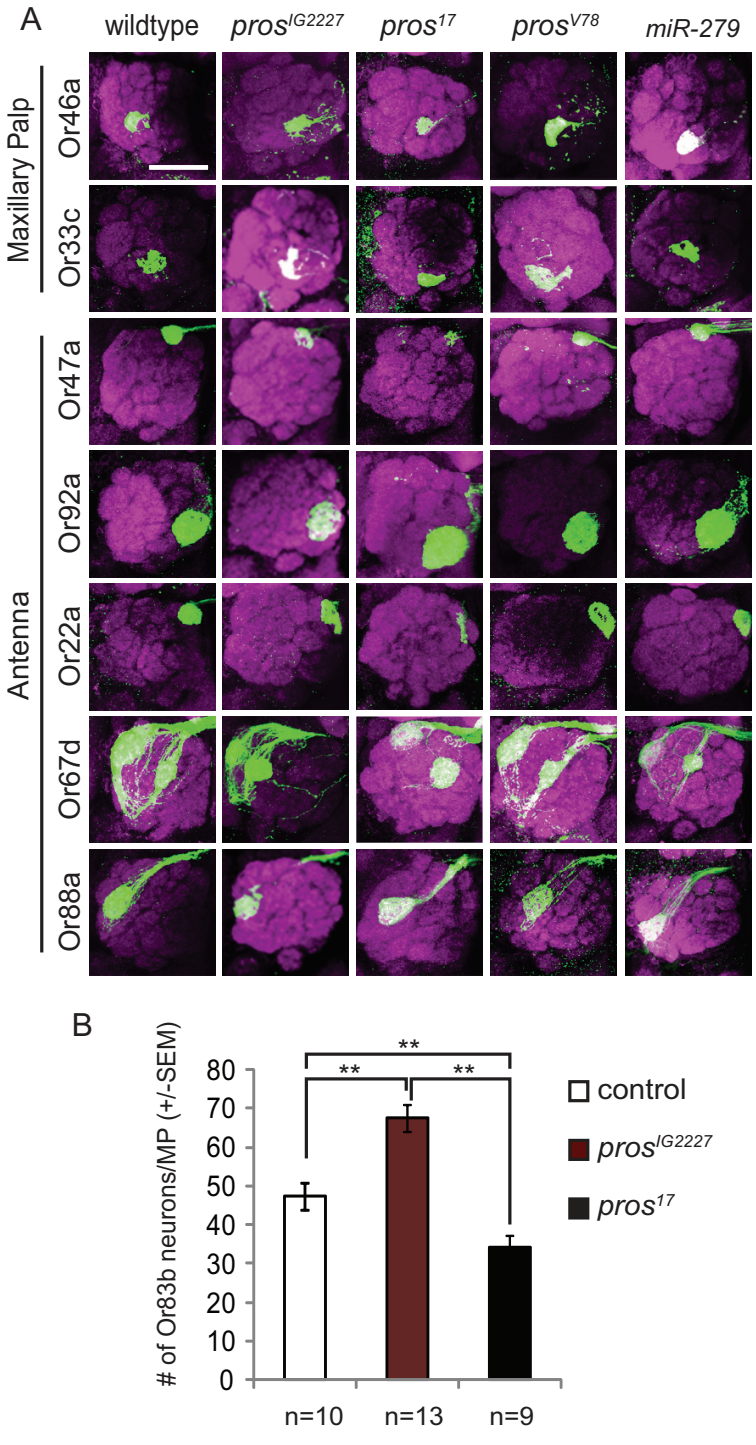
A
wildtype
pros^IG2227
pros^17
pros^V78
miR-279
Maxillary Palp
Or46a
Or33c
Antenna
Or47a
Or92a
Or22a
Or67d
Or88a
B
# of Or83b neurons/MP (+/-SEM)
80
70
60
50
40
30
20
10
0
**
**
**
control
pros^IG2227
pros^17
n=10
n=13
n=9

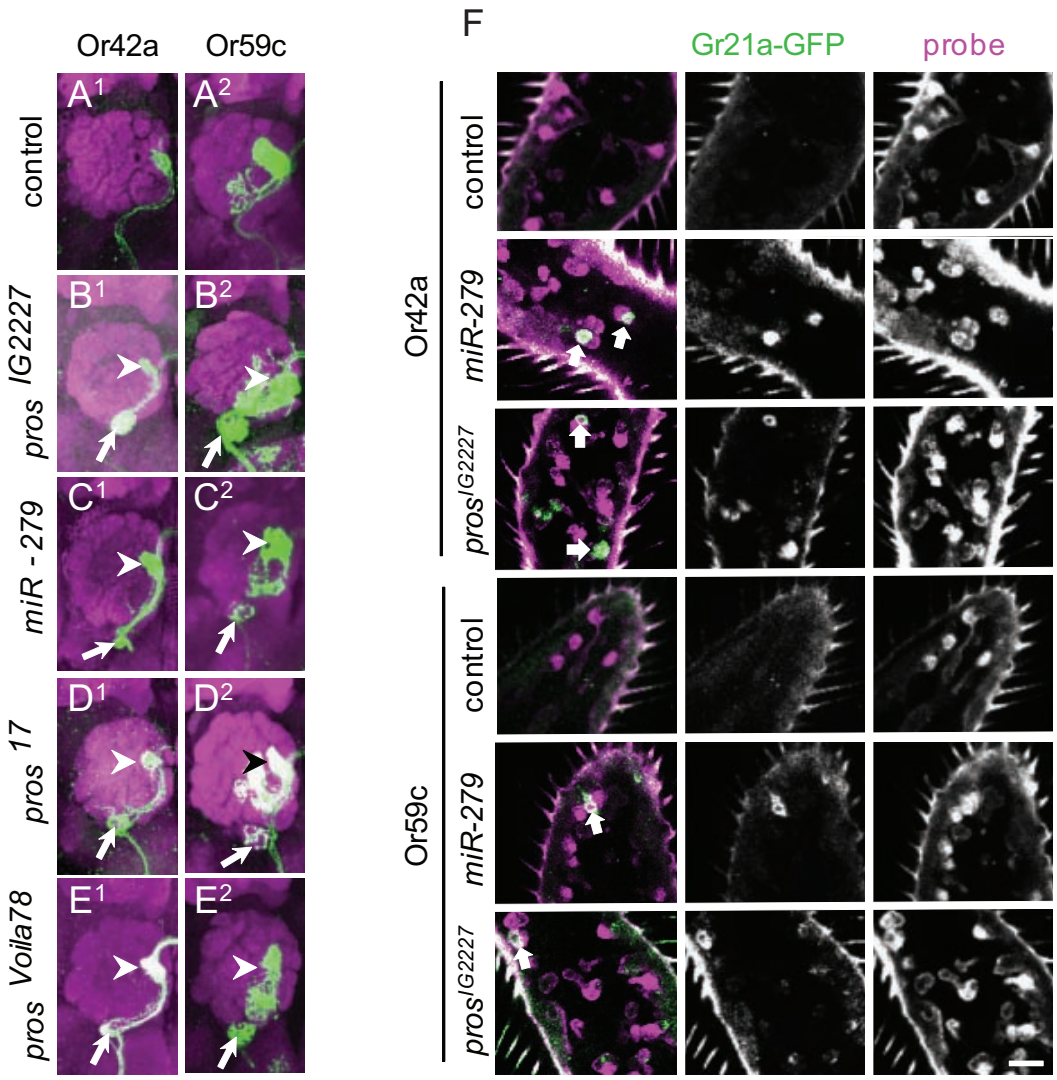

Figure 2.4: Or42a and Or59c are co-expressed with ectopic CO_2 neurons and mistarget to the V-glomerulus **A-E**. Or42a and Or59c targeting is altered in the *miR-279* and various Prospero mutant background. Additionally to the medial food-associated glomerulus (arrowhead), the V-glomerulus is innervated (arrow). **F**. *In situs* on mutant maxillary palps show that ectopic Gr21a positive neurons co-express the receptors Or42a and Or59c. The third ectopic neuron is integrated in the basiconic sensilla structures.

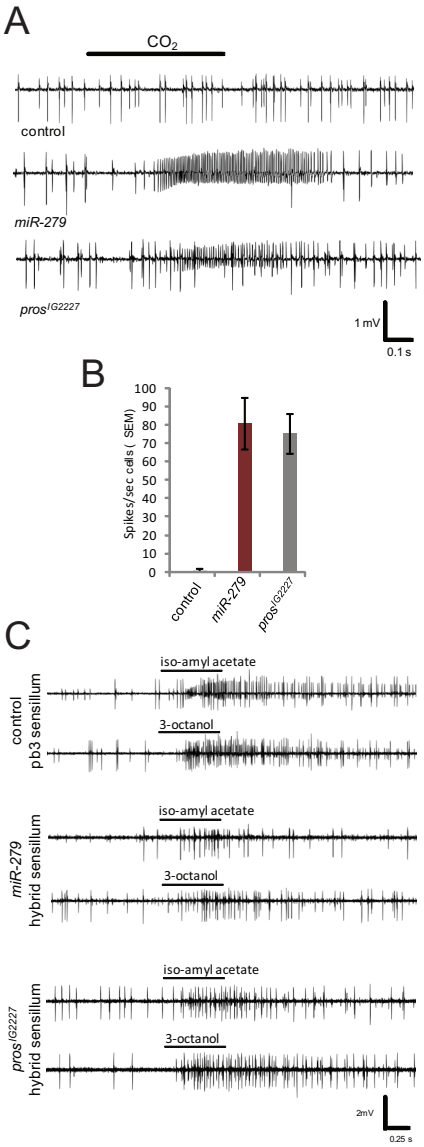

Figure 2.5: Ectopic CO_2 neurons functionally respond to CO_2, isoamylacetate and 3-octanol. Single sensillum recordings (SSR) of wildtype and mutant sensilla. **A**. Stimulation with CO_2 triggered no response in wildtype palps. In contrast, mutant palps of *miR-279* $^{962-7}$ and *pros*^{IG2227} were responding to CO_2. **B**. Both mutants respond with a comparable spike number to the given stimulus. **C.** Also the ligands of Or42a (isoamylacetate) and Or59c (3-octanol) trigger activity in the mutant sensilla.

2.2 *miR-279* and Prospero Expression Throughout MP Development

The similarity of the *miR-279* $^{962-7}$ and *pros*^{IG2227} phenotypes suggested that both molecules act in the same pathway to suppress CO_2 neuron formation on wildtype maxillary palps. As a prerequisite, I tested in collaboration with Dr. Laura Loschek whether both molecules are co-expressed in relevant developmental stages. The olfactory appendages, antennae and maxillary palp, develop throughout the pupal stage. The maxillary palp develops from the antennal part of the eye-antennal disc (Lebreton et al., 2008). The olfactory lineage starts to develop from a

sensory organ precursor (SOP) cell. The SOP gives rise to the precursors of the non-neuronal lineage (pIIa) and the neuronal lineage (pIIb). The marker for the neuronal lineage is Elav.

In the developing maxillary palp, Elav was already expressed at 6 hrs APF. At this timepoint, only a few cells expressed Prospero (Fig.2.6 A,A^{1,2}). At 25 hrs APF, two populations of cells expressed Prospero in a low and a high intensity. At this stage various combinations of Prospero and Elav positive cells were found. Next to cells that either expressed Elav or Prospero, other cells were found that expressed high levels of Prospero and low levels of Elav, and vice versa (Fig.2.6 B, B^{1,2}). At 45 hrs APF, the sensilla were fully differentiated with two cells expressing the neuronal marker Elav as a marker for mature neurons and a third cell positive for Prospero labeling the sheath cell (Fig.2.6 C, C^{1,2}). These findings were consistent with previous published data on sensillum development (Doe et al., 1991). Therefore, I concluded that the maxillary palp develops according to the canonical pathway of sensillum formation.

To assess the expression of *miR-279* during MP development a 2kb-enhancer fragment of *miR-279* fused to Gal4 was used which drove the expression of GFP. In a previous study, this enhancer fragment was sufficient to rescue the *miR-279* $^{962-7}$ phenotype (Cayirlioglu et al., 2008). The expression of *miR-279* started similar to Prospero and Elav at 6 hrs APF (Fig.2.6 D, D$^{1-5}$). At 30 hrs APF, *miR-279* was highly expressed in the future MP and again overlapped with Prospero (Fig.2.6 E, E^{1,2}). At 42 hrs APF, the broad expression of *miR-279* was largely reduced to only a few cells that still overlapped with Prospero expression but both were no longer co-expressed with Elav (Fig.2.6 F, F^{1,2}, G, G^{1,2}). At 70 hrs APF, Prospero and *miR-279* were still co-expressed in sheath cells of the MP (Fig.2.6 H, H^{1,2}).

Thus, *miR-279* and Prospero were co-expressed in the neuronal lineage during sensilla development on the maxillary palp. The expression of Prospero started early in pIIB, while the onset of *miR-279* was slightly delayed and started in late pIIb or early pIIIb. In the fully differentiated sensilla, *miR-279* and Prospero were excluded from neurons and confined to the sheath cells.

2.3 The Development of Mutant Sensilla on the Maxillary Palp

2.3.1 Extra Neurons Develop within Basiconic Sensilla in the Maxillary Palp

The extra neurons formed on the maxillary palp of *miR-279* $^{962-7}$ and *pros*^{IG2227} mutants could develop either within an extra sensillum containing only one single neuron or the extra neuron was integrated within the basiconic sensilla. To test which possibility accounted for the analyzed mutants, *Elav-Gal4* and MARCM in wildtype and mutant flies was used to selectively label the neuronal lineage. In collaboration with Dr. Laura Loschek, palps were dissected at 45 hrs APF. At this stage, it was not possible to use the specific driver for CO_2 neurons, since the onset of *Gr21a-Gal4* was later than the analyzed timepoint. In wildtype palps, I only saw basiconic sensilla carrying two neurons positive for *Elav-Gal4* and α-Elav staining. Next to the neurons a single cell, the sheath cell, was positively labeled with α-Prospero. Interestingly, mutant sensilla of *miR-279* $^{962-7}$ and *pros*^{IG2227} contained three cells positive for *Elav-Gal4* and Elav protein. Attached to the three neuron cluster, the sheath cell could be identified through positive staining for Prospero. The mutant *pros*^{IG2227} palps exhibited the same phenotype, however, with a lower expression of Prospero in the sheath due to hypomorphic mutation. Hence, the mutation in *miR-279* $^{962-7}$ or *pros*^{IG2227} induced a phenotype with tree instead of two neurons in the basiconic sensilla.

In adult sensilla, the CO_2 neuron specific driver *Gr21a-Gal4* could be used to label the neurons. In the *miR-279* $^{962-7}$ and *pros*^{IG2227}, sensilla carried three neurons positive for *Elav-Gal4* and α-Elav staining and one was positive for *Gr21a-Gal4*.

Figure 2.6 *(following page)*: Expression of Prospero and *miR-279* throughout the development of the maxillary palp. **A.** Prospero starts to be expressed at 6 hrs APF in the primordium of the maxillary palp and overlaps with Elav (A, A^1 and A^2). **B.** At 25 hrs APF, Prospero is more largely expressed and partially overlaps with Elav (B, B^1 and B^2). **C.** At 45 hrs APF, Prospero labels the sheath cell in the differentiated sensillum and is excluded from neurons that are positive for Elav (C, C^1 and C^2). **D.** *miR-279* starts to be expressed at low levels at 6 hrs APF and is overlapping with Prospero (D,D^1 and D^2) as well as with Elav (D^3-D^5). **E.** At 30 hrs APF, the expression of *miR-279* is increased and does also partially overlap with Prospero. **F.** At 42 hrs APF, levels of *miR-279* are again reduced, but still overlap with α Prospero staining. **G.** At 42 hrs APF, *miR-279* is no longer co-expressed in α Elav positive cells (G, G^2). **H.** Also in the mature palp at 72hrs APF, Prospero positive cells co-express *miR-279*.

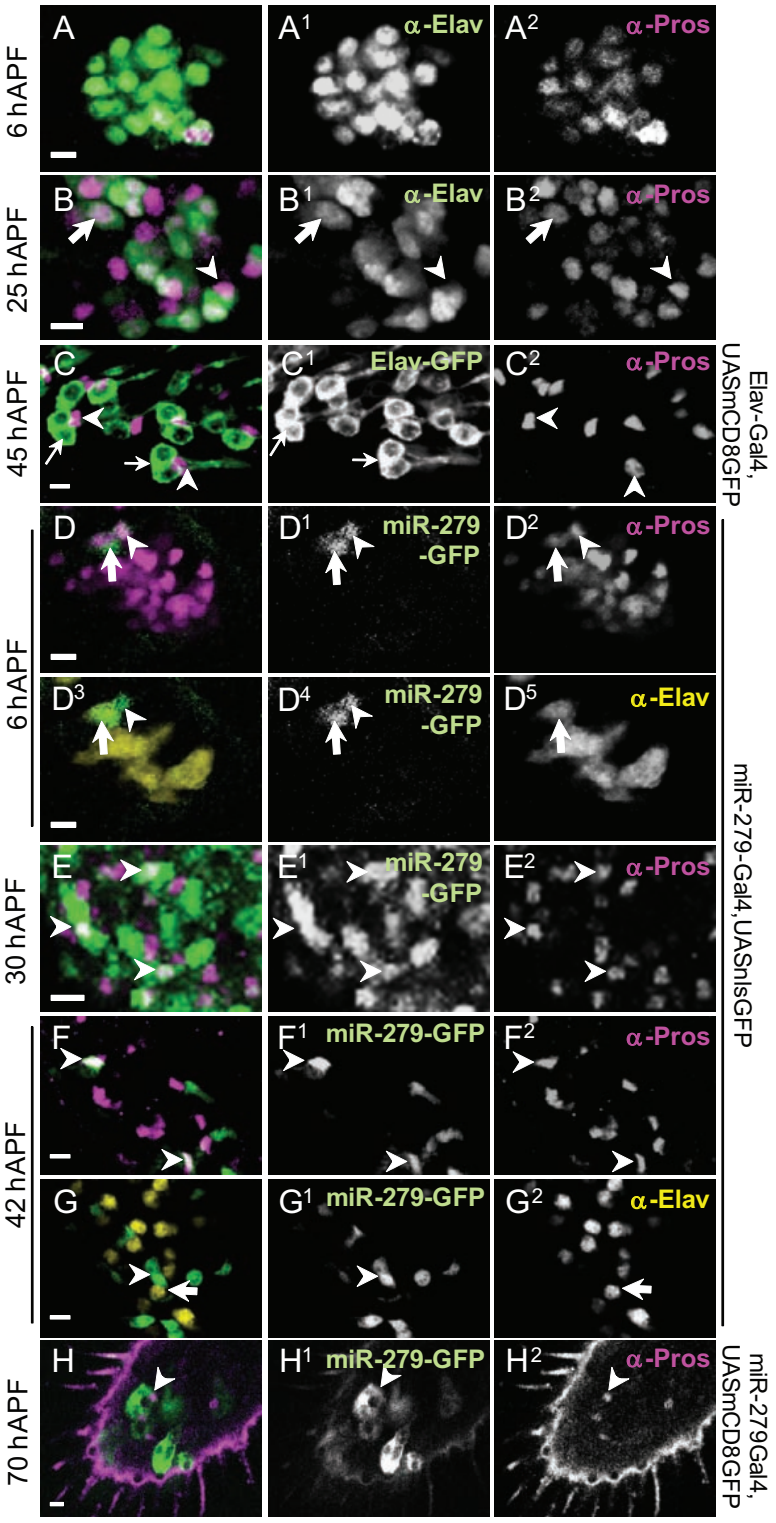
6 hAPF
25 hAPF
45 hAPF
6 hAPF
30 hAPF
42 hAPF
70 hAPF
A
A1 α-Elav
A2 α-Pros
B
B1 α-Elav
B2 α-Pros
C
C1 Elav-GFP
C2 α-Pros
D
D1 miR-279 -GFP
D2 α-Pros
D3
D4 miR-279 -GFP
D5 α-Elav
E
E1 miR-279 -GFP
E2 α-Pros
F
F1 miR-279-GFP
F2 α-Pros
G
G1 miR-279-GFP
G2 α-Elav
H
H1 miR-279-GFP
H2 α-Pros
Elav-Gal4, UASmCD8GFP
miR-279-Gal4,UASnlsGFP
miR-279Gal4, UASmCD8GFP

In addition, maxillary palps of *pros*^{17} mutants were analyzed. Besides the sensilla with three neurons (in 54% of analyzed palps), two more types of altered sensilla were present: sensilla with only one neuron (31% of palps analyzed) and sensilla containing four *Elav-Gal4* positive cells but none expressing Elav protein (15.5%). Probably, these sensilla failed to fully differentiated due to the complete loss of Prospero in the *pros*^{17} background. In line with previous reports in other sensilla lineages (Manning and Doe, 1999), both effects are likely due to a conversion of the neuronal (pIIb) to the non-neuronal (pIIa) lineage. Therefore, also during sensilla development of maxillary palps, Prospero functioned to distinguish the neuronal versus the non-neuronal lineage as a full loss of Prospero resulted partially in undifferentiated neurons. Moreover, the hypomorphic allele of Prospero, *pros*^{IG2227}, uncovered a second, later role of Prospero within the pIIb lineage of the maxillary palp sensilla. Here, Prospero restricted neuron number within one sensillum and thereby suppressed specifically the formation of ectopic CO_2 neurons on the MP. In contrast, the number and the development of sheath cells was not affected.

Taken together, Prospero and *miR-279* accounted for neuron number per sensillum as the mutant sensilla on the maxillary palp expressed three instead of two neurons in the pupal stage. In adult palps, ectopic CO_2 receptor neurons developed within sensilla containing three neurons. Unlike the hypomorphic allele, a complete loss of Prospero in *pros*^{17} showed additional phenotypes as, for instance, the lack of neuronal differentiation and conversion of the pIIb in the pIIa lineage.

2.3.2 The Development of CO_2 Neurons is not Induced by Late Cell Division

To test whether additional neurons occurred because of an extra cell division post-differentiation, I labeled new born neurons at different time points of MP development with *Elav-Gal4*. Previous experiments suggested that the development of the olfactory sensilla was completed at around 30 hrs APF. Therefore, I chose different time points before and after 30 hrs APF and induced via heatshock the expression of *ElavGal4-UASmcD8GFP* (*Elav:GFP*) which labeled all neurons and

Figure 2.7 *(following page)*: *miR-279* and Prospero mutant sensilla on the maxillary palp. A. At 45hrs APF, wildtype MPs only carry basiconic sensilla, with two neurons positive for αElav. **B-D.** Mutant sensilla of *miR-279* $^{962-7}$, *pros*^{IG2227} and *pros*^{17} have an extra neurons and carry sensilla with three neurons on their MPs. **E.** On adult maxillary palps, in the *miR-279* mutant background, three neurons are formed in the sensilla with one being positive for the CO_2 neuron marker (*Gr21a Gal4 UASmcD8GFP*). **F.** In the *pros*^{IG2227} mutant background, sensilla that carry the ectopic CO_2 neuron, express three neurons.

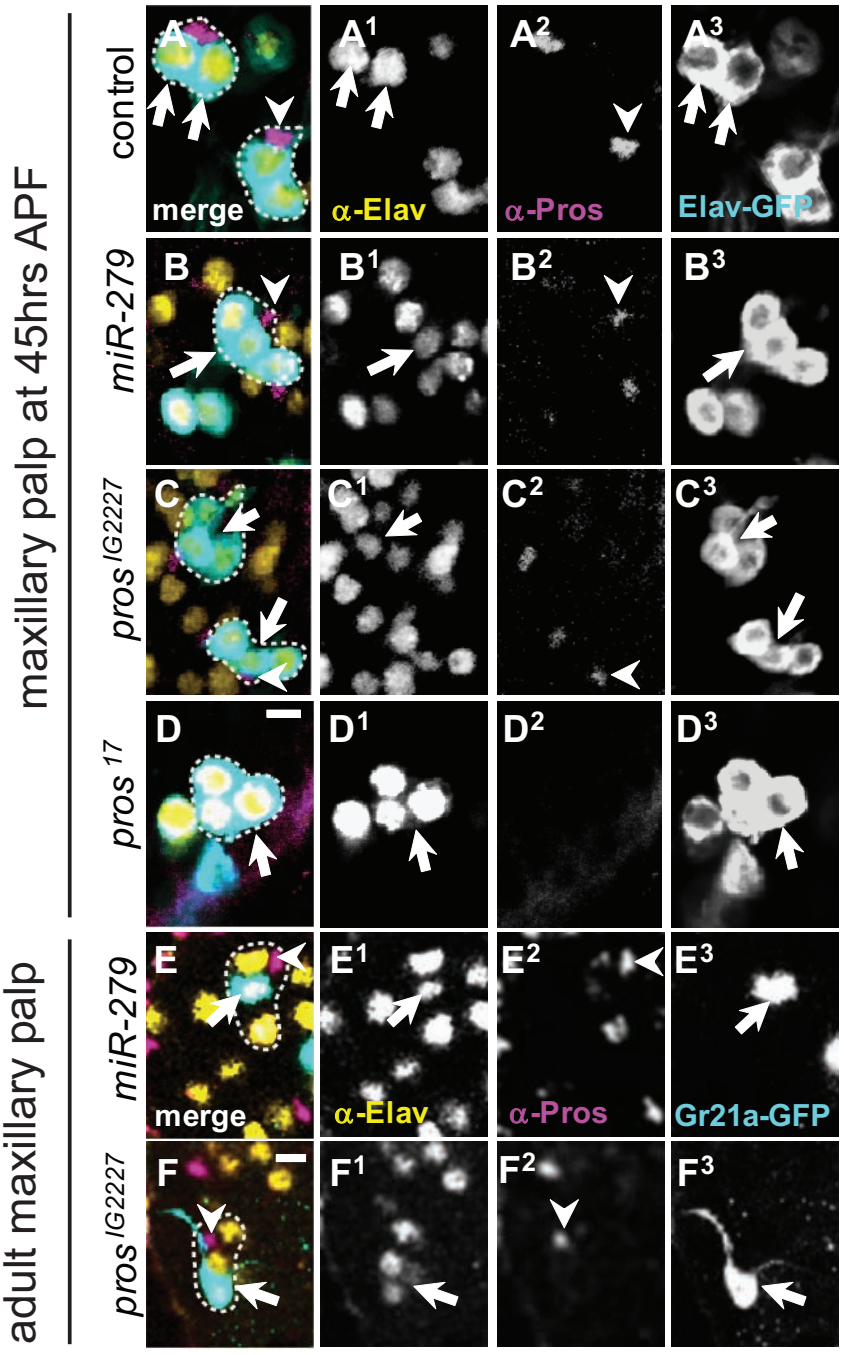
maxillary palp at 45hrs APF
adult maxillary palp
control
miR-279
pros IG2227
pros 17
miR-279
pros IG2227
A
A1
A2
A3
merge
α-Elav
α-Pros
Elav-GFP
B
B1
B2
B3
C
C1
C2
C3
D
D1
D2
D3
E
E1
E2
E3
merge
α-Elav
α-Pros
Gr21a-GFP
F
F1
F2
F3

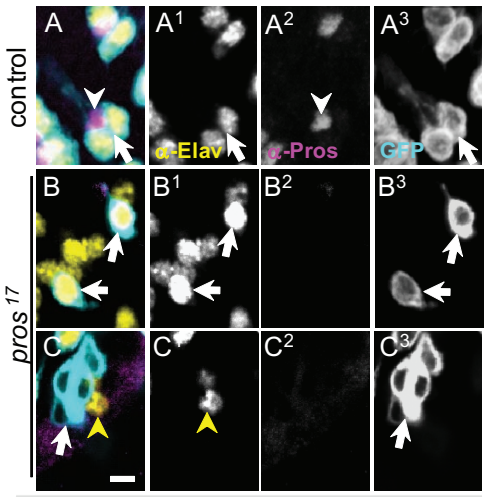

D

	Phenotype in maxillary palp		
	ectopic neuron	pIIb to pIIa conversion	
genotype	3-neuron sensillum	1-neuron sensillum	undiff. neuron
WT	0 %	0 %	0 %
pros^{IG2227}	100 %	10 %	0 %
miR-279	100 %	4 %	0 %
pros^{17}	54 %	31 %	15.5 %

Figure 2.8: Additional phenotypes in *pros*^{17} mutants. A. At 45 hrs APF control sensilla on the maxillary palp form two neurons. **B-C.** In the *pros*^{17} background, sensilla with only one neuron positive for Elav protein (B, B1, B2, B3) were observed. A second phenotype was observed, where sensilla formed 4 cells positive for *Elav-Gal4* but not for Elav protein (C, C1, C2, C3). **D.** Quantification of phenotypes on the maxillary palps in the mutant background.

the projections that were formed after the heatshock. I compared *Elav:GFP* labeled neurons on adult maxillary palps of all analyzed Prospero mutant alleles and the *miR-279* mutant with wildtype palps which were treated in the same conditions. In summary, all flies of any mutant background and wildtype had *Elav:GFP* positive cells on the MP before 25hrs APF. Any heatshock applied after this timepoint did not result in Elav positive cells on the maxillary palp. Hence, all analyzed mutants were not delayed in sensilla development as the neurons did not form after 30hrs APF. Moreover, the development of extra neurons did not occur due to an additional late cell division in mutant sensilla as compared to wildtype.

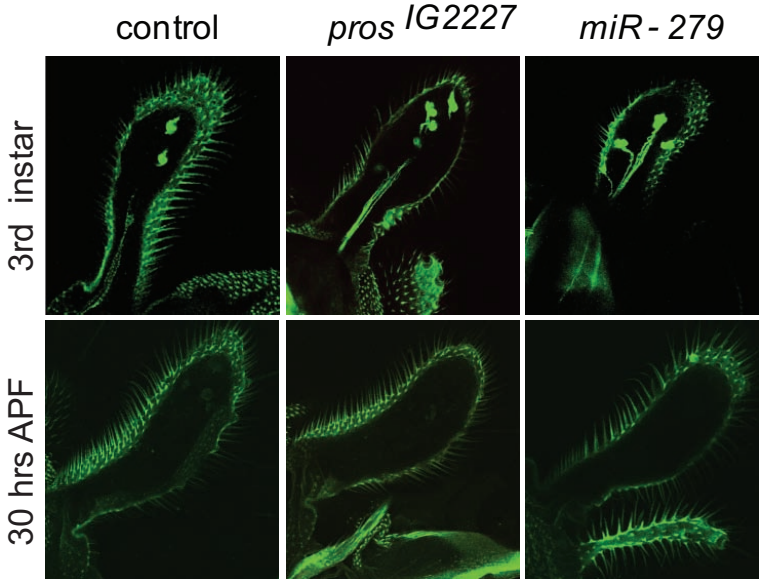

Figure 2.9: Ectopic CO_2 neurons do not form after 30 hrs APF. Adult maxillary palps that underwent heatshock at 3rd instar and at 30 hrs APF. *Elav-Gal4* is only expressed before 30 hrs APF. Mutant palp development is not delayed and extra neurons do not occur because of extra cell divisions after 30 hrs APF.

2.3.3 Mutant Sensilla are not Formed Upon Lack of Cell Death or Altered Cell Cycle Activity

Next, I tested whether extra neurons are formed due to a lack of apoptosis or because of a general failure in cell cycle. I chose the apoptosis inhibitor p35 and the cell cycle protein CyclinE and overexpressed both in wildtype flies. A previous study showed that CyclinE is a downstream target of Prospero (Choksi et al., 2006). For overexpression in mutant clones, I used a direct fusion of *Gr21-sytGFP* recombined to β-*actin-Gal4* and induced eyeless Flp (eyFLP) clones (see methods). β-*actin-Gal4* was only active in eyFLP induced clones. The entire population of CO_2 neurons were labeled with *Gr21a-sytGFP*. The antennal lobes of these flies were analyzed for the presence or absence of a *miR279* $^{962-7}$-like mistargeting phenotype. None of the analyzed flies developed extra CO_2 neurons on the MP which mistargeted to the medial glomerulus. The finding that changes in general cell cycle and apoptosis factors were not sufficient to induce ectopic neurons suggested that more specific (e.g. neurogenic) factors might be required to induce the formation of ectopic CO_2 neurons. Moreover, CyclinE as a downstream target of Prospero was not sufficient to induce the expression of extra CO_2 neurons on the maxillary palp and might not directly be involved in the pathway to suppress CO_2 neurons.

2.4 The Molecular Interaction of Prospero and *miR-279*

2.4.1 Overexpression of *miR-279* Rescues the *pros*^{IG2227} Phenotype

As both *miR-279* and Prospero were co-expressed in the neuronal lineage of MP development, I tested whether Prospero activity was necessary for the expression of *miR-279*. To this end, I performed a rescue experiment, where Prospero or *miR-279* were overexpressed in the mutant background. The overexpression constructs contained the cDNA of the respective gene fused to a UAS transcriptional response element. To express either *miR-279* or a full length version of Prospero, I used a flystock that contained a *Gr21a-synaptotagmin-GFP* direct fusion recombined to β-*actin-Gal4*. As a result, overexpression of *miR-279* completely rescued the *miR-279* $^{962-7}$ mutant phenotype. Similarly, the *pros*^{IG2227} mutant phenotype could be completely rescued by expressing a full length version of Prospero. Surprisingly, also expression of *miR-279* in the *pros*^{IG2227} mutant background led to a rescue of 80%. Contrarily, when Prospero was expressed in the *miR-279* $^{962-7}$ mutant background, only a partial rescue of 37% was detected (Fig. 2.10).

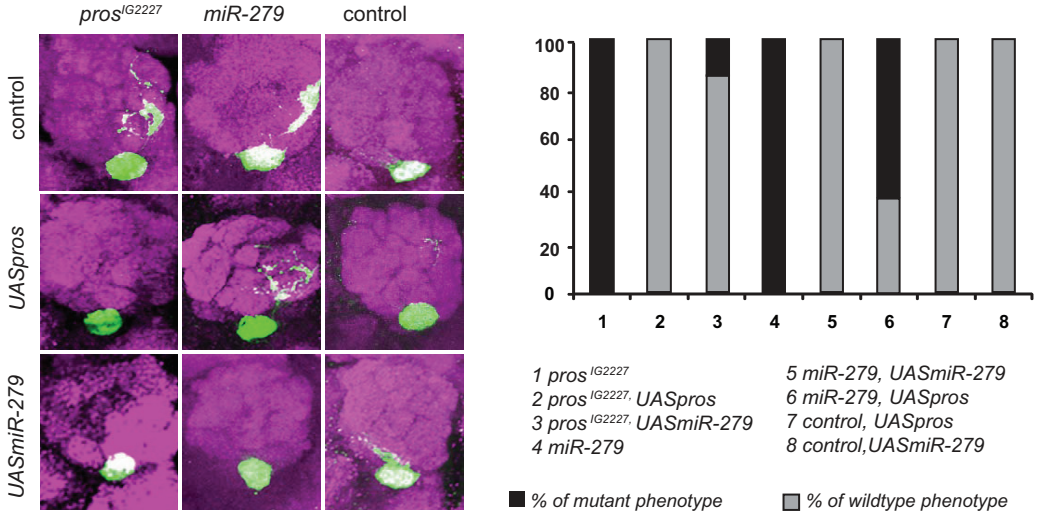

Figure 2.10: Genetic interaction and rescue experiments of *miR-279* and Prospero. Expression of *UASprospero* rescues the *pros*^{IG2227} phenotype to 100%, while expression in the *miR-279* mutant rescues only 37% of the mutant phenotype. Re-expressing *UASmiR-279* in the *miR-279* mutant background results in a full rescue, and also the *pros*^{IG2227} phenotype is rescued to 80%.

These results indicated that Prospero and *miR-279* act in a common pathway suppressing CO_2 neuron formation in the wildtype maxillary palp. In this regulatory network, Prospero is

putatively upstream of *miR-279* as expression of *miR-279* almost fully rescued the *pros*^{IG2227} phenotype. As expression of Prospero in the *miR-279* $^{962-7}$ mutants partially rescued the phenotype, it could not be excluded that Prospero is able to act independently and in parallel to *miR-279* to suppress CO_2 neuron formation on the maxillary palp. However, as the rescue of the *miR-279* $^{962-7}$ phenotype by expressing full length Prospero was only 37%, this parallel pathway might be less efficient than the miR-mediated suppression.

2.4.2 Prospero Binds Directly to the *miR-279* Enhancer

Given that Prospero and *miR-279* genetically interact, I hypothesized that Prospero being a transcription factor could directly bind to the *miR-279* enhancer region. The 2kb upstream region of the *miR-279* gene was shown to be sufficient to rescue the *miR-279* $^{962-7}$ phenotype (Cayirlioglu et al., 2008). Therefore, I refer to this genomic region as *miR-279* enhancer. To identify putative binding sites of Prospero, I used the already published motifs: TWAGVYD (Cook et al., 2003) and CWYNNCY (Choksi et al., 2006). Using bioinformatic tools, a search for these two motifs in the *miR-279* enhancer region was performed. In total 18 predicted Prospero binding sites were identified in the enhancer region (Fig. 2.11). By comparing these predicted sites with the same genomic region of five other Drosophila species (*D.simulans*, *D.yakuba*, *D.erecta*, *D.ananassae*, *D.pseudoobscura*), I found five highly conserved Prospero binding sites (Fig. 2.11).

MicroRNAs are transcribed as a longer pri-microRNAs, before they get exported and further trimmed to shorter pre-miRs yielding mature microRNAs (Lee et al., 2003). To define the length of the primary transcript of *miR-279*, I conducted a 5'RACE. The resulting PCR product had a length of 1.2 kb and matched the sequence of the *miR-279* upstream region (Fig. 2.12).

According to the distribution of predicted binding sites, I found that three putative Prospero binding sites lay outside of the primary transcript and two sites within the primary transcript (see Fig.2.12).

To test the functionality of these sites, I used an electromobility shift assay (EMSA). Using this assay, I tested whether Prospero could *in vitro* directly bind to the predicted Prospero binding sites found in the *miR-279* enhancer fragment. I focused on two predicted Prospero binding sites, P1 and P4, where the former lay within the primary transcript and the latter outside (see Fig.2.12). For the EMSA, I purified the Prospero homeobox motif and assayed with oligos containing one of the predicted Prospero sites, P1 or P4. Prospero bound oligos were identified by a shifted band due to the higher molecular weight of the protein-DNA complex. On the gel, only the oligos containing the P4 site were shifted (Fig.2.13 lane 3). In a control

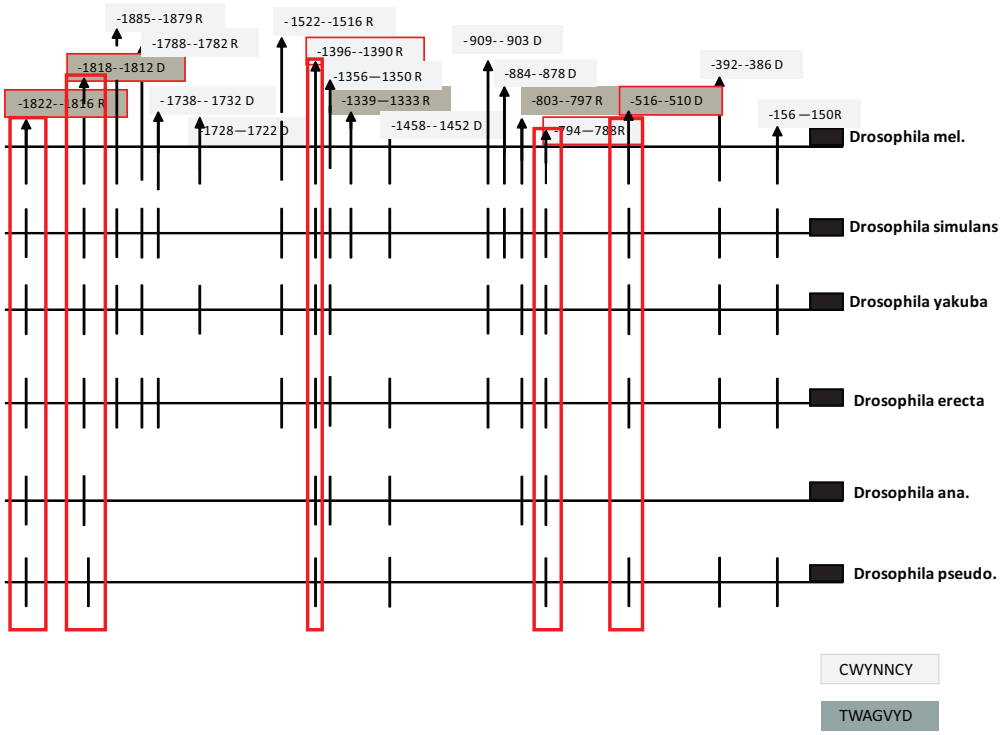

Figure 2.11: Putative Prospero binding sites in the *miR-279* enhancer. Predicted Prospero binding sites in the *miR-279* enhancer fragment are compared to the same genomic region in 6 different Drosophila species. The most conserved sites are highlighted (red).

experiment, where I mutagenized the binding motifs, the shift of P4 oligos was strongly reduced (Fig.2.13 lane 4). Hence, purified Prospero directly bound to the *miR-279* enhancer *in vitro*. The binding was mediated by the highly conserved Prospero binding site P4 which lay outside the primary transcript.

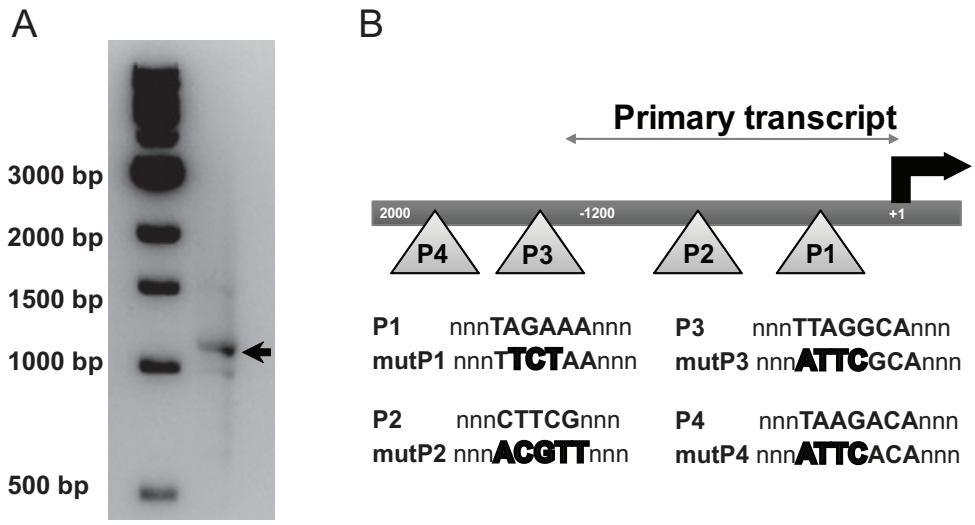

Figure 2.12: 5'RACE PCR product of the *miR-279* RNA. **A**. The PCR product of the 5'RACE indicates that *miR-279* is transcribed as a longer mRNA around 1.2kb. **B**. The *miR-279* enhancer fragment contains predicted Prospero binding sites. The length of the primary transcript is indicated. The sequence of the motifs is shown as well as the sequences of the mutagenized motifs.

2.4.3 Prospero Activates *miR-279* Expression in S2 Cells

As Prospero is known to act both as activator and repressor of its target genes (Choksi et al., 2006), I assessed the effect of Prospero binding to the *miR-279* enhancer using a luciferase reporter assay in S2 cells. In this assay, luciferase was expressed under the control of the *miR-279* enhancer. I compared the expression of the wildtype enhancer with the mutated enhancer containing mutations in the Prospero binding sites (Fig.2.12B). The wildtype enhancer was highly activated in S2 cells. By mutating four of the predicted binding sites of Prospero (Fig.2.12 B), the expression of the reporter dropped to 60%$\pm$10% (compare panel 1 and 5 in Fig.2.14).

To further measure the effect of Prospero to the *miR-279* expression, I increased and decreased the levels of Prospero in S2 cells. In case of both the wildtype and mutated enhancer, overexpression of full length Prospero using *ubiquitin-Gal4* did not affect the level of luciferase expression (compare panel 2 and 6 in Fig.2.14). This suggested that the amount of Prospero which was endogenously expressed in S2 cells was already sufficient to express the maximum level of the *miR-279* enhancer reporter. In contrast, decreasing the level of Prospero using RNAi against Prospero (*RNAipros*), reduced substantially the expression of the wildtype enhancer reporter by 70$\pm$6.2% (see panel 3 Fig.2.14). Likewise, the reporter expression under the control

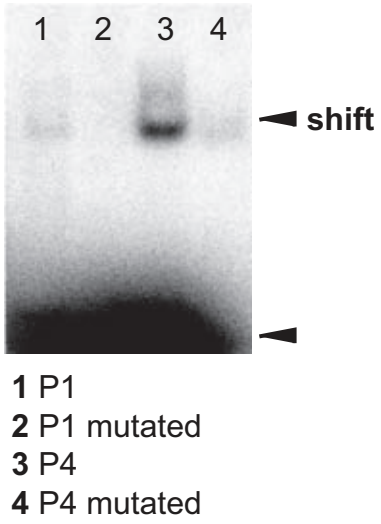

Figure 2.13: Purified Prospero binds to the *miR-279* enhancer. Only P4 containing oligos are bound by purified Prospero which results in a shifted band (lane 3). Oligos containing a mutated Prospero binding motif do not bind the transcription factor anymore (lane 4).

of the mutated enhancer was reduced to 49± 7% (see panel 7 Fig.2.14). In a control experiment, I transfected an unrelated RNAi construct against insulin receptor (InR) together with the reporter constructs. Unlike *RNAipros*, *RNAiInR* did not affect the expression of any reporter construct (panel 4 and 8 Fig.2.14). Hence, Prospero could activate the expression of *miR-279* by directly binding to the enhancer. The activation was in part mediated via the predicted Prospero binding sites as mutating these sites decreased the expression level. Moreover, the *mir-279* enhancer was less expressed when Prospero levels were reduced in the cell using RNAi. Nevertheless, in these conditions the *miR-279* enhancer was still expressed suggesting that either additional Prospero binding sites might be involved in the activation of *miR-279* or other factors might be important for *miR-279* activation.

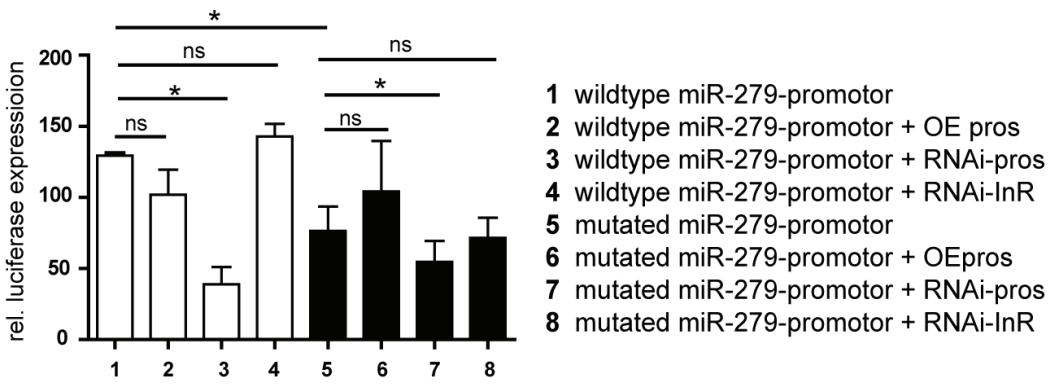

Figure 2.14: Quantification of *miR-279* reporter luciferase assay in S2 cells. The wildtype *miR-279* enhancer is expressed in S2 cells (column 1). Mutating the predicted Prospero binding sites in the *miR-279* enhancer reduces the expression of the luciferase reporter (column 5). Overexpression of Prospero does not significantly affect the expression of the wildtype enhancer nor of the mutated version (columns 2 and 6). The expression of the wildtype enhancer is strongly reduced when levels of Prospero are reduced using RNAi (column 4). The transfection of *RNAiInR* does not affect the expression of *miR-279* enhancer reporter (column 8). The firefly luciferase expression is normalized to the expression of a co-transfected renilla luciferase.

2.4.4 Prospero Binds to the *miR-279* Enhancer *in vivo*

To test whether Prospero binds to the *miR-279* enhancer *in vivo*, I performed a chromatin immunoprecipitation (ChIP) experiment. To do so, I overexpressed a FLAG-tagged version of Prospero in *Drosophila* embryos. To preserve the interaction of Prospero with genomic DNA, the tissue was crosslinked. Chromatin was extracted, sheared and further mixed with α-FLAG antibody. The antibody bound to FLAG-tagged Prospero also recovered chromatin which was recognized by the transcription factor. To verify, whether Prospero bound to DNA flanking the P4 site in the *miR-279* enhancer, I performed a PCR with the recovered chromatin and primers flanking this site. Compared to the input, 48% of chromatin was recovered by immunoprecipitation using an α-FLAG antibody, while no PCR product was detected in the samples which were probed with an unspecific mouse IgG instead of the α-FLAG antibody. The same was true for a third control, where instead of an antibody water was added to the mix (Fig.2.15). In conclusion, Prospero bound the P4 site *in vivo*, corroborating the findings of the EMSA experiment.

Next, to tested whether Prospero was modifiying the activity of *miR-279 in vivo*, I used a miR sensor flystock. The miR sensor contained a GFP gene, which was expressed under the control of two regulatory sequences. First, the GFP expression was driven by a tubulin

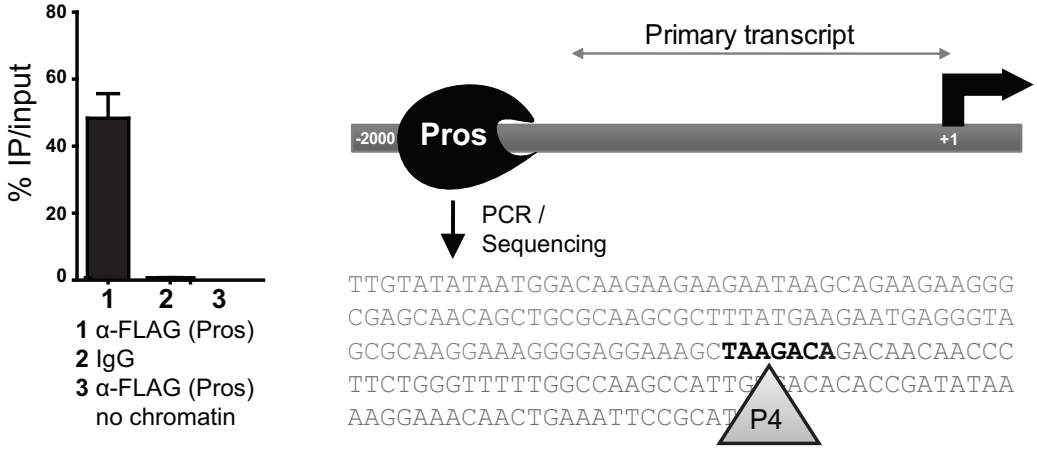

Figure 2.15: Prospero binds to the *miR-279* enhancer in a ChIP assay. Quantification of the immunoprecipitated fraction of chromatin using α-Flag-Prospero to the input chromatin. Sequence of the *in vivo* binding site of Prospero to the *miR-279* enhancer.

promotor and therefore broadly expressed. To restrict the GFP expression, the cDNA was fused to a 3'UTR sequence which contained multiple *miR-279* binding sites and therefore restricted the expression of GFP to cells lacking *miR-279* expression. Hence, in tissues expressing *miR-279*, GFP was repressed while in tissues with no *miR-279*, GFP was expressed. The sensor could be used to distinguish cells with a mature, functional form of *miR-279* from cells which lack *miR-279*. As a control, I analyzed a control sensor flystock which broadly expressed GFP driven by the tubulin promotor. The control sensor was not regulated by microRNAs as a 3'UTR sequence was missing. Therefore, this construct might be active in any cell which expresses *tubulin Gal4*.

I analyzed the embryonic CNS at stage 16 with either the miR sensor or the control sensor in the genetic background. The CNS of embryos expressing the control sensor, was broadly labeled with GFP which overlapped with α-Prospero staining (Fig.2.16A). Interestingly, the miR-sensor was more sparsely expressed in the embryonic CNS and not a single GFP positive cell overlapped with α-Prospero staining (Fig.2.16A). According to the logic of the sensor constructs, the GFP positive cells in the miR sensor background did not express an active version of *miR-279*, whereas non-labeled cells expressed an active version of *miR-279*, which repressed the sensor-GFP mRNA. The missing overlap of GFP positive cells with α-Prospero staining indicated that Prospero positive cells expressed an mature *miR-279*. Together with the previous results showing that Prospero directly bound to the *miR-279* promotor *in vitro* and *in*

vivo to activate the microRNA, I further found *in vivo* evidence that Prospero was overlapping with a mature form of *miR-279* in the embryonic CNS.

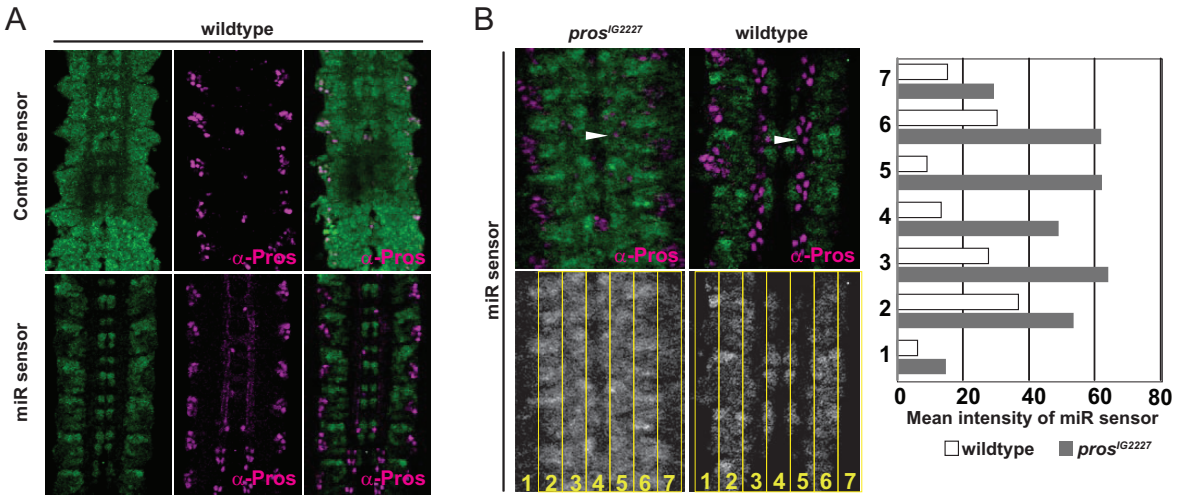

Figure 2.16: Prospero activates *miR-279* in the CNS of *Drosophila* embryos. A. Expression of *miR-279* sensor and control sensor constructs in the embryonic CNS of embryos at stage 16. **B**. *miR-279* sensor expression in embryonic CNS at stage 16 in the $pros^{IG2227}$ mutant background. Quantification of *miR-279* sensor intensity using the Region of interest (ROI) in different panels.

To test whether Prospero was indeed activating *miR-279*, I expressed the miR sensor under the control of a tubulin promotor element in the background of the $pros^{IG2227}$ mutant. In the hypomorphic mutant allele, the residual Prospero protein was sufficent for a immunochemical detection. Here, GFP was expressed in α-Prospero positive cells indicating that *miR-279* was less active in the Prospero mutant background (Fig.2.16B). Unfortunately, I was not able to test the sensor constructs in the developing maxillary palp as the control sensor was not expressed in MPs at 6 hrs APF (Fig.2.17). Therefore, I could not draw any conclusion from experiments performed with the miR sensor in the developing olfactory system.

To analyze, how reduced levels of Prospero affected the expression of *miR-279* in the developing olfactory system, I used a miR-reporter construct (*miR-279-Gal4*) containing the *miR-279* enhancer fused to Gal4. I tested the miR-reporter at 6 hrs APF, when *miR-279* was first detected in Prospero positive cells. In wildtype palps, 75% of the analyzed palps co-expressed Prospero and the miR-reporter (Fig.2.18 A,B). Also, in *miR-279* $^{962-7}$ mutant palps the reporter co-labeled Prospero positive cell in 69% of the palps analyzed (Fig.2.18 A,B). This indicated that *miR-279* expressing cells were fully differentiated in the *miR-279* $^{962-7}$ mutant background. In contrast, only in 16% of the analyzed $pros^{IG2227}$ mutant palps co-expressed

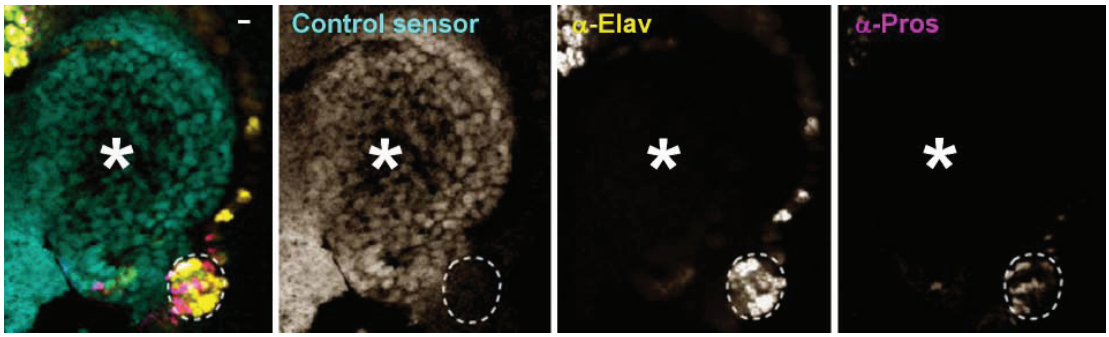

Figure 2.17: Expression of the control sensor in developing MPs at 6 hrs APF. At 6 hrs APF, the control sensor is only expressed in the antenna (asterisk) but not in the MP (circle)(data obtained from Laura Loschek). The reason for this is currently not known. Scale bar 5 microns.

Prospero. Similar results were obtained in adult palps. In this case, the miR reporter was visible in 100% and 80% of the analyzed wildtype palps and *miR-279* $^{962-7}$ mutant palps. Whereas in *pros*^{IG2227} mutant palps only 54% expressed the miR-reporter. In the *pros*^{17} mutant background, the miR-reporter was only in 42% of analyzed palps detectable (Fig.2.18 C).

In summary, I could show that Prospero bound to chromatin of the *miR-279* enhancer *in vivo* employing the conserved binding site P4. The same site was also *in vitro* bound by purified Prospero (Fig 2.13). Flies that carry a construct that monitored the activity of *miR-279* showed that in the embryonic CNS, Prospero overlapped with the mature *miR-279*. In the Prospero hypomorphic mutant background, the activity of *miR-279* was reduced. Moreover, in the developing and adult olfactory system, *miR-279* expression was dependent on Prospero as in the *pros*^{IG2227} mutant background the *miR-279* reporter was less expressed. Taken together, Prospero directly activates *miR-279 in vivo*.

2.5 Common Targets of *miR-279* and Prospero

2.5.1 Identification of Common *miR-279* and Prospero Targets

The experiments showed, that Prospero regulates the expression of *miR-279* to suppress the formation of CO_2 neurons on the maxillary palp of wildtype flies. As the two molecules are involved in the same developmental process, I tried to unravel downstream regulated factors. To find common targets of *miR-279* and Prospero, I compared a list of verified *in vivo* Prospero targets (Choksi et al., 2006) with lists of putative *miR-279* targets taken from prediction tools e.g.,TargetScan (`www.targetscan.org/fly/`) (see methods). Thereby, I could identify 20

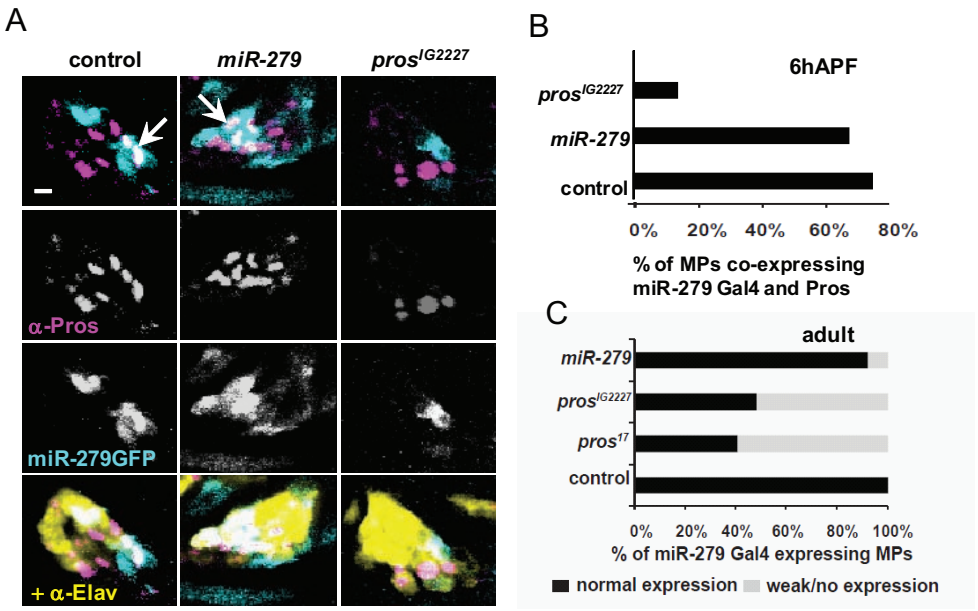

Figure 2.18: *miR-279* reporter expression is reduced in Prospero mutant palps *in vivo* A. Expression of *miR-279* reporter constructs in the developing maxillary palps at 6 hrs APF. **B**. Quantification of the *miR-279* reporter and Prospero expressing cells in the genetic background of the mutants at 6 hrs APF. **C**. Quantification of *miR-279* reporter expressing cells in adult maxillary palps in wildtype and mutant background of *miR-279* $^{962-7}$, *pros*^{IG2227} and *pros*^{17}.

common targets (Fig.2.19). The intersection of *miR-279* and Prospero targets was subjected to a Gene Ontology (GO) term analysis to classify the targets according to their function. I found that 12 out of 20 common targets were highly enriched in the three functional groups, cell fate determination, nervous system development and neurogenesis (Fig.2.20). As these functions were highly related to the phenotype observed, I investigated some of the targets more closely in a genetic interaction experiment. I hypothesized if *miR-279* and Prospero acted as repressors, a reduction of the target level would lead to a rescue of the observed phenotype. To reduce the target level, I used transgenic *UAS-RNAi* fly lines that were expressed using the above described *Gr21a-sytGFP* β*-actin-Gal4* stock. The following targets were chosen: *RNAi Ptx, RNAi lola, RNAi scute, RNAi spineless*, *RNAi nerfin-1* and *RNAi escargot*. Out of these, only *RNAi nerfin-1* altered the mistargeting pattern of both mutants. Reducing the levels of Nerfin-1 surprisingly rescued the phenotype of *miR-279* $^{962-7}$ completely and of *pros*^{IG2227} mutant to 80% (Fig.2.21). For the other RNAi lines, I could not finally clarify whether they were not involved in the pathway or the RNAi lines were not functional. At least none of the

common target	gene	molecular function
CG13906	nerfin-1	Transcription factor
CG3758	escargot	Transcription factor
CG11988	neuralized	Ubiquitin ligase
CG3827	scute	Transcription factor
CG9626	unknown	unknown
CG13521	robo	receptor
CG9239	B4	unknown
CG10580	fringe	UDP-glycosyltransferase
CG9739	frizzled-2	Wnt receptor
CG17835	invected	Transcription factor
CG12245	gcm	Transcription factor
CG1447	Ptx-1	Transcription factor
CG6993	spineless	Transcription factor
CG1072	Arrowhead	Transcription factor
CG18408	Cap	Vinculin binding
CG2679	goliath	Transcription factor
CG9623	inflated	Receptor cell adhesion
CG1004	rhomboid	peptidase, cleaves EGF
CG5507	Transcript 48	unknown
CG31048	unknown	unknown

Figure 2.19: List of common targets. Prospero and *miR-279* share 20 common targets.

used RNAi lines resulted in additional phenotypes.

In summary, *miR-279* and Prospero shared common predicted targets which fell predominantly into the three different functional groups cell fate determination, nervous system development and neurogenesis. Out of these, the previously identified *miR-279* target Nerfin-1 (Cayirlioglu et al., 2008), showed an effect on the suppression of CO_2 neurons. When Nerfin-1 was downregulated by RNAi in the *miR-279* and the Prospero mutant background, both phenotypes were rescued. Hence, Nerfin-1 could be verified as a downstream target of *miR-279* and Prospero *in vivo*. Since downregulation of Nerfin-1 rescued the phenotype, the target must be repressed by the microRNA and the transcription factor in the wildtype. The effect of Escargot could not be determined using RNAi as the available construct was not functional.

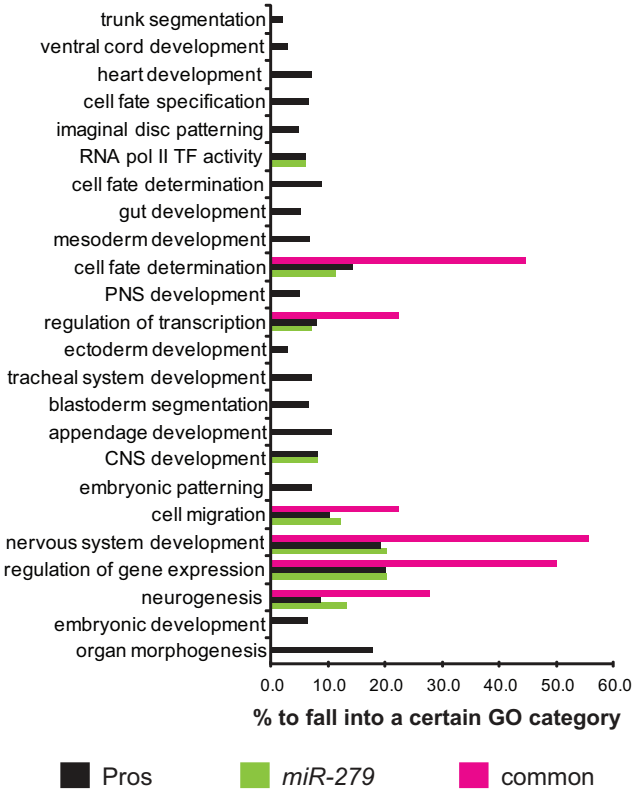

Figure 2.20: Gene Ontology (GO) analysis of common *miR-279* and Prospero targets. Percentage of *miR-279*, Prospero and common targets to fall in a given Gene Ontology (GO) category. Common targets are enriched in the categories cell fate determination, nervous system development, regulation of gene expression and neurogenesis.

2.5.2 Escargot and Nerfin-1 are Targets of *miR-279* in S2 Cells

To test whether Escargot was a target of *miR-279*, I expressed a 3'UTR reporter construct in S2 cells. The reporter construct contained the 3'UTR of escargot fused to a Renilla luciferase gene. The vector was transfected into S2 cells together with *UAS-miR279* construct which was driven with ubiquitin-Gal4. Upon binding of *miR-279*, the escargot reporter expression was downregulated to $51\pm9\%$. As a control, *miR-315* was expressed together with the 3'UTR reporter, which didn't affect the escargot reporter expression (Fig.2.22 B). Nerfin-1 was already shown to be a target of *miR-279* in S2 cells (Cayirlioglu et al., 2008). As a positive control, I repeated a nerfin-1 3'UTR reporter construct in S2 cells. Binding of *miR-279* to the nerfin-1 3'UTR reporter resulted in a reduction to $27\pm10\%$ of the reporter expression. Again increased levels of *miR-315* had no effect on the nerfin-1 3'UTR reporter (Fig.2.22 A). This experiment

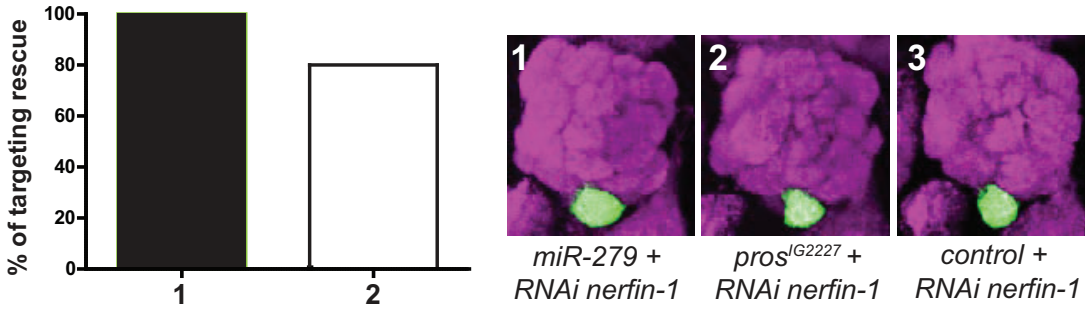

Figure 2.21: Reducing levels of Nerfin-1 in the mutant background rescues the mistargeting phenotype. *RNAi nerfin-1* in the mutant background of *miR-279* $^{962-7}$ and *pros*^{IG2227} rescues the mistargeting phenotype to 100% and 80%, respectively (column 1 and 2). Expressing *RNAi nerfin-1* in the control does not alter the targeting of CO_2 neurons (3).

showed that both Escargot and Nerfin-1 were directly suppressed by *miR-279* in S2 cells.

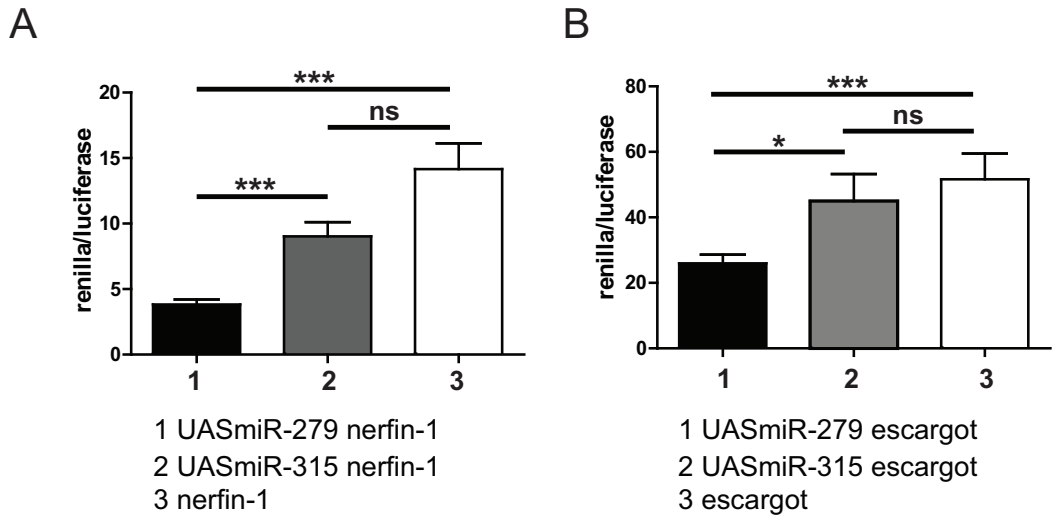

Figure 2.22: *miR-279* represses the expression of Escargot and Nerfin-1 in S2 cells. A. The expression of the nerfin-1 3'UTR reporter expression is significantly reduced upon overexpressing *miR-279* to $27\pm10\%$. **B**. The expression of the escargot 3'UTR reporter is significantly suppressed to $51\pm9\%$ upon *miR-279* overexpression. In both cases, overexpression of *miR-315* does not affect the expression.

2.5.3 Expression of the Common Targets, Escargot and Nerfin-1, in the Developing MP

To assess the expression of the transcription factor Escargot, I used a fly stock containing a lacZ labeled P-element insertion in the escargot locus (esg-P[lacZ]). In collaboration with Dr.Laura Loschek, maxillary palps were dissected at various stages of development. At 6 hrs APF, the transcription factor was broadly expressed in the MP (Fig.2.23 A) and stayed switched on until 25 hrs APF, when the expression was slightly decreased (Fig.2.23 B). At 30 hrs APF, the expression of esg-P[lacZ] was no longer detectable (Fig.2.23 C). At even later stages (48 hrs APF), Escargot expression was completely absent on the MP (Fig.2.23 D). Co-staining with α-Prospero revealed that only at 6 hrs APF a few cells co-expressed Prospero and Escargot (Fig.2.23).

In a previous publication, Nerfin-1 was shown to be expressed in the olfactory appendages (Cayirlioglu et al., 2008). I could not reproduce the staining to analyze all the relevant stages during MP development, because a functional antibody could not be obtained.

An alternative strategy to determine the expression of a gene is the use of fosmids. The fosmid vectors include a large piece of genomic DNA around 36 kb in average, together with an attB site for site-directed integration into the fly genome (Ejsmont et al., 2009). The DNA

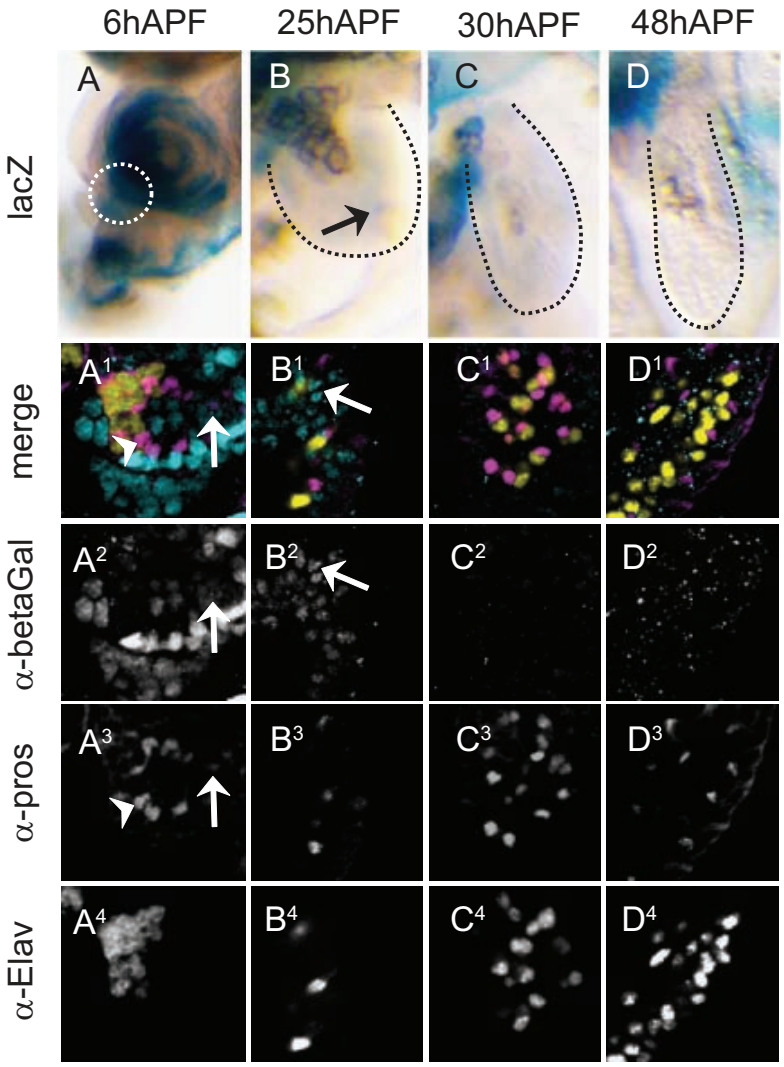

Figure 2.23: Escargot is expressed early steps of MP development. A. At 6 hrs APF esg-lacZ is present in the developing MP (white dashed circle). Cells expressing esg-lacZ (blue) are overlapping with Prospero staining (magenta) (see arrows $A^{1,2,3}$). **B**. At 25 hrs APF the expression of esg-lacZ is drastically reduced. Only a few cells express esg-lacZ ($B^{1,2}$), **C** and **D**. At 30 and 48 hrs APF the esg-lacZ expression is no longer detectable in the MP (C^2, D^2).

fragments resulted from a random restriction digest of whole genomic DNA. The single pieces contained genes together with the surrounding genomic environment which putatively covers a large part of the regulatory elements. Through recombineering the genomic region could be tagged with cassettes containing a fluorescent protein e.g. GFP, mcherry with or without localization signals. The tagged fosmid could be used to study the endogenous expression pattern *in vivo*. Due to the lack of a functional antibody for Nerfin-1, I tagged the fosmid clone of *nerfin-1* gene with nls-mcherry tagging. The tag was inserted 5' of the gene to avoid a damage of the 3'UTR. I received two fly lines and tested the expression of the Nerfin-1 fosmid in embryos. Unfortunately, in all stages tested the expression of the fosmid was not detectable in any of the lines. The reasons for this are currently unknown. A possible explanation might be that important regulatory elements for Nerfin-1 expression were missing in the fosmid or that the expression of Nerfin-1 was overall very low. To test the latter possibility the fosmid lines could be analyzed in the *miR-279* mutant background.

2.5.4 Nerfin-1 and Escargot are Targets of *miR-279* and Prospero *in vivo*

Since reducing levels of Nerfin-1 using RNAi rescued the phenotype of *miR-279* $^{962-7}$ and *pros*^{IG2227}, I tested whether *miR-279* and Prospero repress Escargot *in vivo*. Nerfin-1 was already shown to be upregulated in *miR-279* mutant palps and to co-localise with the ectopic CO_2 neurons (Cayirlioglu et al., 2008). As the anti-body for Nerfin-1 was not working for me, I was not able to perform the same experiment in the *pros*^{IG2227} mutants. To assess the impact of the mutations of *miR-279* and *pros*^{IG2227} mutation on Escargot, I analyzed the expression of esg-P[lacZ] in the mutant background in developing palps at 6 hrs APF. At this timepoint, around 16% of the palps co-expressed Escargot and Prospero in the wildtype. In the *miR-279* $^{962-7}$ and *pros*^{IG2227} mutant palps the level of Escargot was increased. Moreover, 90% and 61% of the *miR-279* $^{962-7}$ and *pros*^{IG2227} mutant palps co-expressed Prospero and Escargot (Fig.2.24). Surprisingly, as the escargot-lacZ allele was an insertion into the *escargot* enhancer, also in the *miR-279* $^{962-7}$ background the expression was increased. Given that *miR-279* mediated a post-transcriptional repression, the increase of the esg-lacZ reporter reflecting the enhancer activity was surprising since no Escargot-lacZ fusion mRNA was transcribed. The reasons for that are still unknown. Nevertheless, the experiment demonstrated that Prospero acts on the genomic level to repress the expression of Escargot in the wildtype. When the levels of Prospero are decreased, the repression was removed and Escargot expression was increased

in the MP.

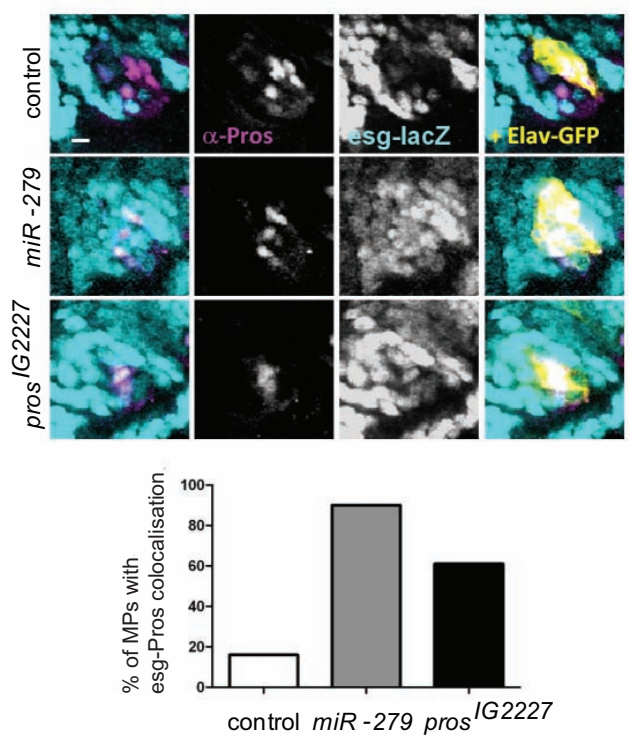

Figure 2.24: Escargot expression in the MP is elevated in the mutant background. The expression of esg-lacZ in wildtype and mutant background at 6 hrs APF. In the wildtype esg-lacZ is only sparsely expressed in the developing MP area. In *miR-279* $^{962-7}$ mutants the expression of esg-lacZ is enhanced compared to wildtype MPs. Also the percentage of cells co-expressing Prospero and esg-lacZ is increased. Similarly in *pros*^{IG2227} mutant MPs, the expression of esg-lacZ and also the overlap with Prospero staining are increased.

As the experiments suggested that *miR-279* and Prospero repress the level of their targets, I tested whether decreased target levels in the mutant background reduced the number of ectopic CO_2 neurons on the MP. To do so, I crossed a heterozygous mutant allele of either *nerfin-1*, *escargot* or a combination of both to the *miR-279* $^{962-7}$ or the *pros*^{IG2227} background. By reducing the level of Nerfin-1 in *pros*^{IG2227}, I detected a reduction of the number of ectopic CO_2 neurons by 40%. Similarly, decreased levels of Escargot in the *miR-279* $^{962-7}$ and the *pros*^{IG2227} mutant palps reduced the number of ectopic CO_2 neurons to 44% and 33%, respectively (Fig.2.25 A,B). Although a reduction of Nerfin-1 and Escargot together in the *pros*^{IG2227} mutant background, did not result in a decreased number of ectopic CO_2 neurons compared to the reduction achieved by reducing only one target (Fig.2.25 A). Reducing the levels of Hb9, which was predicted to be a target of *miR-279* but not of Prospero, in the *miR-279* $^{962-7}$ background had no influence on the number of CO_2 neurons (Fig.2.25 B). Therefore, Nerfin-1

and Escargot are common targets of *miR-279* and Prospero and act specifically on MP CO_2 neuron suppression.

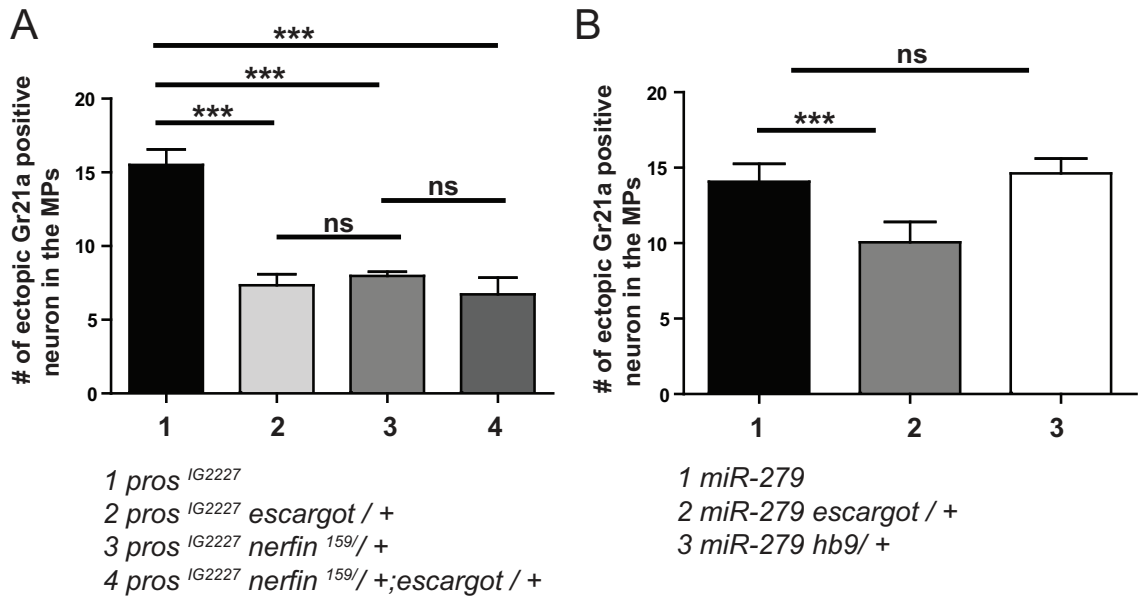

Figure 2.25: Lower levels of Nerfin-1 and Escargot decrease the number of ectopic CO_2 neurons. A. Removing one copy of *escargot* or *nerfin-1* by introducing a heterozygous mutant in the $pros^{IG2227}$ background reduces the number of ectopic neurons to 33% and 40%, respectively. Reducing the levels of both targets in the $pros^{IG2227}$ mutant background, does not significantly further reduce the number of ectopic CO_2 neurons. **B.** Removing one copy of *escargot* in the *miR-279* $^{962-7}$ background reduces the number of ectopic CO_2 neurons to 44%. Reducing the level of Hb9 in the *miR-279* $^{962-7}$ background has no influence on the number of CO_2 neurons.

In conclusion, reduction of the levels of Nerfin-1 and Escargot, diminished the number of ectopic CO_2 neurons and also rescued the mistargeting phenotype in both mutants. Therefore, both Nerfin-1 and Escargot are involved in the regulatory network that is responsible to repress the formation of CO_2 neurons on the maxillary palps of wildtype flies.

2.5.5 Nerfin-1 and Escargot Are Necessary and Sufficient for the Formation of CO_2 Neurons

As I characterized candidate molecules which were important to generate mosquito-like CO_2 neurons on the maxillary palps of *Drosophila*, I addressed the question whether the target molecules that were tightly suppressed by *miR-279* and Prospero *in vitro* and *in vivo*, are sufficient to induce the formation of ectopic MP CO_2 neurons in the wildtype flies. To do so, I overexpressed in eyFLP-clones Nerfin-1 and Escargot and a combination of the two using the above described *Gr21asytGFP actin-Gal4* stock in wildtype flies. Overexpression of a either Escargot or Nerfin-1, never altered the targeting of the Gr21a positive neurons (Fig.2.26). In stark contrast, overexpression of a combination of Nerfin-1 and Escargot led to a mistargeting in 40% of the analyzed brains. The phenotype highly resembled the *miR-279* $^{962-7}$ and *pros*^{IG2227} phenotype as axons innervated the antennal lobe via the labial nerve and mistargeted a medial glomerulus (Fig.2.26). Therefore, high levels of Nerfin-1 and Escargot together were sufficient to generate a *miR-279* $^{962-7}$ and *pros*^{IG2227} like phenotype in maxillary palps. Additionally, the axon bundle from the antennal nerve was thiner as compared with the wildtype situation potentially suggesting that Escargot and Nerfin-1 were also involved in the development of the antennal CO_2 neurons.

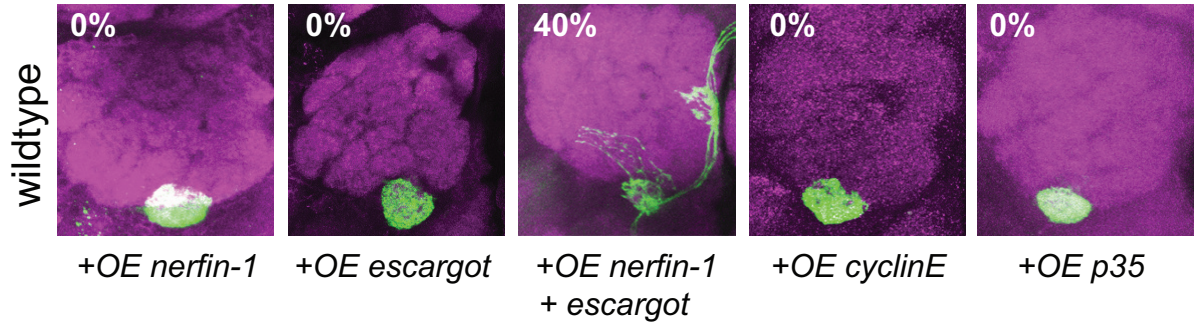

Figure 2.26: Elevated Nerfin-1 and Escargot levels are sufficient to form ectopic CO_2 neurons in the wildtype. Overexpression of Nerfin-1 and Escargot independently in the wildtype background does not effect the targeting pattern of CO_2 neurons. In contrast, overexpression of both targets together leads to mistargeting to a medial glomerulus via the labial nerve in 40% of the analyzed brains, indicating the formation of ectopic CO_2 neurons on the MP. As a control, also overexpression of CyclinE and p35 as markers for cell cycle defects or apoptosis does not alter the targeting pattern of CO_2 neurons.

2.6 A Model on CO_2 Neuron Suppression on the MP

In conclusion, I formulated a model of the factors that were required to suppress the formation of CO_2 neurons on the maxillary palp in *Drosophila*. I found that Prospero via activation of *miR-279* and also independently- although less sufficient- suppressed the expression of Escargot and Nerfin-1. As a consequence of this effective suppressive network, no ectopic CO_2 neurons developed on the fly maxillary palp. If either of the suppressors was missing for instance in *miR-279* $^{962-7}$ or *pros*^{IG2227} mutants, the levels of Escargot and Nerfin-1 were elevated and around 20 cells on the maxillary palp started expressing the receptor for CO_2. These extra neurons sent their axons to the antennal lobe via the labial nerve and mistargeted a medial glomerulus (Fig.2.27). All analyzed aspects of the ectopically formed neurons highly resembled in localization, targeting pattern and ligand specificity the CO_2 neurons found in mosquitoes.

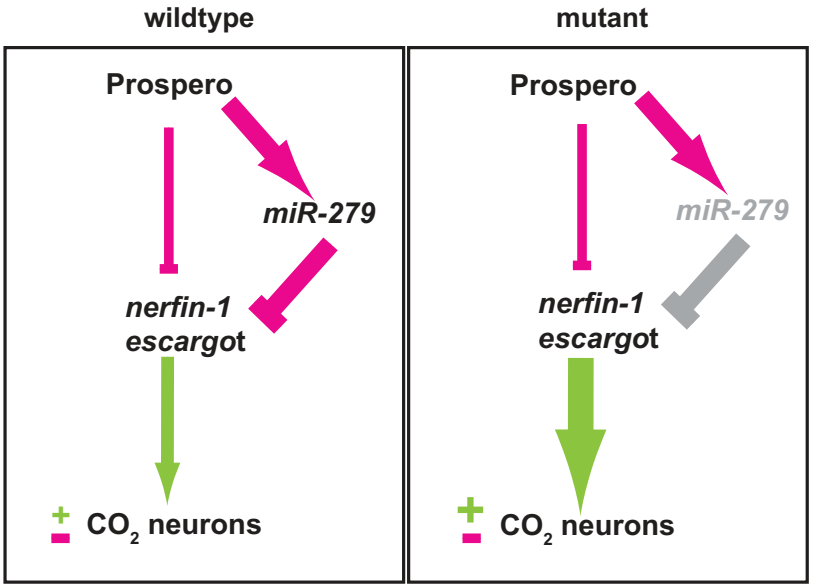

Figure 2.27: Model on CO_2 neuron suppression on the MP in *Drosophila*. In wildtype flies Prospero can suppress the expression of the two targets Nerfin-1 and Escargot directly by binding to the enhancer and indirectly through *miR-279*. *miR-279* downregulates Nerfin-1 and Escargot on the post-transcriptional level and thereby, suppresses the formation of CO_2 neurons. If either Prospero or *miR-279* are missing, the levels of Nerfin-1 and Escargot are elevated and lead in turn to the formation of ectopic CO_2 neurons on the MP.

2.7 The Candidate Circuit in Mosquito

Due to the mosquito-like phenotype it was tempting to ask whether the candidate molecules were conserved and involved in CO_2 neuron development in mosquitoes. The *Anopheles gambiae* genome was fully sequenced in 2002 (Holt et al., 2002) and meanwhile the annotation progressed (e.g.`www.vectorbase.org`). I found that all identified candidate genes are conserved in *Anopheles gambiae*. An interesting aspect for future research might be, whether changes in 3'UTRs of *aga-escargot* and *aga-nerfin-1* evolved that inhibit the binding of *aga-miR-279*. According to prediction tools, *aga-miR-279* has 150 predicted targets, but *aga-escargot* as well as *aga-nerfin-1* are not among them (see Materials and Methods). To verify this experimentally, I performed a 3'RACE of *aga-nerfin-1* for which I extracted mRNA from mosquito pupae. Preliminary results suggested that the non-translated 3'UTR region of *aga-nerfin-1* was reduced compared with the nerfin-1 3'UTR in *Drosophila melanogaster*. As the 3'UTR length was shown to be variable in different developmental stages as well as in different tissues especially in the nervous system (Hilgers et al., 2011), the experiments need to be repeated in various tissues at different developmental time points. Another possibility that might have led to changes in localization might be differences in the expression of the candidate genes. To address this question, I identified putative enhancer regions of *Anopheles gambiae* candidate genes to generate fly reporter lines carrying mosquito enhancer fragments. These reporter constructs will be used to establish transgenic fly lines.

Chapter 3

Discussion

The presented work unraveled a regulatory gene network that specifically suppressed the formation of CO_2 neurons on the maxillary palp of *Drosophila melanogaster*. The network contains the neurogenic, atypical homeobox transcription factor Prospero which controls the expression of Escargot and Nerfin-1, both being transcription factors implicated in neuronal development. To do so, Prospero controls the target expression directly on the genomic level and in parallel on the post-transcriptional level through *miR-279*. *In vitro* and *in vivo* experiments showed that *miR-279* is in turn directly activated by Prospero. If either *miR-279* or Prospero were missing in the maxillary palps, ectopic CO_2 neurons formed. These ectopic neurons expressed the receptor for CO_2 and also either Or42a or Or59c. In addition, ectopically formed neurons also responded to CO_2 and to the ligands of Or42a and Or59c. The targeting of these olfactory neurons was altered. Gr21a positive neurons mistargeted a medial glomerulus instead of the V-glomerulus. Or42a and Or59c positive neurons usually targeted the medial glomerulus, but in the mutant background additionally to the V-glomerulus. Interestingly, the pattern of the ectopic CO_2 neurons highly resembled the location and the targeting of mosquito CO_2 neurons. In mosquitoes, CO_2 neurons are expressed on the maxillary palp and target a medial glomerulus in the antennal lobe. Since the mutant CO_2 neurons resemble the mosquito CO_2 neurons in location and targeting, makes the unraveled network interesting in order to gain some insight how CO_2 detection in flies and mosquitoes evolved. Future studies will focus on the regulation of MP CO_2 neuron development in mosquitoes. In *Drosophila*, *miR-279* and Prospero were expressed throughout the development of the neuronal lineage of olfactory sensilla. Sensilla on the maxillary palp form according to the canonical model of sensilla development (Lai and Orgogozo, 2004). In the mutant background of either *miR-279* or Prospero, the predominant basiconic sensilla type on the maxillary palp innervated by two neurons is altered to three neu-

rons. Therefore, the ectopic neurons formed within a basiconic sensillum on the maxillary palp. The developmental analysis demonstrated clearly that Prospero and *miR-279* were co-expressed in the developing olfactory tissue and regulated the neuron number per sensillum by specifically suppressing the developmental program to form CO_2 neurons. Furthermore, *in vitro* and *in vivo* experiments showed that Prospero directly bound to the *miR-279* enhancer. The binding exhibited a strong activation of *miR-279* as in S2 cells downregulation of Prospero through RNAi led to a strong decrease of luciferase reporter activity. Moreover, *in vivo* reporter of *miR-279* expression were strongly decreased in the Prospero mutant.

To define the downstream targets of *miR-279* and Prospero, lists of predicted or experimentally verified targets were compared. The overlap was clustered into functional groups using GO term analysis. The predicted common targets of *miR-279* and Prospero fell into three categories: nervous system development, cell fate determination and neurogenesis. As these categories were highly connected to the phenotypes observed, a couple of targets were subjected to an RNAi screen. Out of the tested targets, RNAi against nerfin-1 strongly rescued the phenotype of *miR-279* and Prospero. In S2 cell reporter assays, *miR-279* could be shown to suppress besides Nerfin-1, also Escargot. Escargot was expressed in early stages of maxillary palp development but downregulated in later stages. In contrast, in the *miR-279* and Prospero mutant background, Escargot expression was highly upregulated in the developing maxillary palp. Together with the S2 cell results, these data suggested that Escargot was repressed by *miR-279* and Prospero. Furthermore, elevated levels of Escargot and Nerfin-1 together in the wildtype maxillary palp, led to the formation of ectopic MP CO_2 neurons which mistargeted the medial glomerulus. As a result, Escargot and Nerfin-1 were shown to be necessary and sufficient to induce the formation of ectopic CO_2 neurons.

Taken together, the tight regulation of *miR-279* and Prospero acting on Escargot and Nerfin-1 suppresses the formation of ectopic mosquito-like CO_2 neurons on the maxillary palp of *Drosophila melanogaster*. The mutation of either Prospero and *miR-279* uncovered an evolutionary intermediate state of mosquito and *Drosophila* CO_2 neurons through the missing suppression of Escargot and Nerfin-1.

3.1 Prospero and *miR-279* Together Define Neuron Number

According to Dr. Laura Loschek's and my data, MP sensillum development follows the canonical model of sensilla formation (Lai and Orgogozo, 2004). Comparable to other sensilla, Prospero is expressed in the neuronal lineage and labels the sheath cell in the mature MP sensillum. In line with studies on bristle sensilla (Manning and Doe, 1999), where complete loss of Prospero led to a conversion of the pIIb to the pIIa lineage and subsequently to neuron loss, loss-of-function of Prospero (*pros*^{17}) results in a loss of neurons in several OR classes on the antenna and the MP (Fig.2.8). In addition to this phenotype, the new hypomorphic allele of Prospero, *pros*^{IG2227}, uncovered a second function of Prospero during late stages of olfactory MP development. In this case, Prospero together with *miR-279* defines the correct number of neurons in basiconic sensilla on the MP by preventing the formation of an additional neuron. In both, *pros*^{IG2227} and *miR-279* $^{962-7}$ mutant palps, the 2-neuron basiconic sensilla type develops a third neuron positive for the neuronal marker Elav. Interestingly, the 3-neuron hybrid sensillum expresses both CO_2 receptors and either one of the food odor receptors, Or42a or Or59c. This specific phenotype of Prospero resembles the role in the embryonic CNS, where Prospero prevents overproliferation likely through repression of mitosis (Choksi et al., 2006).

As Prospero acts on a variety of processes and tissues during neuronal development (Manning and Doe, 1999; Choksi et al., 2006), the OR-type specific phenotype of the hypomorphic allele is surprising. The appendage specificity might be influenced by proneuronal genes that define antennal and MP regions. Prior to the onset of neurogenic factors, the activity of two pro-neuronal genes, *amos* and *atonal* (Gupta and Rodrigues, 1997b; Goulding et al., 2000) determines the fate of the sensory precursor cells. Indeed, antennal and maxillary palp sensilla belong to different lineages. While *amos* defines the fate of some types of sensilla belonging to the future antenna, sensilla on the MP are derived from the *atonal* lineage (Gupta and Rodrigues, 1997b; Goulding et al., 2000). Within these lineages, different transcription factors pre-pattern the fate of the cells through activation of different developmental signaling pathways which finally determine the choice of receptors. Interestingly, CO_2 neurons of mosquito share the developmental origin with fly MP sensilla and therefore of the ectopic CO_2 neurons in *pros*^{IG2227} and *miR-279* $^{962-7}$ mutants as both belong to the *atonal* lineage (Lu et al., 2007). Hence, the activity of proneuronal genes might predefine the expression of certain types of olfactory receptor neurons and inhibit the development of other subsets.

Given that the activity of proneuronal genes apparently relays the development of sensory

organs in one direction, another factor could be important for the specificity of the observed phenotype. Generally to specify distinct subtypes of olfactory sensory neurons, either the expression of cell type specific factors is required or different levels of the same factors are expressed. According to the canonical model of sensilla development, various subtypes of sensilla employ the same set of transcription factors and signalling pathways. Therefore, varying the expression level of these factors might differentially affect the specification of distinct sensilla subtypes. This hypothesis can account for the phenotypes in the *pros*^{17} full mutant and the *pros*^{IG2227} hypomorphic allele. Whereas the full mutant of Prospero affects largely olfactory sensilla development on both appendages, the hypomorphic allele only affects two OSNs on the MP. Moreover, in the external sensory organ, Prospero was shown to cooperate with Notch to prevent additional cell divisions in the neuronal pIIB lineage (Simon et al., 2009). The differential expression and activity of neuronal determinants like Prospero and Notch might have contributed to the overall variety of sensilla types. Such mechanism are required to generate the large diversity of olfactory sensilla. The hypomorphic *pros*^{IG2227} allele revealed a specific effect of Prospero on the neuronal lineage of MP sensilla especially affecting CO_2 neuron suppression. Whether or how Notch signaling is involved in this process remains to be studied.

Besides a specific effect on the MP, inducing mutant clones of *pros*^{IG2227} and *miR-279* $^{962-7}$ in the less diverse external sensory organs on the thorax, resulted occasionally in the formation of an additional neuron suggesting a more general role of Prospero and *miR-279* in regulation of neuron number (Fig.3.1). Hence, the combined action of Prospero and *miR-279* seems to be conserved in at least two sensory neuron lineages.

Taken together, the hypomorphic allele of Prospero revealed a new, specific role in the regulation of neuron number in two lineages of olfactory receptors in late MP development. The temporal activity of Prospero on suppression of CO_2 neuron development is enhanced through the interaction with *miR-279*. The fact that only MP neurons are affected might be due to the different pro-neuronal genes initiating the development of olfactory sensilla on the MP and antenna. As Prospero and Notch were shown to interact in the determination of neuron number in the external sensory organs, the effect of Notch signaling remains to be studied on CO_2 neuron suppression. In bristle sensilla which contain only one neuron of the same type, *miR-279* and Prospero also influence the number of neurons suggesting a more general role of the microRNA and the transcription factor. Interestingly, in parallel to basiconic sensilla on the MP also bristle sensilla are dependent on *atonal* (Gupta and Rodrigues, 1997a).

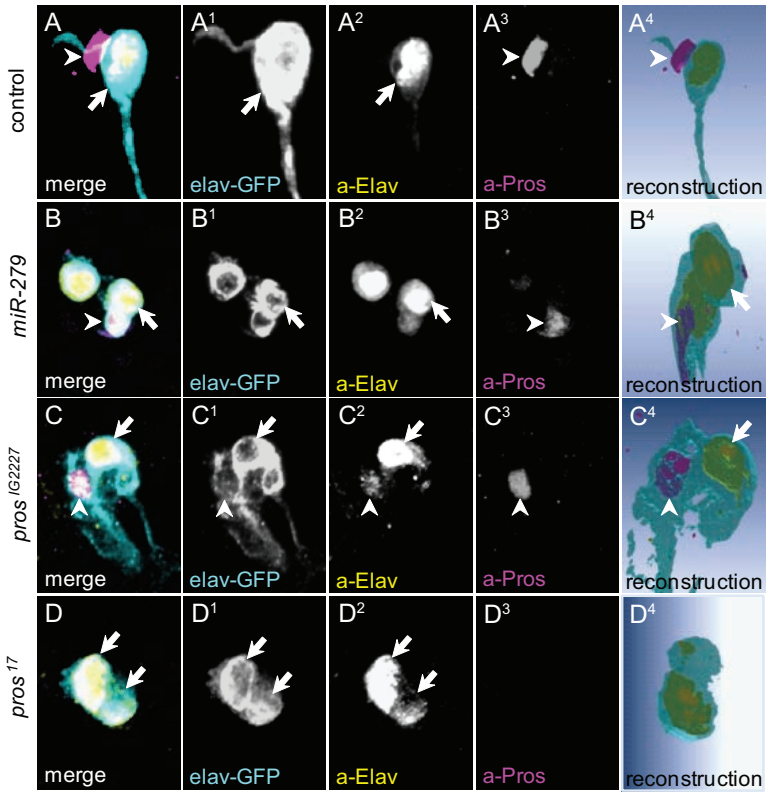

Figure 3.1: Prospero and *miR-279* define neuron number in bristle sensilla Wildtype ES organ sensillum carrying one neuron positively labeled for *Elav-Gal4 UASmcD8GFP* (A^1) and stained α-Elav (A^2), and one sheath cell positive for α-Prospero. A 3D-reconstruction of the sensillum is shown (A^4). Mutant ES organ sensilla of *miR-279* $^{962-7}$(B, B^{1-4}), *pros*^{IG2227} (C, C^{1-4}) and *pros*^{17} (D, D^{1-4}) develop a second extra neuron within the sensillum positively labeled for the neuronal marker Elav (data obtained by Laura Loschek).

3.2 *miR-279* and Prospero Act in a Coherent Feed-Forward Loop

The expression of microRNAs depends on transcription factors (TFs). So far there are only few studies on TFs activating microRNAs are available (Bethke et al., 2009) as previous work mainly focused on the identification of post-transcriptional targets. The presented model intergrates *miR-279* in a regulatory network governed by Prospero and regulating Escargot and Nerfin-1 (Fig.3.2). Prospero and *miR-279* share common targets and cooperate in repressing their expression. In genetic rescue experiments, re-expression of the microRNA in the hypomorphic Prospero mutant background yielded to a higher rescue than vice versa. These data suggest that the suppression of Escargot and Nerfin-1, through a combination of *miR-279* and Prospero

is more efficient than Prospero's suppression on the genomic level. There are several possibilities, why the combined repression by the transcription factor and the microRNA is stronger. Developmental processes require the expression of potent transcription factors that control the expression of a battery of genes e.g. Prospero was shown to bind to the regulatory regions of more than 1.800 genes during embryonic development (Choksi et al., 2006). These powerful genes have a restricted time slot of action, which requires a tight regulation. microRNAs could act as a fail-safe mechanism in case the genomic repression of a TF is either to slow or to weak and would therefore lead to excessive mRNA levels of the targets. Interestingly, in adult neuronal stem cells prior to differentiation, mRNAs of developmental regulators are already excessively transcribed, which leads to an accumulation of the respective mRNA (Beckervordersandforth et al., 2010). To eliminate these mRNAs from the cell, microRNAs seem to be an appropriate way as repression on the genomic level can only inhibit *de novo* transcription. I propose that through *miR-279*, Prospero is able to potentiate the repression of Escargot and Nerfin-1 by extending the mode of action to the post-transcriptional level. The two identified target genes are powerful genes involved in nervous system development and differentiation. For example, Nerfin-1 is necessary for proper neuron differentiation in the embryonic CNS by controlling the expression of guidance factors like robo2, wnt5, derailed, Go-alpha47a, Lar and futsch that are necessary for proper neuron targeting (Kuzin et al., 2005). Moreover, Escargot was shown to regulate neuronal differentiation in the external sensory organ lineage, where mutants of Escargot developed a double-bristle phenotype (Yang et al., 2010). Interestingly, adult stem cells in the midgut of *Drosophila* are further examples for a general role of Escargot and Prospero in cell proliferation. Here, Escargot labels a population of diploid cell, which give rise to Prospero positive cells (Micchelli and Perrimon, 2006).

On wildtype palps, increased levels of Escargot and Nerfin-1 induced ectopic CO_2 neuron development. This effect was not induced by sheer inhibition of apoptosis through p35 or enhancement of cell cycle progression through CyclinE. Thus, Escargot and Nerfin-1 in combination are necessary and sufficient for CO_2 neuron suppression on the MP.

In conclusion, *miR-279* and Prospero act in a powerful and temporally defined way on CO_2 neuron suppression on the maxillary palp in *Drosophila*. This suppression is achieved through the tight repression of Escargot and Nerfin-1, both being powerful regulators of nervous system development (Kuzin et al., 2005; Yang et al., 2010). The combinatorial effect of Escargot and Nerfin-1 could be shown to act specifically on CO_2 neuron development. Therefore, I identified a regulatory network acting on a subsystem of olfactory sensilla. The question how Escargot and Nerfin-1 are cooperating on neuronal differentiation and specification is still not understood.

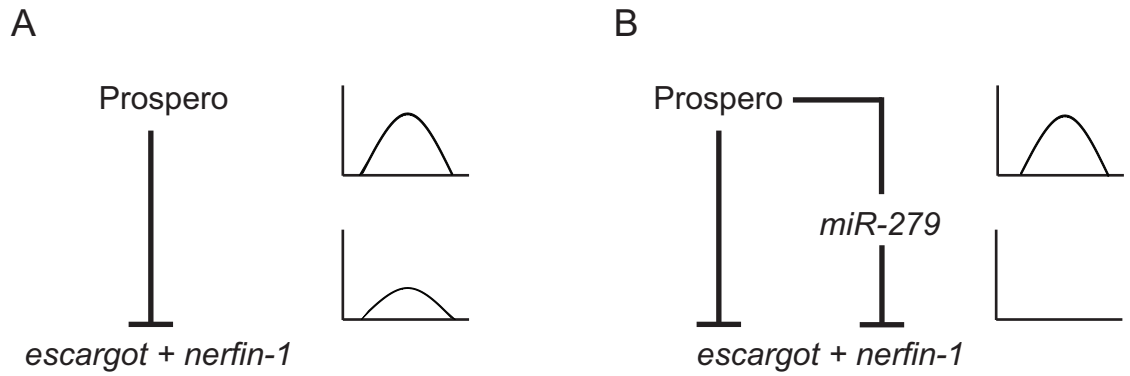

Figure 3.2: Enhancing repression through the use of microRNAs. A. Effect of Prospero's genomic repression on the protein level of Escargot and Nerfin-1. **B.** Prospero's enhanced repressive effect by including *miR-279* in the network. The upper panel illustrates the protein level before repression while the lower panel illustrates the protein level after repression of either Prospero alone or together with *miR-279*.

This question might be resolved by uncovering genes that underly the control of Escargot and Nerfin-1. So far, single mutants neither of Escargot nor Nerfin-1 show a phenotype in the development of CO_2 neurons.

The question which factors are actually directly regulating the expression of the CO_2 receptors remains open. Several steps could be tested to find some answers. One possibility is that Escargot and Nerfin-1 are directly regulating the receptor expression. This hypothesis is rather unlikely since the two transcription factors are expressed really early in development and the expression of the receptors starts only in the late pupal stages. Hence, the temporal overlap between the expression of Escargot and Nerfin-1 and the receptors, Gr21a and Gr63a, might be missing. Therefore the factors which are in the *miR-279*/ Prospero pathway to regulate CO_2 receptor expression remain to be elucidated. Interestingly, mutations in components of the DREAM complex resulted in mistargeting of the CO_2 receptor expressing neurons to the medial glomerulus (personnel communication by Anananda Ray). The DREAM complex is predicted to directly bind to the Gr21a receptor enhancer. Whether this complex is downstream of Escargot and Nerfin-1 is still elusive.

3.3 Evolvability of sensory systems

The olfactory receptors for CO_2 of flies and mosquitoes are highly conserved (Jones et al., 2007; Kwon et al., 2007). In contrast to the sequence similarity, the localization and the targeting pattern of CO_2 neurons differ between both species (Jones et al., 2007; Kwon et al., 2007;

Ghaninia et al., 2007; Lu et al., 2007). Moreover, the behavior triggered by CO_2 is opposite, as flies strongly avoid CO_2, whereas mosquitoes are highly attracted and use the cue for host detection (Suh et al., 2004; Guerenstein and Hildebrand, 2008). I showed that flies mutant for either Prospero or *miR-279*, develop ectopic CO_2 neurons on the maxillary palp whithout affecting the antennal CO_2 neurons. The ectopic neurons mistarget to a medial glomerulus and respond to CO_2. Throughout development, the ectopic neurons are formed within basiconic sensilla altering the 2-neuron sensilla type to a 3-neuron type. In all analyzed aspects, the ectopic CO_2 neurons due to the *pros*^{IG2227} or *miR-279* $^{962-7}$ mutations highly resemble mosquito CO_2 neurons (Ghaninia et al., 2007; Lu et al., 2007). Together with the intact antennal CO_2 neurons, the mutant flies might represent an evolutionary intermediate state between fly and mosquito (Cayirlioglu et al., 2008; Jones, 2008). Interestingly, a single mutation in only one microRNA or a transcription factor can promote such dramatic changes in OSN choice and wiring.

Do the genes identified as supressors of CO_2 neurons also play a role in the malaria mosquito *Anopheles gambiae (aga)*? The comparison is worthwhile as all candidate genes are conserved in *Anopheles gambiae*. Two different changes might have occurred in the evolution of *Anopheles* and *Drosophila*. First, the homologues of *escargot* and *nerfin-1* in mosquito might not be recognized by *aga-miR-279* and therefore might not be suppressed. Variations in the 3'UTR sequences and length are most likely to trigger such changes. According to prediction tools, *aga*-Nerfin-1 and *aga*-Escargot are no longer targets of *aga-miR-279*. A preliminary 3'RACE to determine the length of the mosquito nerfin-1 3'UTR indeed showed that the sequence is shortened as compared the *Drosophila* nerfin-1 3'UTR. Predictions and preliminary results suggest that the regulatory 3'UTR changed throughout evolution and might have varied the target selection of *miR-279*. Second, the expression of all mosquito candidate genes including *miR-279* might be altered through changes in the enhancer that could lead in turn to a recruitment of different *trans* factors.

Another interesting aspect of these results is that relocation of OSNs from MP to antenna might have triggered the expression of a different behavior from attraction to avoidance. The relocation of the OSNs coincided with a change in wiring of the neurons. The ectopic CO_2 neurons target to the medial glomerulus, which is in mosquito and *Drosophila* associated with the detection of food odors (Ghaninia et al., 2007; Fishilevich and Vosshall, 2005; Couto et al., 2005). Interestingly, a recent study showed that attraction behavior is dependent on a single glomerulus (Semmelhack and Wang, 2009). Redirecting the wiring to another glomerulus might be sufficient to connect an odor to different neuronal circuits that in turn change the behavior. However, mutant flies of *miR-279* tested in a behavioral paradigm still avoid CO_2, which might

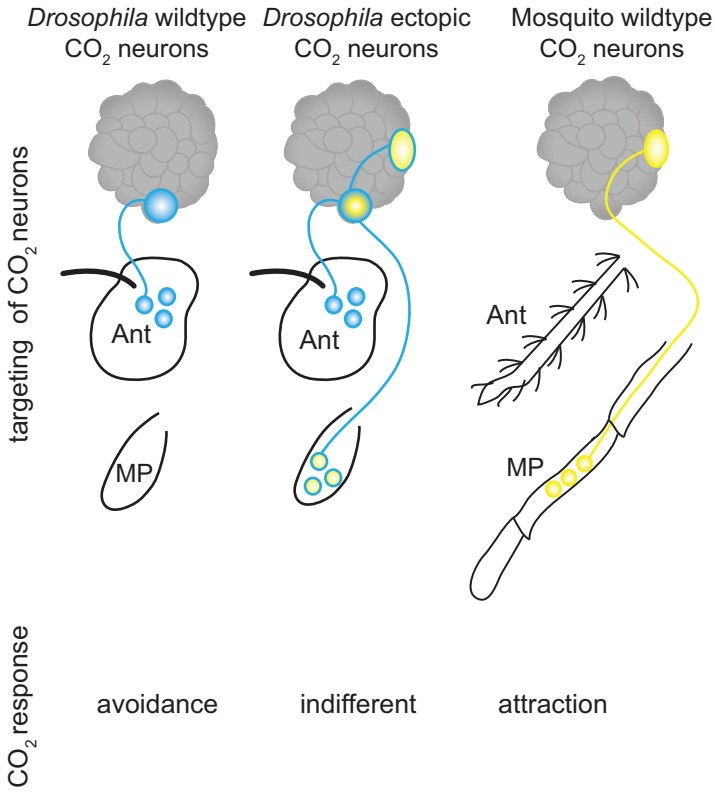

Figure 3.3: Comparison of CO_2 neuron targeting and behavioral output. In wildtype Drosophila CO_2 neurons are expressed on the antenna and target the V-glomerulus. These flies strongly avoid the gas. In *miR-279* and Prospero mutant flies, CO_2 neurons are also expressed on the maxillary palp and target the medial glomerulus. Mutant flies behave indifferent toward the gas. Mosquito CO_2 neurons are formed exclusively on the maxillary palp and target a medial food-associated glomerulus. Blood-feeding mosquitoes use CO_2 for host detection and are highly attracted to the gas.

be due to the unimpaired CO_2 neurons on the antennae (Cayirlioglu et al., 2008). After removal of the antennae, flies were still not attracted but indifferent to CO_2. Given that the sensilla of the ectopic CO_2 neurons connect to a food related glomerulus are functional, starvation might promote attraction behavior.

In case of blood-feeding mosquitoes the advantage to be attracted to CO_2 as part of host detection and thereby ensuring food supply is obvious, however, the avoidance of *Drosophila* is not fully understood yet. Although CO_2 is probably used as a conspecific alarm signal, flies do not avoid CO_2 emitted by yeast and fruits. How flies can distinguish in a context dependent manner, maybe in computing food odors and CO_2 is only studied in the periphery. Chemicals present in ripening fruits and produced as by-product of fermentation can inhibit the activity of CO_2 neurons (Turner and Ray, 2009). Moreover, how gustatory attraction to CO_2 (Fischler

et al., 2007) is integrated with olfaction-mediated avoidance, is also not studied yet. Possibly, the different qualities of short, when the fly tastes CO_2, versus long range stimulation, when the fly smells CO_2, allow for an appropriate discrimination (Scott, 2011). However, the involved cellular mechanisms are not yet identified.

3.4 Conclusion

The presented work unraveled a regulatory network that is involved in the suppression of CO_2 neuron formation on the maxillary palp of Drosophila. The identified network shows for the first time that the broadly acting transcription factor Prospero employs a microRNA to tightly control the expression of targets that are also repressed on the genomic level. This finding first exemplifies the need of tight regulation of developmentally powerful genes. Second it shows how a broadly acting factor acts on a defined subset of olfactory neurons. Prospero is expressed in almost every neuronal cell in the fly. Therefore it is hard to imagine, how the transcription factor might contribute to the differentiation of specific cell types. In this study, the usage of a specific microRNA to tightly regulate target genes or mRNAs might be one answer to this question. Another aspect might be the hypomorphic nature of the studied Prospero allele. In contrast, to the complete loss of Prospero, which additionally and more prominently showed a neuronal loss, the hypomorphic allele specifically acted in the neuron number in two olfactory neuron classes on the MP. This argues for the observation that neurogenic factors act on a temporally and level dependent manner to generate variety in different sensilla subtypes.

Since the formation of ectopic MP CO_2 neurons which perform mistargeting to the medial glomerulus highly resembles the CO_2 neuron pattern found in mosquito, the regulatory elements detected might have played a role in the evolution of flies and mosquitoes. Whether these factors also play a role in mosquito might be the next interesting question to answer. Studying the factors further might answer, how sensory neurons relocate throughout evolution from one appendage to another and why this re-location alters wiring and the underlying behavior. The comparison of flies and mosquito and their behavior toward CO_2 is especially interesting since the two species represent two extreme cases. How in evolution attraction was changed into avoidance could be answered by elucidating the mosquito factor guiding CO_2 neuron development.

Apart from that, studying microRNAs seemed to be feasible in a model organism like *Drosophila* which proofed to be genetically easily modifiable and the number of *Drosophila* microRNAs is limited. However, *miR-279* is among the few microRNAs which show a phenotype. Recent studies showed that apart from the CO_2 neurons the microRNA is also involved in specifying migratory border cells vs. non-migratory follicle cells in the *Drosophila* ovary (Yoon et al., 2011). Non-migratory cells distinguish themselves from migratory cells through low levels of unpaired (Upd) and hence reduced STAT levels. *miR-279* was shown to directly repress STAT and thereby reinforces the cellular fate to become a follicle cell. In another context,

miR-279 mutants showed a phenotype in the circadian rhythm. Unlike control flies, *miR-279* mutants exhibited arrhythmic behavior. On the molecular level, *miR-279* was shown to repress *Upd* in the output neurons of the circadian clock. Interestingly, the microRNA could be a molecular link between the internal clock to cells that regulated rest and activity (Luo and Sehgal, 2012). In both studies, *miR-279* is regulating components of the JAK/STAT pathway. The two studies exemplify that microRNAs are important in developmental processes but also act in the fully differentiated organism to regulate behavior. Therefore *miR-279* could be used to study, how a single microRNA is differently regulated in various systems imposing different cell fates. Thereby, a more complete picture how cellular identities are specified using common factors would be achieved.

Chapter 4

Material and Methods

4.1 Molecular techniques

4.1.1 Media

LB media (per liter)

- 10g NaCl
- 10g tryptone
- 5g yeast extract
- 20g agar
- pH 7 (NaOH)

For selection:

- add appropriate antibiotic e.g.100 μg/ml Ampicilin, 50 μg/ml Kanamycin or 30 μg/ml Chloramphenicol
- for plates + 15g Agar

NZY plus media (per liter)

- 10g NZ amine
- 5g yeast extract

- 5g NaCl
- pH 7.5

after autoclaving, add the following sterile filtered solutions:

- 12.5ml of 1M $MgCl_2$
- 12.5ml of 1M $MgSO_4$
- 10ml of 2M glucose solution

4.2 Enzymes and Standards

Polymerases:

- Taq (NEB)
- Takara Taq

Restriction enzymes were purchased from NEB and used according to the manufacturers instructions.

4.3 Commercial Kits

- Maxi prep Kit (Qiagen)
- Spin Mini prep Kit (Qiagen)
- Gel Extraction Kit (Qiagen)
- PCR product purification Kit (Qiagen)
- MultiSite Directed Mutagenesis (Stratagene)
- Magna EZ ChIP Kit (Millipore)
- Effectene Transfection Reagent (Qiagen)

4.4 Oligonucleotides

mutagenesis primer

mutP1 fwd acagttcaaatgtgccgtctaatttctaatgatttaatttc

mutP2 fwd gcgcgtgtgtaagacgttgattgttagtgtacgg

mutP3 fwd cctggtacaatgaagattcgcatttagaataaggca

mutP4 fwd gggaggaaagcattcacagacaacaacccttctggg

EMSA oligos

P1 fwd gatgcaagcagcatttacagttcaaatgtgccgtctaattagaaatgatttaatttcaat

mutP1 fwd gatgcaagcagcatttacagttcaaatgtgccgtctaatttctaatgatttaatttcaat

P4 fwd gagggtagcgcaaggaaaggggaggaaagctaagacagacaacaacccttctggg

mutP4 fwd gagggtagcgcaaggaaaggggaggaaagcattcacagacaacaacccttctggg

3'UTR primer

3'UTR escargot primer fwd acctcgagggcaatatatttatatatac

3'UTR escargot primer rev acgcggctgtatgtaaataaaat

miR-279 promotor primer

miR-279 promotor fwd gagctcgaaatgccagtattgcaaac

miR-279 promotor rev ctcgagcaaatactaagaaaatcaat

4.5 Plasmids

- TOPO-TA (Invitrogen)
- TOPO pENTR (Invitrogen)
- pGEX-prosL (Cook et al., 2003)
- pUAStattB-prospero (fulllength)

- RNAi prospero (VDRC)
- RNAi insulin receptor (VDRC)
- pGl3 (empty) (Promega)
- miR-279 promotor-pGl3 (Hartl et al., 2011)
- miR-279 promotor-2x mutated-pGL3
- miR-279 promotor-4x mutated-pGl3
- pTK Renilla (Promega)
- psi-CHECK2 (Promega)
- psi-CHECK2-nerfin-1 3'UTR (Cayirlioglu et al., 2008)
- psi-CHECK2-escargot 3'UTR (Hartl et al., 2011)
- UAS-dsred-miR-279 (Cayirlioglu et al., 2008)
- UAS-dsred-miR-315 (Cayirlioglu et al., 2008)
- ubiquitin-Gal4 (Cayirlioglu et al., 2008)

4.6 Bacteria Strains

Chemically competent cells, TOP10, were purchased from Invitrogen and were used for amplification of plasmids and cloning. For overexpression of the homeodomain of Prospero, Bl21 cells were used, as these strain is deficient of the *lon(8)* and the *ompT* proteases. The strain purchased from Novagen (Bl21(DE3)plysS) had an additional copy of a lysis enzyme that allowed for an easier lysis of the cells.

4.7 Antibodies

4.7.1 Primary and Secondary Antibodies for Immunohistochemistry

Primary antibodies were used in the following dilutions:

- mouse α-NC82 (DSHB), 1:20;
- mouse α-Disclarge (DSHB), 1:50;
- mouse α-Prospero (DSHB), 1:20;
- mouse and rat α-Elav (DSHB), 1:50;
- rabbit and mouse α-GFP (Clontech), 1:2000 and 1:500, respectively.

All secondary antibodies were ordered from Dianova and used at 1:200:

- α-mouse-CY5
- α-rat-CY3
- α-rabbit-488

4.7.2 Antibodies for ChIP Assay

For Chromatin Immunoprecipitation of FLAG-Prospero, the M2 α-FLAG antibody from Sigma was used.

4.8 Molecular Techniques

4.8.1 Molecular Cloning

Molecular cloning was performed using the classical restriction enzyme digest which leads to sticky ends followed by a ligation of the digested vector and insert using the T4 ligase (NEB).

4.8.2 Electromobility Shift Assay (EMSA)

For the electromobility shift assay the homeodomain of Prospero was purified from BL21 cells transfected with the construct pGex-prosL that was kindly provided by Tiffany Cook. Oligos containing the predicted Prospero binding sites were annealed and radiolabeled with $[\gamma^3 2P]$ ATP using T4 polynucleotide kinase (Fermentas).

P1fwd gatgcaagcagcatttacagttcaaatgtgccgtctaattagaaatgatttaatttcaat

mutP1fwd gatgcaagcagcatttacagttcaaatgtgccgtctaatttctaatgatttaatttcaat

P4fwd gagggtagcgcaaggaaaggggaggaaagctaagacagacaacaacccttctggg

mutP4fwd gagggtagcgcaaggaaaggggaggaaagcattcacagacaacaacccttctggg

The labeled oligos were mixed with the purified proteins in binding buffer (20mM HEPES pH7.5, 100mM NaCl, 1mM DTT, 5mM $MgCl_2$) and incubated for 20min at RT. Subsequently the mixture was loaded on a 0.5% TBE pre-run minigel. The gel was dried and exposed to a Phospho screen overnight.

4.8.3 Chromatin immunoprecipitation (ChIP)

Embryos (*UAS-Flag-Pros*/X; *actin-Gal4*/+) were collected and fixed as previously described (Sandmann et al., 2006). The embryos were fixed in a crosslinking solution (50mM HEPES, 1mM EDTA, 0.5mM EGTA, 100mM NaCl, pH 8,0) for 15min under vigorous shaking. The crosslinking solution was stopped by adding PBS with 125mM glycine and 0.1% Triton-X. Embryos were washed twice with PBT (0,1% Triton-X), dried and frozen in -80 C. For cell lysis embryos were dounced in PBS with 0.1% Triton-X and protease inhibitor, centrifuged and the pellet dissolved in cell lysis buffer (5mM HEPES pH 8.0, 85mM KCl, 0.5% NP-40 and protease inhibitor). After the centrifugation, the pellet was dissolved in nuclear lysis buffer (50mM HEPES pH 8.0, 10mM EDTA, 0,5% N-Laurylsarkosin and protease inhibitor) and incubated at room temperature for 20min. Lysates were sonicated (Sonicator sonoplus, Bandelin) until an approximate fragment length of 500-1000bp was achieved. The sheared chromatin fragments were incubated overnight with magnetic beads and α-FLAG M2 (Sigma) to detect Flag-Prospero or mouse IgG as unspecific binding control. Beads were washed and the bound chromatin was eluted according to the manufacturer's instructions (Magna ChIP G Kit, Millipore). The chromatin was checked for the presence of *miR-279* enhancer fragments by PCR using the following primer sets:

ChIP P4 fwd gtatataatggacaagaagaagaataagcag

ChIP P4 rev catgcggaatttcagttgtttccttttatatc

An input control was included into the PCR.

4.9 Cell Culture Lines

Drosophila Schneider cells (S2) (Invitrogen) were grown in cell culture. The S2 cell line was derived from a primary culture of late stage (20-24 hours old) *Drosophila melanogaster* embryos

(Schneider, 1972). S2 cells were incubated at 25°C without CO_2 as a loose, semi-adherent monolayer in tissue culture flasks. For maintenance, S2 cells were splitted in a ratio of 1:3 or 1:10 and further incubated for 3 or 7 days, respectively.

4.9.1 Promotor S2 Cell Analysis

The genomic 2kb upstream region of *miR-279* was amplified and cloned into the pGL3 vector. This putative enhancer region was further mutagenised at the predicted conserved Prospero binding sites using the Stratagene QuickChange Lightning Multi Site-Directed Mutagenesis Kit. The following primers were used to perform the nucleotide exchange:

mutP1 fwd acagttcaaatgtgccgtctaatttctaatgatttaatttc

mutP2 fwd gcgcgtgtgtaagacgttgattgttagtgtacgg

mutP3 fwd cctggtacaatgaagattcgcatttagaataaggca

mutP4 fwd gggaggaaagcattcacagacaacaacccttctggg

S2 cells were transfected with a reporter construct carrying either the wild type enhancer fragment, a promoter fragment with mutated sites P1 and P2 or a construct with mutations at all putative and conserved Prospero binding sites. For normalization, the pTK Renilla vector that expresses the Renilla luciferase was co-transfected. Both vectors were used in a concentration of 500ng. The 10^6 cells were seeded in 6-well plates and transfected the next day with the constructs described. For transfection the Effectene transfection reagent (Qiagen) was used according to the manual provided. Approximately 16h after transfection the cells were lysed and luciferase expression assayed using the Dual Luciferase Kit (Promega) according to the manufacturer's instructions. For overexpression of Prospero, a full length EST (LD37627 from BDGP) was subcloned into the pattB-UAS vector (donation from the Basler lab). The RNAi pros construct was a gift from the VDRC library (Construct ID 109284). To drive the expression of both constructs ubiquitin-Gal4 was co-transfected. All experiments were performed in triplicates.

4.9.2 3'UTR S2 Cell Assay

To generate luciferase targets, we amplified a 1.8kb *nerfin-1* fragment (including the entire 3'UTR and 220bp of downstream sequence), and a 644bp *escargot* 3'UTR fragment and cloned

these downstream of the renilla luciferase coding region in psiCHECK2; this vector contains an internal firefly luciferase gene that serves as an internal control. For the *miR-279* expression construct, I cloned 415 bp of genomic sequence, centered on the *miR-279* hairpin, into the 3'UTR of UAS-DsRed. Different 3'UTRs were fused to a luciferase reporter construct. psiCheck, a control 3'UTR; the entire nerfin-1 3'UTR; escargot 3'UTR with one predicted *miR-279* binding sites. Subsequently, I transfected 100 ng target, 50 ng ub-Gal4 and 100 ng UAS-DsRed-*miR-279* plasmids into 1x10^6 S2 cells in 24 well format. For transfection the Effectene transfection reagent (Qiagen) was used according to the manufacturer's instructions. Three days later, the cells were lysed, subjected to the dual luciferase assay (Promega) and analyzed on a plate luminometer (Tecan). Triplicate transfections were performed and data of four repetitions were pooled.

4.10 Fly Maintenance and Genetics

4.10.1 Fly Food and Rearing Conditions

Crosses and weak stocks were maintained on standard medium at 25°C at around 60-70% humidity. The general stock maintenance was at 18°C. For selection of markers, flies were anesthetized using CO_2.

4.10.2 Genotypes

Control:

eyflp;Gr21a-Gal4,UAS-mCD8GFP/+;FRT82/FRT82Gal80E2F

eyflp;Gr21-sytGFP/+;FRT82/FRT82Gal80E2F

eyflp;miR-279-Gal4,UAS-mCD8GFP/+; FRT82/FRT82Gal80E2F

hsflp;Elav-Gal4,UAS-mCD8GFP/+; FRT82/FRT82Gal80

hsflp;miR-279-Gal4,UAS-mCD8GFP/+; FRT82/FRT82Gal80E2F

eyflp; Gr21a-sytGFP actGal4;FRT82/FRT82ClGal80

eyflp; Gr21a-sytGFP actGal4/RNAipros; FRT82/FRT82ClGal80

eyflp; Gr21a-Gal4 UASmCD8GFP/ RNAinerfin-1; FRT82 /FRT82ClGal80

eyflp; Gr21a-sytGFP actGal4/RNAispineless; FRT82/FRT82ClGal80

(a.o. RNAi constructs against *gcm*, *senseless*, Ptx1)

eyflp; Gr21a-Gal4 UASmCD8GFP/ escargotk00606; FRT82 /FRT82ClGal80

eyflp; Gr21a-Gal4 UASmCD8GFP/ +; FRT82 hb9^{kk30}/FRT82ClGal80

eyflp; Gr21a-Gal4 UASmCD8GFP/ +; FRT82 /FRT82ClGal80

eyflp; OrX-Gal4 UASsytGFP/+; FRT82/FRT82ClGal80

eyflp; OrX-Gal4 UASmCD8GFP/+; FRT82/FRT82ClGal80

eyflp; FRT40A/FRT40A GAL80 or CL;Gr21a-GAL4,UASmCD2

Mutants: The *miR-279* $^{962-7}$ resulted from a P-element insertion in the enhancer region of the *miR-279* gene (Cayirlioglu et al., 2008). The hypomorphic allele of Prospero, *pros*^{IG2227}, resulted from a point mutation due to EMS mutagenesis (Hartl et al., 2011). *pros*^{17} is a complete loss-of-function allele of Prospero (Manning and Doe, 1999). *pros*^{voila78} represents a hypomorphic allele of Prospero which resulted from a P-element insertion into the enhancer region of Prospero followed by an imprecise excision (Grosjean et al., 2001).

eyflp;Gr21a-Gal4,UAS-mCD8GFP/+;FRT82 mutant/FRT82Gal80E2F

eyflp;Gr21-sytGFP/+;FRT82 mutant/FRT82Gal80E2F

eyflp;miR-279-Gal4,UAS-mCD8GFP/+; FRT82 mutant/FRT82Gal80E2F

hsflp;miR-279-Gal4,UAS-mCD8GFP/+; FRT82 mutant/FRT82Gal80E2F

hsflp, Elav-Gal4UASmCD8GFP; FRT82 mutant/FRT82Gal80

eyflp; Gr21a-sytGFP actGal4; FRT82 mutant/FRT82ClGal80

eyflp; Gr21a-sytGFP actGal4/ UASmiR-279 or UASpros or UASnerfin-1;FRT82 mutant/FRT82ClGal80

eyflp; Gr21a-sytGFP actGal4/ RNAinerfin-1; FRT82 mutant/FRT82ClGal80

eyflp; Gr21a-Gal4 UASmCD8GFP/ RNAipros; FRT82 mutant/FRT82ClGal80

eyflp; Gr21a-sytGFP actGal4/RNAispineless; FRT82 mutant/FRT82ClGal80

(a.o. RNAi constructs against *gcm*, *senseless*, Ptx1)

eyflp; Gr21a-Gal4 UASmCD8GFP/ +; FRT82 mutant hb9kk30/FRT82ClGal80

eyflp; Gr21a-Gal4 UASmCD8GFP/ escargot^{k00606}; FRT82 mutant/FRT82ClGal80

eyflp; Gr21a-Gal4 UASmCD8GFP/+; FRT82 mutant nerfin^{159}/FRT82ClGal80

eyflp; OrX-Gal4 UASsytGFP/+; FRT82 mutant/FRT82ClGal80

eyflp; OrX-Gal4 UASmCD8GFP/+; FRT82 mutant/FRT82ClGal80

eyflp; FRT40A escargot^{k00606}/FRT40A GAL80 or CL;Gr21a-GAL4,UASmCD2

eyflp;Gr21a-sytGFP actGal4/ UASescargot or UASnerfin-1

or *UASescargot, UASnerfin-1; FRT82/FRT82ClGal80*

eyflp;Gr21a-sytGFP actGal4/ UASp35 or UAScyclinE; FRT82/FRT82ClGal80

4.10.3 eyeless Flp

For large clones in the antenna and the maxillary palp an eyeless-FLP insertion on the X chromosome was used. The eyeless promotor used was previously described for the visual system (Newsome et al., 2000). The construct used generates around 50-70% mutant cells in the olfactory appendages.

4.10.4 MARCM

The Mosaic Ananlysis with a Repressible Cell Marker technique (MARCM) is widely used in *Drosophila* in order to generate and label mutant cells in a tissue specific manner (Lee and Luo, 2001). To do so, the Gal4/UAS system (Brand and Perrimon, 1993) is combined with Gal80 to repress the expression of Gal4. Heterozygous cells carry the Gal80 transgene *in trans* to the mutation but on the same chromosomal arm as the mutated gene of interest. Upon mitotic recombination mediated by the FRT/FLP system, Gal80 is removed from the homozygous mutant cell. Hence, the expression of the fluorescent label by the Gal4/UAS system is possible and allows the detection of mutant cell and their daughters.

4.10.5 The Screen for Mutant Alleles

The screen that revealed the hypomorphic Prospero and the loss-of-function *miR-279* $^{962-7}$ (Cayirlioglu et al., 2008) mutant alleles was performed on a library of P-element insertion lines and EMS mutants that were *per se* lethal. In order to be able to analyze them MARCM and FRT/FLP mosaic analysis that rendered only the tissues where *eyFLP* was active mutant while the rest of the fly remained wildtype. To analyse phenotypes, the mutant cells were labeled by three different subsets of olfactory receptors (Or47a, Or47b and Gr21a). The screen resulted in three *miR-279*-like mutants out of 6000 analyzed mutants on the third chromosome that were analyzed.

4.10.6 MARCM Analysis of Lethal Mutant Alleles

MARCM analysis was carried out on flies of either sex of the following genotype: *hsFLP or eyFLP; OR-gal4 UAS-sytGFP (or UAS-mCD8GFP)/+; FRT82 mutation/FRT82 Gal80 (E2F)*. ORN labeling was achieved by fusing the promoter-elements to *GAL4* or directly to synaptotagmin-GFP. Mutations included *FRT82B miR-279*$^{962-7}$ (Cayirlioglu et al., 2008), *FRT82B pros*^{17} (Manning and Doe, 1999), *FRT82B pros*^{IG2227} (Hartl et al., 2011), and *FRT82B pros*^{voila78} (Grosjean et al., 2001). All analyses were done in mosaic animals. Gr21a transcriptional reporter was used for CO_2 neurons (i.e. *Gr21a-GAL4* driving membrane-bound GFP (UAS-mCD8GFP)), to detect cell bodies in the antenna and the maxillary palp. *Elav-GAL4* was used to label neurons. *miR-279-GAL4* contains the 2kb DNA stretch upstream of *miR-279* gene. As previously shown, this driver rescues the mutant phenotype of *miR-279* loss-of-function allele (Cayirlioglu et al., 2008). *miR-279-GAL4* was used to label cells and their daughter cells expressing *miR-279* in mosaic animals. Alternatively, a transgene provided by S. Cohen was used to detect *miR-279* activity *in vivo*: miR-sensor. Sensor constructs contain a green fluorescent protein (GFP) driven by a tubulin-promotor. The GFP is fused to a 3'UTR that in our case contained several binding for *miR-279*. In cells where the microRNA is present the GFP in the miR-sensor is downregulated, while in cells without *miR-279*, GFP is expressed. Therefore, the miR-sensor is a reporter for the activity of the microRNA in the tissue. In the control sensor construct any 3'UTR is absent. Therefore, the construct is expressed wherever the utilized tubulin-promotor is active. I analyzed the expression of the sensor constructs in the embryonic CNS.

4.10.7 Rescue and Genetic Interaction Experiments

Rescue and genetic interaction experiments were carried out by using cDNAs fused to UAS transcriptional response elements. UAS-construct expression was under the control of the β-actin promoter, but the expression was restricted to only the mutant tissue in the MP and antenna upon eyFLP expression and mitotic recombination. *UAS-Pros* constructs were generated and generously provided by F. Matsuzaki, C. Doe, and A. Brand. *UAS-dsred-miR-279* was a gift by E. Lai. *UAS-nerfin* transgenic flies and *nerfin-1* loss-of-function alleles were generously provided by Ward Odenwald. *UAS-escargot* was ordered from Bloomington.

4.10.8 RNAi Flies

Transgenic flies carrying RNAi constructs were ordered from the VDRC or Kyoto stock centers. RNAi was expressed in exactly the same manner as the UAS constructs in mutant tissue of antenna and MP only.

4.10.9 Genetic Interaction Using Loss-of-Function Alleles

The number of ectopic CO_2 neurons was tested mutant alleles of Prospero *pros*^{IG2227} and in the *miR-279* mutant background. Also heterozygous mutations of *escargot* (P(lacZ)esg) and *nerfin-1*(*nerfin*^{159}) and a combination of both was introduced in the mutant background. The ectopic neurons in the MPs were counted and compared. *Escargot* loss-of-function and P(lacZ)esg flies were ordered from the Bloomington stock center.

4.10.10 Collection of Embryos

The plates for embryo collection contained 23g of danish agar (Roth) boiled in 1l of apple juice. The flies were put in a collection cage that was closed by a apple agar plate. The plates were exchanged twice per day, in the morning after an overnight collection and in the evening. The collected eggs covered all developmental stages in about the same ratios. The embryos were on the plate dechorinated in 30% bleach(Sigma) for 2 min at RT. The dechorinated embryos were collected in a sieve and rinsed extensively with tap water. It is important to remove the bleach completely from the embryos. For fixation the embryos were transferred in an Eppendorf tube that contained 50% Heptan, 45% PBS and 5% Formaldehyde. Under vigorous shaking to mix the two phases of the solution the tissue was fixed for 21min at RT. The lower layer was subsequently removed, replaced with Methanol and again removed. These sequence was

repeated until the embryos were fully soaked with Methanol and sink down in the Eppendorf tube. At this step they can be frozen at -20°C. To avoid bleaching of GFP, methanol can be replaced by 70% Ethanol.

4.10.11 Tissue Dissection and Antibody Staining

For the analysis of ORN axon targeting in the adult brain, eyFLP mosaic flies were dissected, adult brains were fixed, and immunostained. For analysis of cell body number and position, heatshock and eyFLP were used to create mosaic mutant tissue. Quantifications of ORN number were carried out on adult MPs and antennae. Detailed developmental analysis was carried out with eyFLP mosaic clones. Analysis in the developing olfactory neurons was carried out with the use of eyFLP and hsFLP. White pupae were selected and incubated at 25°C until the stage of interest was reached. MPs and antenna regions were dissected in ice cold PBS and collected in 4% PFA on ice. Upon fixation for 1h at RT in 4% PFA in PBL, tissues were washed 2x 15 min in PBS-0.5% Triton, followed by 1h incubation in blocking solution (20% donkey serum, 0.5% Triton in PBS). Primary antibody was incubated over night at 4°C in blocking solution without Triton. After washing 2x 15 min in PBS-0.5% Triton, tissues were incubated with secondary antibody for 1h at RT in blocking solution without Triton. Tissues were washed once again for 2x 15 min in PBS-0.5% Triton and mounted with Vectashield mounting medium. Dechorinated and fixed Embryos were first stained following the same procedure as described above. After staining the embryonic CNS was dissected using thin needles. All tissues were analyzed using confocal microscopy at an Olympus FV1000 or a Leica SP2 confocal. Pictures were processed in Adobe Photoshop, Adobe Illustrator, ImageJ, and Microsoft PowerPoint. For sensor quantification, single sections at comparable position between wild type and mutant, taken at same intensities and resolution, were divided into seven regions of interest (ROI). The mean of pixel intensity was quantified using ImageJ software and plotted using Microsoft Excel.

solution:

PBL:

PBS + Triton-X

4% PFA

0.1M Na_2 HPO_4

100 mM Lysine (1) HCl

pH 7.4

Primary antibodies were used in the following dilutions:

- mouse α-NC82 (DSHB), 1:20;
- mouse α-disclarge (DSHB), 1:50;
- mouse α-prospero (DSHB), 1:20;
- mouse and rat α-Elav (DSHB), 1:50;
- rabbit and mouse anti-GFP (Clontech), 1:2000 and 1:500, respectively

All secondary antibodies were ordered from Dianova and used at 1:200:

- α-mouse-CY5
- α-rat-CY3
- α-rabbit-488

4.10.12 Electrophysiology

genotype of control fly analysed: *eyflp; Gr21aGal4 UASmcD8GFP; FRT82ClGal80/FRT82*

genotype of mutant fly analysed: *eyflp; Gr21aGal4 UASmcD8GFp; FRT82 pros*^{IG2227} *or miR-279* $^{962-7}$

Extracellular single sensillum recordings from maxillary palp were performed according to the procedure described previously (de Bruyne et al., 1999). Briefly, a fly was trapped into a truncated pipette tip with its proboscis protruding out and mounted on a glass slide. The protruding proboscis and maxillary palps were secured and stabilized on a coverslip with the help of a tapered glass micro pipette. The preparation was visualized with a Leica DM6000 FS microscope at 750X magnification and maxillary palp basiconic sensilla were identified by the expression of GFP in mutant flies *eyflp; Gr21aGal4 UASmcD8GFp; FRT82 pros*^{IG2227} *or miR-279* $^{962-7}$. A glass reference electrode filled with 0.01M KCl was inserted into the eye and a recording glass electrode filled with the same solution was used to record from the maxillary palp basiconic sensilla. Action potentials were recorded using a CV-7B headstage and MultiClamp 700B amplifier (Molecular Devices). The signals were sampled at 10 KHz and digitized and fed

into a computer by Digidata 1440A. The spikes were visualized and recorded in Clampex 10.2 acquisition software and sorting of spikes were done manually with Clampfit 10.2 software off line. A continuous and humidified airstream (2000 ml/min) was delivered to the fly throughout the experiment via an 8mm diameter glass tube positioned 10mm away from the preparation. A custom-made odor delivery system was used for stimulation in all experiments (Smartec, Martinsried). For CO_2 stimulation, 500 ms pulses of CO_2 were delivered into the continuous airstream with the help of mass flow controllers and solenoid valves. For odor stimulation, specific odors were diluted 1:10 in paraffin oil and 300 ml/min odor pulse were delivered into the continuous airstream using headspace method. During the odor stimulation the continuous airstream flow was maintained always at 2000 ml/min with the help of mass flow controllers and solenoid valves. The spikes in the recorded traces were sorted according to spike amplitude. The spike quantification was done by counting number of spikes over 500 ms duration immediately after the onset of CO_2 response and subtracting from the number of spikes counted over a 500 ms window before the stimulation. The obtained number of spikes were doubled and presented as spikes/s.

4.11 *in silico* Analysis

4.11.1 Bioinformatic Analysis

The presence of the Prospero binding motifs TWAGVYD (Cook et al., 2003) or CWYNNCY (Choksi et al., 2006) in the 2kb upstream region of the *miR-279* gene was tested using the RSA tools software. The predicted putative binding sites were further evaluated by testing the conservation in 6 different Drosophila species (*D. melanogaster, D. yakuba, D.simulans, D. erecta, D. ananassae, D. pseudoobscura*) using the VISTA genome browser.

RSA tools software: `http://rsat.ulb.ac.be/rsat/genome-scale-dna-pattern_form.cgi`

VISTA genome browser: `http://pipeline.lbl.gov/cgi-bin/gateway2`

4.11.2 GO term Analysis and *miR-279* Prediction Tools

A genome wide list of Prospero *in vivo* targets was previously published (Choksi et al., 2006). *miR-279* target gene predictions were generated with the following online software:

TargetScan http://www.targetscan.org/fly_12,

PicTar http://pictar.mdc-berlin.de/cgi-bin/new_PicTar_fly.cgi?species=fly,

miRBase http://www.mirbase.org

Only targets that appeared at least in two of the predictions were used for the comparison to the list of *Prospero* target genes. Gene ontology analysis was carried out using GOstat (Beissbarth and Speed, 2004). All predictions were Benjamini-corrected and GO terms with a $p>0.01$ were disregarded. Targets for aga-miR-279 were predicted using miRBase.

Results can be found here:

http://www.ebi.ac.uk/enright-srv/microcosm/cgi-bin/targets/v5/hit_list.pl?genome_id=377&mirna_id=aga-miR-279&external_name=&gene_id=&go_class=function&go_term=&logic=phrase&terms=

aga-nerfin-1 is AGAP002601, and aga-escargot is AGAP008274

Bibliography

L. Abuin, B. Bargeton, M.H. Ulbrich, E.Y. Isacoff, S. Kellenberger, and R. Benton. Functional architecture of olfactory ionotropic glutamate receptors. *Neuron*, 69:44–60, 2011.

D.-B.G. Akalal, C.F. Wilson, L. Zong, N.K. Tanaka, K. Ito, and R.L. Davis. Roles for *Drosophila* mushroom body neurons in olfactory learning and memory. *Learn Mem*, 13:659–668, 2006.

V. Ambros. The functions of animal microRNAs. *Nature*, 431:350–355, 2004.

C.I. Bargmann. Comparative chemosensation from receptors to ecology. *Nature*, 444:295–301, 2006.

D.P. Bartel. MicroRNAs: Genomics, biogenesis, mechanism, and function. *Cell*, 116:281–297, 2004.

D.P. Bartel. MicroRNAs: Target recognition and regulatory functions. *Cell*, 136:215–233, 2009.

R. Beckervordersandforth, P. Tripathi, J. Ninkovic, E. Bayam, A. Lepier, B. Stempfhuber, F. Kirchhoff, J. Hirrlinger, A. Haslinger, D.C. Lie, J. Beckers, B. Yoder, M. Irmler, and M. Götz. In vivo fate mapping and expression analysis reveals molecular hallmarks of prospectively isolated adult neural stem cells. *Cell Stem Cell*, 7:744–758, 2010.

T. Beissbarth and T.P. Speed. GOstat: Find statistically overrepresented Gene Ontologies within a group of genes. *Bioinformatics*, 20:1464–1465, 2004.

R. Benton, S. Sachse, S.W. Michnick, and L.B. Vosshall. Atypical membrane topology and heteromeric function of *Drosophila* odorant receptors in vivo. *PLoS Biol*, 4:e20, 2006.

R. Benton, K.S. Vannice, C. Gomez-Diaz, and L.B. Vosshall. Variant ionotropic glutamate receptors as chemosensory receptors in *Drosophila*. *Cell*, 136:149–162, 2009.

A. Bethke, N. Fielenbach, Z. Wang, D.J. Mangelsdorf, and A. Antebi. Nuclear hormone receptor regulation of microRNAs controls developmental progression. *Science*, 324:95–98, 2009.

A.H. Brand and N. Perrimon. Targeted gene expression as a means of altering cell fates and generating dominant phenotypes. *Development*, 118:401–415, 1993.

L. Buck and R. Axel. A novel multigene family may encode odorant receptors: A molecular basis for odor recognition. *Cell*, 65:175–187, 1991.

S. Campuzano and J. Modolell. Patterning of the *Drosophila* nervous system: The achaete-scute gene complex. *Trends Genet*, 8:202–208, 1992.

P. Cayirlioglu, I.C.Grunwald Kadow, X. Zhan, K. Okamura, G.S.B. Suh, D. Gunning, E.C. Lai, and S.L. Zipursky. Hybrid neurons in a microRNA mutant are putative evolutionary intermediates in insect CO2 sensory systems. *Science*, 319:1256–1260, 2008.

S.P. Choksi, T.D. Southall, T. Bossing, K. Edoff, E. de Wit, B.E. Fischer, B. van Steensel, G. Micklem, and A.H. Brand. Prospero acts as a binary switch between self-renewal and differentiation in *Drosophila* neural stem cells. *Dev Cell*, 11:775–789, 2006.

T.A. Christensen, B.R. Waldrop, I.D. Harrow, and J.G. Hildebrand. Local interneurons and information processing in the olfactory glomeruli of the moth *Manduca sexta*. *J Comp Physiol A*, 173:385–399, 1993.

T. Cook, F. Pichaud, R. Sonneville, D. Papatsenko, and C. Desplan. Distinction between color photoreceptor cell fates is controlled by Prospero in *Drosophila*. *Dev Cell*, 4:853–864, 2003.

A. Couto, M. Alenius, and B.J. Dickson. Molecular, anatomical, and functional organization of the *Drosophila* olfactory system. *Curr Biol*, 15:1535–1547, 2005.

J.R. Crittenden, E.M. Skoulakis, K.A. Han, D. Kalderon, and R.L. Davis. Tripartite mushroom body architecture revealed by antigenic markers. *Learn Mem*, 5:38–51, 1998.

B.R. Cullen. Derivation and function of small interfering RNAs and microRNAs. *Virus Res*, 102:3–9, 2004.

J.S. de Belle and M. Heisenberg. Associative odor learning in *Drosophila* abolished by chemical ablation of mushroom bodies. *Science*, 263:692–695, 1994.

M. de Bruyne, P. J. Clyne, and J. R. Carlson. Odor coding in a model olfactory organ: The *Drosophila* maxillary palp. *J Neurosci*, 19:4520–4532, 1999.

M. de Bruyne, K. Foster, and J. R. Carlson. Odor coding in the *Drosophila* antenna. *Neuron*, 30:537–552, 2001.

T. Dekker, B. Steib, R.T. Cardé, and M. Geier. L-lactic acid: A human-signifying host cue for the anthropophilic mosquito Anopheles gambiae. *Med Vet Entomol*, 16:91–98, 2002.

T. Dekker, M. Geier, and R.T. Cardé. Carbon dioxide instantly sensitizes female yellow fever mosquitoes to human skin odours. *J Exp Biol*, 208:2963–2972, 2005.

C.Q. Doe, Q. Chu-LaGraff, D.M. Wright, and M.P. Scott. The prospero gene specifies cell fates in the *Drosophila* central nervous system. *Cell*, 65:451–464, 1991.

R.K. Ejsmont, M. Sarov, S. Winkler, K.A. Lipinski, and P. Tomancak. A toolkit for high-throughput, cross-species gene engineering in *Drosophila*. *Nat Methods*, 6:435–437, 2009.

T. Elkins, M. Hortsch, A.J. Bieber, P.M. Snow, and C.S. Goodman. *Drosophila* fasciclin I is a novel homophilic adhesion molecule that along with fasciclin III can mediate cell sorting. *J Cell Biol*, 110:1825–1832, 1990.

K. Endo, T. Aoki, Y. Yoda, K.-I. Kimura, and C. Hama. Notch signal organizes the *Drosophila* olfactory circuitry by diversifying the sensory neuronal lineages. *Nat Neurosci*, 10:153–160, 2007.

K. Endo, M.R. Karim, H. Taniguchi, A. Krejci, E. Kinameri, M. Siebert, K. Ito, S.J. Bray, and A.W. Moore. Chromatin modification of Notch targets in olfactory receptor neuron diversification. *Nat Neurosci*, 15:224–233, 2011.

C. Faucher, M. Forstreuter, M. Hilker, and M. de Bruyne. Behavioral responses of *Drosophila* to biogenic levels of carbon dioxide depend on life-stage, sex and olfactory context. *J Exp Biol*, 209:2739–2748, 2006.

W. Fischler, P. Kong, S. Marella, and K. Scott. The detection of carbonation by the *Drosophila* gustatory system. *Nature*, 448:1054–1057, 2007.

E. Fishilevich and L.B. Vosshall. Genetic and functional subdivision of the *Drosophila* antennal lobe. *Curr Biol*, 15:1548–1553, 2005.

A. García-Bellido. Genetic Analysis of the Achaete-Scute System of DROSOPHILA MELANOGASTER. *Genetics*, 91:491–520, 1979.

A. Garces and S. Thor. Specification of *Drosophila* aCC motoneuron identity by a genetic cascade involving even-skipped, grain and zfh1. *Development*, 133:1445–1455, 2006.

D.M. Garcia, D. Baek, C. Shin, G.W. Bell, A. Grimson, and D.P. Bartel. Weak seed-pairing stability and high target-site abundance decrease the proficiency of lsy-6 and other microRNAs. *Nat Struct Mol Biol*, 18:1139–1146, 2011.

M. Ghaninia, B.S. Hansson, and R. Ignell. The antennal lobe of the African malaria mosquito, Anopheles gambiae - innervation and three-dimensional reconstruction. *Arthropod Struct Dev*, 36:23–39, 2007.

A. Ghysen, C. Dambly-Chaudière, L.Y. Jan, and Y.N. Jan. Cell interactions and gene interactions in peripheral neurogenesis. *Genes Dev*, 7:723–733, 1993.

J.B. Golding, D. Shearer, W.B. McGlasson, and S.G. Wyllie. Relationships between respiration, ethylene, and aroma production in ripening banana. *J Agric Food Chem*, 47:1646–1651, 1999.

A.L. Goldman, W. Van der Goes van Naters, D. Lessing, C.G. Warr, and J.R. Carlson. Coexpression of two functional odor receptors in one neuron. *Neuron*, 45:661–666, 2005.

S.E. Goulding, P. zur Lage, and A.P. Jarman. amos, a proneural gene for *Drosophila* olfactory sense organs that is regulated by lozenge. *Neuron*, 25:69–78, 2000.

Y. Grosjean, M. Balakireva, L. Dartevelle, and J.F. Ferveur. PGal4 excision reveals the pleiotropic effects of Voila, a *Drosophila* locus that affects development and courtship behaviour. *Genet Res*, 77:239–250, 2001.

Y. Grosjean, R. Rytz, J.-P. Farine, L. Abuin, J. Cortot, G.S.X.E. Jefferis, and R. Benton. An olfactory receptor for food-derived odours promotes male courtship in *Drosophila*. *Nature*, 478:236–240, 2011.

P.G. Guerenstein and J.G. Hildebrand. Roles and effects of environmental carbon dioxide in insect life. *Annu Rev Entomol*, 53:161–178, 2008.

B.P. Gupta and V. Rodrigues. Atonal is a proneural gene for a subset of olfactory sense organs in *Drosophila*. *Genes Cells*, 2:225–233, 1997a.

B.P. Gupta and V. Rodrigues. Atonal is a proneural gene for a subset of olfactory sense organs in *Drosophila*. *Genes Cells*, 2:225–233, 1997b.

B.P. Gupta, G.V. Flores, U. Banerjee, and V. Rodrigues. Patterning an epidermal field: *Drosophila* lozenge, a member of the AML-1/Runt family of transcription factors, specifies olfactory sense organ type in a dose-dependent manner. *Dev Biol*, 203:400–411, 1998.

T.S. Ha and D.P. Smith. A pheromone receptor mediates 11-cis-vaccenyl acetate-induced responses in *Drosophila*. *J Neurosci*, 26:8727–8733, 2006.

E.A. Hallem and J.R. Carlson. Coding of odors by a receptor repertoire. *Cell*, 125:143–160, 2006.

M. Hartl, L.F. Loschek, D. Stephan, K.P. Siju, C. Knappmeyer, and I.C.Grunwald Kadow. A new Prospero and microRNA-279 pathway restricts CO2 receptor neuron formation. *J Neurosci*, 31:15660–15673, 2011.

B. Hassan, L. Li, K.A. Bremer, W. Chang, J. Pinsonneault, and H. Vaessin. Prospero is a panneural transcription factor that modulates homeodomain protein activity. *Proc Natl Acad Sci USA*, 94:10991–10996, 1997.

L. He and G.J. Hannon. MicroRNAs: Small RNAs with a big role in gene regulation. *Nat Rev Genet*, 5:522–531, 2004.

G. Heimbeck, V. Bugnon, N. Gendre, A. Keller, and R.F. Stocker. A central neural circuit for experience-independent olfactory and courtship behavior in *Drosophila melanogaster*. *Proc Natl Acad Sci USA*, 98:15336–15341, 2001.

M. Heisenberg. Mushroom body memoir: From maps to models. *Nat Rev Neurosci*, 4:266–275, 2003.

M. Heisenberg, A. Borst, S. Wagner, and D. Byers. *Drosophila* mushroom body mutants are deficient in olfactory learning. *J Neurogenet*, 2:1–30, 1985.

V. Hilgers, M.W. Perry, D. Hendrix, A. Stark, M. Levine, and B. Haley. Neural-specific elongation of 3' UTRs during *Drosophila* development. *Proc Natl Acad Sci USA*, 108:15864–15869, 2011.

O. Hobert. Gene regulation by transcription factors and microRNAs. *Science*, 319:1785–1786, 2008.

R.A. Holt, G.M. Subramanian, A. Halpern, G.G. Sutton, R. Charlab, D.R. Nusskern, P. Wincker, A.G. Clark, J.M.C. Ribeiro, R. Wides, S.L. Salzberg, B. Loftus, M. Yandell, W.H. Majoros, D.B. Rusch, Z. Lai, C.L. Kraft, J.F. Abril, V. Anthouard, P. Arensburger, P.W. Atkinson, H. Baden, V. de Berardinis, Danita Baldwin, Vladimir Benes, Jim Biedler, Claudia Blass, Randall Bolanos, Didier Boscus, Mary Barnstead, Shuang Cai, Angela Center, Kabir Chaturverdi, G.K. Christophides, Mathew A. Chrystal, Michele Clamp, Anibal Cravchik, Val Curwen, Ali Dana, Art Delcher, Ian Dew, Cheryl A. Evans, Michael Flanigan, Anne Grundschober-Freimoser, Lisa Friedli, Zhiping Gu, Ping Guan, Roderic Guigo, Maureen E. Hillenmeyer, Susanne L. Hladun, James R. Hogan, Young S. Hong, Jeffrey Hoover, Olivier Jaillon, Zhaoxi Ke, Chinnappa Kodira, Elena Kokoza, Anastasios Koutsos, I. Letunic, A. Levitsky, Yong Liang, Jhy-Jhu Lin, Neil F. Lobo, John R. Lopez, Joel A. Malek, Tina C. McIntosh, Stephan Meister, Jason Miller, Clark Mobarry, Emmanuel Mongin, Sean D. Murphy, David A. O'Brochta, Cynthia Pfannkoch, Rong Qi, Megan A. Regier, Karin Remington, Hongguang Shao, Maria V. Sharakhova, Cynthia D. Sitter, Jyoti Shetty, Thomas J. Smith, Renee Strong, Jingtao Sun, Dana Thomasova, Lucas Q. Ton, Pantelis Topalis, Zhijian Tu, Maria F. Unger, Brian Walenz, Aihui Wang, Jian Wang, Mei Wang, Xuelan Wang, Kerry J. Woodford, Jennifer R. Wortman, Martin Wu, Alison Yao, Evgeny M. Zdobnov, Hongyu Zhang, Qi Zhao, Shaying Zhao, Shiaoping C. Zhu, Igor Zhimulev, Mario Coluzzi, Alessandra della Torre, Charles W. Roth, Christos Louis, Francis Kalush, Richard J. Mural, Eugene W. Myers, Mark D. Adams, Hamilton O. Smith, Samuel Broder, Malcolm J. Gardner, Claire M. Fraser, Ewan Birney, Peer Bork, Paul T. Brey, J Craig Venter, Jean Weissenbach, Fotis C. Kafatos, Frank H. Collins, and Stephen L. Hoffman. The genome sequence of the malaria mosquito Anopheles gambiae. *Science*, 298:129–149, 2002.

J. Huang, W. Zhang, W. Qiao, A. Hu, and Z. Wang. Functional connectivity and selective odor responses of excitatory local interneurons in *Drosophila* antennal lobe. *Neuron*, 67: 1021–1033, 2010.

Y.N. Jan and L.Y. Jan. Genetic control of cell fate specification in *Drosophila* peripheral nervous system. *Annu Rev Genet*, 28:373–393, 1994.

D. Jhaveri, A. Sen, and V. Rodrigues. Mechanisms underlying olfactory neuronal connectivity in *Drosophila*-the atonal lineage organizes the periphery while sensory neurons and glia pattern the olfactory lobe. *Dev Biol*, 226:73–87, 2000.

W.D. Jones. MicroRNA mutant turns back the evolutionary clock for fly olfaction. *Bioessays*, 30:621–623, 2008.

W.D. Jones, P. Cayirlioglu, I.C.Grunwald Kadow, and L.B. Vosshall. Two chemosensory receptors together mediate carbon dioxide detection in *Drosophila*. *Nature*, 445:86–90, 2007.

U.B. Kaupp. Olfactory signalling in vertebrates and insects: Differences and commonalities. *Nat Rev Neurosci*, 11:188–200, 2010.

A.C. Keene and S. Waddell. *Drosophila* olfactory memory: Single genes to complex neural circuits. *Nat Rev Neurosci*, 8:341–354, 2007.

M. Kiriakidou, G.S. Tan, S. Lamprinaki, M.. Planell-Saguer, P.T. Nelson, and Z. Mourelatos. An mRNA m7G cap binding-like motif within human Ago2 represses translation. *Cell*, 129: 1141–1151, 2007.

M.J. Krashes, A.C. Keene, B. Leung, J.D. Armstrong, and S. Waddell. Sequential use of mushroom body neuron subsets during drosophila odor memory processing. *Neuron*, 53: 103–115, 2007.

A. Kuzin, T. Brody, A.W. Moore, and W.F. Odenwald. Nerfin-1 is required for early axon guidance decisions in the developing *Drosophila* CNS. *Dev Biol*, 277:347–365, 2005.

A. Kuzin, M. Kundu, T. Brody, and W.F. Odenwald. The *Drosophila* nerfin-1 mRNA requires multiple microRNAs to regulate its spatial and temporal translation dynamics in the developing nervous system. *Dev Biol*, 310:35–43, 2007.

J.Y. Kwon, A. Dahanukar, L.A. Weiss, and J.R. Carlson. The molecular basis of CO2 reception in *Drosophila*. *Proc Natl Acad Sci USA*, 104:3574–3578, 2007.

E.C. Lai and V. Orgogozo. A hidden program in *Drosophila* peripheral neurogenesis revealed: Fundamental principles underlying sensory organ diversity. *Dev Biol*, 269:1–17, 2004.

G. Lebreton, C. Faucher, D.L. Cribbs, and C. Benassayag. Timing of Wingless signalling distinguishes maxillary and antennal identities in *Drosophila melanogaster*. *Development*, 135:2301–2309, 2008.

T. Lee and L. Luo. Mosaic analysis with a repressible cell marker (MARCM) for *Drosophila* neural development. *Trends Neurosci*, 24:251–254, 2001.

T. Lee, A. Lee, and L. Luo. Development of the *Drosophila* mushroom bodies: Sequential generation of three distinct types of neurons from a neuroblast. *Development*, 126:4065–4076, 1999.

Y. Lee, C. Ahn, J. Han, H. Choi, J. Kim, J. Yim, J. Lee, P. Provost, O. Rådmark, S. Kim, and V.N. Kim. The nuclear RNase III Drosha initiates microRNA processing. *Nature*, 425: 415–419, 2003.

B. Lilly, D.D. O'Keefe, J.B. Thomas, and J. Botas. The LIM homeodomain protein dLim1 defines a subclass of neurons within the embryonic ventral nerve cord of *Drosophila*. *Mech Dev*, 88:195–205, 1999.

D.M. Lin, R.D. Fetter, C. Kopczynski, G. Grenningloh, and C.S. Goodman. Genetic analysis of Fasciclin II in *Drosophila*: Defasciculation, refasciculation, and altered fasciculation. *Neuron*, 13:1055–1069, 1994.

T. Lu, Y.T. Qiu, G. Wang, J.Y. Kwon, M. Rutzler, H.-W. Kwon, R.J. Pitts, J.J.A. van Loon, W. Takken, J.R. Carlson, and L.J. Zwiebel. Odor coding in the maxillary palp of the malaria vector mosquito *Anopheles gambiae*. *Curr Biol*, 17:1533–1544, 2007.

W. Luo and A. Sehgal. Regulation of circadian behavioral output via a microrna-jak/stat circuit. *Cell*, 148(4):765–779, Feb 2012.

L. Manning and C.Q. Doe. Prospero distinguishes sibling cell fate without asymmetric localization in the *Drosophila* adult external sense organ lineage. *Development*, 126:2063–2071, 1999.

N.Y. Masse, G.C. Turner, and G.S.X.E. Jefferis. Olfactory information processing in *Drosophila*. *Curr Biol*, 19:R700–R713, 2009.

S.E. McGuire, P.T. Le, and R.L. Davis. The role of *Drosophila* mushroom body signaling in olfactory memory. *Science*, 293:1330–1333, 2001.

G. Meister and T. Tuschl. Mechanisms of gene silencing by double-stranded RNA. *Nature*, 431: 343–349, 2004.

C.A. Micchelli and N. Perrimon. Evidence that stem cells reside in the adult *Drosophila* midgut epithelium. *Nature*, 439:475–479, 2006.

K. Mori, H. Nagao, and Y. Yoshihara. The olfactory bulb: Coding and processing of odor molecule information. *Science*, 286:711–715, 1999.

T.P. Newsome, B. Asling, and B.J. Dickson. Analysis of *Drosophila* photoreceptor axon guidance in eye-specific mosaics. *Development*, 127:851–860, 2000.

M. Ng, R.D. Roorda, S.Q. Lima, B.V. Zemelman, P. Morcillo, and G. Miesenböck. Transmission of olfactory information between three populations of neurons in the antennal lobe of the fly. *Neuron*, 36:463–474, 2002.

S. Nottrott, M.J. Simard, and J.D. Richter. Human let-7a miRNA blocks protein production on actively translating polyribosomes. *Nat Struct Mol Biol*, 13:1108–1114, 2006.

S.R. Olsen and R.I. Wilson. Lateral presynaptic inhibition mediates gain control in an olfactory circuit. *Nature*, 452:956–960, 2008.

A. Pascual and T. Préat. Localization of long-term memory within the *Drosophila* mushroom body. *Science*, 294:1115–1117, 2001.

C.P. Petersen, M.-E. Bordeleau, J. Pelletier, and P.A. Sharp. Short RNAs repress translation after initiation in mammalian cells. *Mol Cell*, 21:533–542, 2006.

H.M. Robertson, C.G. Warr, and J.R. Carlson. Molecular evolution of the insect chemoreceptor gene superfamily in *Drosophila melanogaster*. *Proc Natl Acad Sci USA*, 100 Suppl 2:14537–14542, 2003.

V. Rodrigues and T. Hummel. Development of the *Drosophila* olfactory system. *Adv Exp Med Biol*, 628:82–101, 2008.

S. Sachse and C.G. Galizia. Role of inhibition for temporal and spatial odor representation in olfactory output neurons: A calcium imaging study. *J Neurophysiol*, 87:1106–1117, 2002.

K. Sato, M. Pellegrino, T. Nakagawa, T. Nakagawa, L.B. Vosshall, and K. Touhara. Insect olfactory receptors are heteromeric ligand-gated ion channels. *Nature*, 452:1002–1006, 2008.

K. Scott. Out of thin air: Sensory detection of oxygen and carbon dioxide. *Neuron*, 69:194–202, 2011.

J.L. Semmelhack and J.W. Wang. Select *Drosophila* glomeruli mediate innate olfactory attraction and aversion. *Nature*, 459:218–223, 2009.

S.R. Shanbhag, B. Müller, and R.A. Steinbrecht. Atlas of olfactory organs of *Drosophila melanogaster* 2. Internal organization and cellular architecture of olfactory sensilla. *Arthropod Struct Dev*, 29:211–229, 2000.

C.P. Shen, L.Y. Jan, and Y.N. Jan. Miranda is required for the asymmetric localization of Prospero during mitosis in *Drosophila*. *Cell*, 90:449–458, 1997.

A.F. Silbering, R. Rytz, Y. Grosjean, L. Abuin, P. Ramdya, G.S.X.E. Jefferis, and R. Benton. Complementary function and integrated wiring of the evolutionarily distinct *Drosophila* olfactory subsystems. *J Neurosci*, 31:13357–13375, 2011.

F. Simon, P. Fichelson, M. Gho, and A. Audibert. Notch and Prospero repress proliferation following cyclin E overexpression in the *Drosophila* bristle lineage. *PLoS Genet*, 5:e1000594, 2009.

E.P. Spana and C.Q. Doe. The prospero transcription factor is asymmetrically localized to the cell cortex during neuroblast mitosis in *Drosophila*. *Development*, 121:3187–3195, 1995.

D.L. Stern and V. Orgogozo. The loci of evolution: How predictable is genetic evolution? *Evolution*, 62:2155–2177, 2008.

R.F. Stocker. *Drosophila* as a focus in olfactory research: Mapping of olfactory sensilla by fine structure, odor specificity, odorant receptor expression, and central connectivity. *Microsc Res Tech*, 55:284–296, 2001.

N.J. Strausfeld, I. Sinakevitch, and I. Vilinsky. The mushroom bodies of *Drosophila melanogaster*: An immunocytological and golgi study of Kenyon cell organization in the calyces and lobes. *Microsc Res Tech*, 62:151–169, 2003.

G.S.B. Suh, A.M. Wong, A.C. Hergarden, J.W. Wang, A.F. Simon, S. Benzer, R. Axel, and D.J. Anderson. A single population of olfactory sensory neurons mediates an innate avoidance behaviour in *Drosophila*. *Nature*, 431:854–859, 2004.

N.K. Tanaka, T. Awasaki, T. Shimada, and K. Ito. Integration of chemosensory pathways in the *Drosophila* second-order olfactory centers. *Curr Biol*, 14:449–457, 2004.

N.K. Tanaka, H. Tanimoto, and K. Ito. Neuronal assemblies of the *Drosophila* mushroom body. *J Comp Neurol*, 508:711–755, 2008.

E.R. Troemel, J.H. Chou, N.D. Dwyer, H.A. Colbert, and C.I. Bargmann. Divergent seven transmembrane receptors are candidate chemosensory receptors in C. *elegans*. *Cell*, 83:207–218, 1995.

S.L. Turner and A. Ray. Modification of CO2 avoidance behaviour in *Drosophila* by inhibitory odorants. *Nature*, 461:277–281, 2009.

L.B. Vosshall and R.F. Stocker. Molecular architecture of smell and taste in *Drosophila*. *Annu Rev Neurosci*, 30:505–533, 2007.

L.B. Vosshall, H. Amrein, P.S. Morozov, A. Rzhetsky, and R. Axel. A spatial map of olfactory receptor expression in the *Drosophila* antenna. *Cell*, 96:725–736, 1999.

J.W. Wang, A.M. Wong, J. Flores, L.B. Vosshall, and R. Axel. Two-photon calcium imaging reveals an odor-evoked map of activity in the fly brain. *Cell*, 112:271–282, 2003.

D. Wicher, R. Schäfer, R. Bauernfeind, M.C. Stensmyr, R. Heller, S.H. Heinemann, and B.S. Hansson. *Drosophila* odorant receptors are both ligand-gated and cyclic-nucleotide-activated cation channels. *Nature*, 452:1007–1011, 2008.

R.I. Wilson. Understanding the functional consequences of synaptic specialization: Insight from the *Drosophila* antennal lobe. *Curr Opin Neurobiol*, 21:254–260, 2011.

R.I. Wilson, G.C. Turner, and G. Laurent. Transformation of olfactory representations in the *Drosophila* antennal lobe. *Science*, 303:366–370, 2004.

M. Wistrand, L. Käll, and E.L.L. Sonnhammer. A general model of G protein-coupled receptor sequences and its application to detect remote homologs. *Protein Sci*, 15:509–521, 2006.

E. Yaksi and R.I. Wilson. Electrical coupling between olfactory glomeruli. *Neuron*, 67:1034–1047, 2010.

D.-J. Yang, J.-Y. Chung, S.-J. Lee, S.-Y. Park, J.-H. Pyo, N.-C. Ha, M.-A. Yoo, and B.-J. Park. Slug, mammalian homologue gene of *Drosophila* escargot, promotes neuronal-differentiation through suppression of HEB/daughterless. *Cell Cycle*, 9:2789–2802, 2010.

C.A. Yao, R. Ignell, and J.R. Carlson. Chemosensory coding by neurons in the coeloconic sensilla of the *Drosophila* antenna. *J Neurosci*, 25:8359–8367, 2005.

W.H. Yoon, H. Meinhardt, and D.J. Montell. mirna-mediated feedback inhibition of jak/stat morphogen signalling establishes a cell fate threshold. *Nat Cell Biol*, 13(9):1062–1069, Sep 2011.

T. Zars. Behavioral functions of the insect mushroom bodies. *Curr Opin Neurobiol*, 10:790–795, 2000.

Acknowledgements

Making a switch from plant physiology to neurobiology sounds almost unlikely. And wouldn't have been possible for me without my supervisor Ilona Grunwald Kadow. Your constant support and believe in the success of my and the research of my colleagues made this work happen. I was lucky to start my PhD as one of the first of your students. Thanks for giving me the experience of a young enthusiastic boss, who is really protective toward the students and their work.

I would also like to thank my official supervisor Prof.Dr.Klaus Förstemann for taking over the institutional responsibility for my project and your input in my thesis committee.

Many thanks go also to my second thesis committee member Alexander Stark. Thanks for reminding me that doing science makes only sense with an enthusiastic attitude!

I would also like to thank all the members of my defense committee Prof.Dr.Dietmar Martin, Prof.Dr.Mario Halic, Prof.Dr.Karl-Klaus Conzelmann, Prof.Dr.Ulrike Gaul and Prof.Dr.Roland Beckmann.

On the daily basis, I had the opportunity to work in a supportive and warm environment. I'm especially obliged to Dr. Laura Loschek for helping me constantly in my project, to Dr. Siju Purayil for doing the electrophysiology, to Daniel Stephan and Christiane Knappmeyer for great assistance in dissections, to Juhi Sardana for giving me company in endless evenings trying to unravel the mysteries of molecular biology and to Habibe Ucpunar for so much fresh motivation to do science.

Apart from work related support, the atmosphere in the Kadow group made most of the time I spend at the MPI a really pleasant experience. Many Thanks for that to Mo, Lawrence, Cristina, Ramona, Lasse, Irina and all the former members, Verena, Yukiko, Ece, Lauren, Anna 1-3 and Ricardo.

Life is easy if you have such great fellow students like Julia, Klaudiusz, Armin, Thorben, Isabella, Anselm, Liesl, Max, Dodo, Michi, Fiona and so on and so on.....

To ensure that science didn't drive me crazy in all the years I'm very grateful to my lovely

sisters, Birgit and Monika, "meinem Papa" and my loyal friends Fini, Basti, Helen, Mary and Nils, Julia F., Wolfgang, Hubert, Basti 2, Peter, Kerstin, Gerrit and Caj.

Lastly, I have to thank Franz: Thank you so much for the endless support I got from you in the last years! I'm looking forward to the continuation of our story in S.F.!